INVESTIGATION OF GENETICAL MATERIAL DECORATED NANOPARTICLES USABILITY AS A NEW GENERATION BIOCHEMICAL STRATEGY IN CANCER THERAPY

YENİ NESİL BİYOKİMYASAL STRATEJİ OLARAK GENETİK MATERYAL İLE DEKORE EDİLMİŞ NANOPARTİKÜLLERİN KANSER TEDAVİSİNDE KULLANILABİLİRLİĞİNİN ARAŞTIRILMASI

GÖKNUR KARA

Prof. Dr. EMİR BAKİ DENKBAŞ
Supervisor

Submitted to
Graduate School of Science and Engineering of Hacettepe University
as a Partial Fulfillment to the Requirements
for the Award of the Degree of Doctor of Philosopy in Chemistry

2020

To my beloved family

ABSTRACT

INVESTIGATION OF GENETICAL MATERIAL DECORATED NANOPARTICLES USABILITY AS A NEW GENERATION BIOCHEMICAL STRATEGY IN CANCER THERAPY

GÖKNUR KARA

Doctor of Philosophy, Department of Chemistry

Supervisor: Prof. Dr. Emir Baki DENKBAŞ

February 2020, 112 pages

Breast cancer (BC) is the second most frequently diagnosed cancer type worldwide. Triple negative breast cancer (TNBC) type is a considerably aggressive one compared to other breast cancer subtypes with high metastasis, relapse and mortality rate in patients. Due to its significant genetic heterogeneity and deficiency of molecular targets such as estrogen receptor (ER), progesterone receptor (PR) and human epidermal growth factor receptor 2 (HER2), no effective targeted therapy strategies are available for TNBC. In recent years, emerging evidence has revealed that short non-coding microRNAs (miRNA) are broadly involved in various cancer pathophysiological processes including cell cycle, proliferation, differentiation, migration/invasion and aging, via regulating the expression of the target genes that are active in those pathways. miRNAs gain an important role as therapeutics by enabling the degradation of the target mRNA or the inhibition of translation. Therefore, miRNA-based therapeutics may be a novel therapeutic approach, especially for TNBC patients. However, safe and efficient delivery systems are required for miRNAs to be successfully used in clinical trials.

In the presented study, poly-L-lysine (PLL) modified sericin (Ser) coated superparamagnetic iron oxide nanoparticles (SPIONs) (PLL/Ser-SPIONs) were synthesized and characterized as miRNA delivery vehicle for TNBC therapy. PLL/Ser-SPIONs were obtained in a size range of 25-30 nm with a cationic zeta potential value that is +13 mV. The nanoparticles were interacted with different concentrations of miRNA (miR) control and the range of the binding efficiencies was found to be as 97-99%. Transmission electron microscopy (TEM) and confocal microscopy analyses exhibited that miR-control or control small interfering RNA (siRNA) loaded PLL/Ser-SPIONs were successfully uptaken by TNBC (MDA-MB-231) cells. miR-329 was chosen as a target miRNA after analyzing several miRNA databases and discovering that its overexpression is related to high survival rate in patients with TNBC. It was demonstrated by quantitative reverse transcription polymerase chain reaction (RT-qPCR) that miR-329 expression level is significantly reduced in many TNBC cell lines. In vitro delivery of miR-329 either using PLL/Ser-SPIONs or a commercial transfection reagent inhibited proliferation, invasion/migration and enhanced apoptosis rate in TNBC cells. The underlying molecular mechanism of miR-329 based therapy was investigated via a number of target prediction algorithms and they showed that miR-329 has binding sites at three prime untranslated region (3'-UTR) of eukaryotic elongation factor-2 kinase (eEF2K) and AXL genes. In addition, by Western Blot assay, upregulated levels of both eEF2K and AXL were observed in TNBC cells, and it was also found that these genes are associated with shorter overall survival in TNBC patients. More important, after miR-329 delivery in TNBC cells, both eEF2K and AXL expressions were remarkably inhibited. The TNBC cells were also treated with specific siRNAs for eEF2K and AXL, and silencing these genes recapitulated the effects of ectopic expression of miR-329 by reducing the cell growth and invasion/migration. Furthermore, in vivo delivery of miR-329 loaded PLL/Ser-SPIONs led to a drastic inhibition in tumor growth in TNBC orthotopic xenograft models (MDA-MB-231 and MDA-MB-436) in mice. A significant knockdown of eEF2K and AXL levels was also observed in tumor samples by Western Blot analysis. In addition, PLL/Ser-SPIONs-miR 329 treatment in mice did not cause any detectable side effects. These obtained results suggest that miR-329 acts as a tumor suppressor (TS) and its reduced expression results in an increase in eEF2K and AXL expressions that lead to progression of TNBC. Moreover, this work also suggests PLL/Ser-SPION as a potential theranostic (therapy+diagnostic) agent with its multifunctional property. Taken all together, this study shows that PLL/Ser-

SPIONs-miR 329 system may be a promising and novel miR-therapy strategy against TNBC providing a safe and high antitumor efficacy.

Keywords: triple negative breast cancer, super paramagnetic iron oxide nanoparticles, miR-329, eEF2K, AXL

ÖZET

YENİ NESİL BİYOKİMYASAL STRATEJİ OLARAK GENETİK MATERYAL İLE DEKORE EDİLMİŞ NANOPARTİKÜLLERİN KANSER TEDAVİSİNDE KULLANILABİLİRLİĞİNİN ARAŞTIRILMASI

GÖKNUR KARA

Doktora, Kimya Bölümü

Tez Danışmanı: Prof. Dr. Emir Baki DENKBAŞ

Şubat 2020, 112 sayfa

Meme kanseri, dünya çapında ikinci en yaygın görülen kanserdir. Üçlü negatif meme kanseri, hastalarda yüksek metastaz, nüks ve mortalite oranına sahiptir ve diğer meme kanseri alt tiplerine kıyasla oldukça agresif bir tiptir. Önemli genetik heterojenliğe sahip olması, östrojen reseptörü, progesteron reseptörü ve insan epidermal büyüme faktörü reseptörü 2 gibi tanımlanmış moleküler hedeflerin bulunmaması nedeniyle, üçlü negatif meme kanseri için etkili bir hedeflenmiş tedavi stratejisi yoktur. Son yıllarda ortaya çıkan kanıtlar, kısa kodlayıcı olmayan mikroRNA'ların (miRNA), hücre döngüsü, proliferasyon, farklılaşma, migrasyon/invazyon ve yaşlanma gibi yolaklarda aktif olan hedef genlerin ekspresyonunu düzenleyerek çeşitli kanser patofizyolojik süreçlerine geniş ölçüde dahil olduklarını ortaya koymuştur. miRNA'lar, hedef mRNA'nın bozunmasını veya translasyonun inhibisyonunu sağlayarak terapötik olarak önemli bir rol kazanır. Bu nedenle miRNA bazlı terapötikler, özellikle üçlü negatif meme kanseri hastaları için yeni bir

terapötik yaklaşım olabilir. Bununla birlikte, miRNA'ların klinik çalışmalarda başarılı bir şekilde kullanılabilmesi için güvenli ve verimli salım sistemleri gerekmektedir.

Sunulan çalışmada, poli-L-lizin (PLL) ile modifiye edilmiş serisin kaplı süperparamanyetik demir oksit nanopartiküller (SPION'lar) (PLL/Ser-SPIONs'lar) üçlü negatif meme kanseri tedavisi için miRNA salım aracı olarak sentezlendi ve karakterize edildi. PLL/Ser-SPION'lar, + 13 mV olan katyonik zeta potansiyel değerine sahip olarak 25-30 nm boyut aralığında elde edildi. Sentezlenen nanoparçacıklar farklı derişimlerdeki kontrol miRNA ile etkileştirilmiş ve bağlanma verimi aralığı %97-99 olarak bulunmuştur. Transmisyon elektron mikroskopisi (TEM) ve konfokal mikroskopi analizleri ile miR-kontrol veya kontrol-siRNA yüklü PLL/Ser-SPION'ların üçlü negatif meme kanseri (MDA-MB-231) hücreleri tarafından başarılı bir şekilde hücre içine alındığı ortaya konuldu. miR-329, birkaç miRNA veritabanı analiz edildikten ve üçlü negatif meme kanseri hastalarında aşırı ekspresyonunun yüksek sağkalım oranı ile ilişkili olduğu keşfediltikten sonra hedef miRNA olarak seçildi. Kantitatif ters transkripsiyon polimeraz zincir reaksiyonu (RT-qPCR) ile miR-329'un ekspresyon seviyesinin birçok üçlü negatif meme kanseri hücre hattında önemli derecede düşük olduğu gösterilmiştir. miR-329'un hem üretilen PLL/Ser-SPION'lar hem de ticari bir transfeksiyon reaktifi kullanılarak in vitro olarak verilmesi üçlü negatif meme kanseri hücrelerinde çoğalmayı, invazyonu ve migrasyonu inhibe ettiği ve apoptozu arttırdığı gözlemlenmiştir. miR-329 temelli tedavinin altında yatan moleküler mekanizma, bir dizi hedef tahmin algoritması ile araştırılmış ve miR-329'un, ökaryotik uzama faktörü-2 kinaz (eEF2K) ve AXL genlerinin 3'-UTR'sinde bağlanma bölgelerine sahip olduğu gösterilmiştir. Ek olarak, western blot analizi ile üçlü negatif meme kanseri hücre dizilerinde hem eEF2K hem de AXL'in artmış ekpresyon seviyeleri gözlenmiş ve ayrıca bu genlerin üçlü negatif meme kanseri hastalarında daha kısa genel sağkalım ile ilişkili olduğu bulunmuştur. Daha da önemlisi, üçlü negatif meme kanseri hücrelerinde miR-329 verilmesinden sonra, hem eEF2K hem de AXL ekpresyonunun önemli ölçüde inhibe edildiği ortaya konmuştur. Üçlü negatif meme kanseri hücreleri ayrıca eEF2K ve AXL'ye spesifik küçük interfere edici RNA'lar (siRNA'lar) ile muamele edilmiş ve bu genlerin susturulması hücre büyümesini ve invazyon/migrasyonu azaltarak miR-329'un ektopik ekspresyonunun etkilerini tekrar etmiştir. Ayrıca, farelerde üçlü negatif meme kanseri ortotopik ksenograft modellerinde (MDA-MB-231 ve MDA-MB-436) miR-329 yüklü PLL/Ser-SPION'ların in vivo olarak uygulanması, tümör büyümesinin önemli derecede inhibisyonuyla sonuçlanmıştır. Western blot analizi ile tümör örneklerinde

eEF2K ve AXL seviyelerinin de önemli ölçüde azaldığı gözlenmiştir. Ayrıca, farelerde PLL/Ser-SPIONs-miR-329 tedavisinin saptanabilir yan etkilere neden olmadığı gözlemlenmiştir. Bu bulgular, miR-329'un bir tümör baskılayıcı olarak işlev gördüğünü ve azaltılmış ekspresyonunun, üçlü negatif meme kanserinin ilerlemesine yol açan eEF2K ve AXL ekspresyonlarında bir artışla sonuçlandığını düşündürmektedir. Dahası, bu çalışma PLL/Ser-SPION'u çok fonksiyonlu özelliği ile potansiyel bir theranostik (terapi+teşhis) ajan olarak önermektedir. Sonuçlar hep birlikte ele alındığında, bu çalışma PLL/Ser-SPIONs-miR-329 sisteminin üçlü negatif meme kanserine karşı güvenli ve yüksek bir antitümör etkinliği sağlayan umut verici ve yeni bir miR-terapi stratejisi olabileceğini göstermektedir.

Anahtar Kelimeler: üçlü negatif meme kanseri, süperparamanyetik demir oksit nanopartiküller, miR-329, eEF2K, AXL

ACKNOWLEDGEMENTS

First and foremost, I would like to express my sincere gratitude to my supervisor Prof. Dr. Emir Baki DENKBAŞ for his immense knowledge, guidance, support and motivation throughout all my graduate journey.

I'm deeply indebted to Assoc. Prof. Dr. Bülent ÖZPOLAT and to Prof. Dr. Gabriel LOPEZ-BERESTEIN for giving me the opportunity to work as a fellow Ph.D. student in their laboratory and supporting me all the time. It was great to work with them and learn from them.

I would like to thank the members of the thesis examining committee, Prof. Dr. Adil DENİZLİ, Prof. Dr. Handan YAVUZ ALAGÖZ, Assoc. Prof. Dr. Fatih BÜYÜKSERİN and Assist. Prof. Dr. Ebru KILIÇAY for their helpful suggestions, guidance and encouragement.

A special gratitude goes to Prof. Dr. Nagihan UĞURLU and her lab members and Prof. Dr. Bekir SALİH and his lab members for their valuable support whenever I need help.

I also wish to thank all at Chemistry Department of Hacettepe University.

I would like to extend my deepest appreciation to my family for their endless love, encouragement and for believing in me during every moment of my life. Without their support, my dissertation would not have been possible. I'm so lucky to have them.

Last but by no means least, I'm extremely grateful to all my friends who have always loved and supported me unconditionally all along the way. Thank you for the beautiful ways you have touched my life!

This study was supported in 2214-A International Doctoral Research Fellowship Program by The Scientific and Technological Research Council of Turkey (TUBITAK). (Application No: 1059B141700104)

Göknur KARA
February 2020, Ankara

TABLE OF CONTENTS

TABLES

FIGURES

SYMBOLS AND ABBREVIATIONS

Symbols

(g)	Spectroscopic Splitting Factor
ΔH_{pp}	Peak to Peak Linewidth

Abbreviations

BC	Breast Cancer
TNBC	Triple Negative Breast Cancer
ER	Estrogen Receptor
PR	Progesterone Receptor
HER2	Human Epidermal Growth Factor Receptor 2
miRNA	MicroRNA
PLL	Poly-L-lysine
Ser	Sericin
SPIONs	Superparamagnetic Iron Oxide Nanoparticles
MNPs	Magnetic Nanoparticles
TEM	Transmission Electron Microscopy
RT-qPCR	Quantitative Reverse Transcription Polymerase Chain Reaction
eEF2K	Eukaryotic Elongation Factor-2 Kinase
3'-UTR	Three Prime Untranslated Region
siRNA	Small Interfering RNA
TP53	Tumor Protein 53
TS	Tumor Suppressor
mRNA	Messenger RNA
MRI	Magnetic Resonance Imaging

PEG	Polyethylene Glycol
PEI	Polyethylenimine
RTK	Receptor Tyrosine Kinase
BL	Basal-Like
M	Mesenchymal-like
MSL	Mesenchymal stem-like
LAR	Luminal Androgen Receptor
IM	Immunomodulatory
UNS	Unstable
BCS	Breast-Conserving Surgery
pCR	Pathological Complete Response
DDR	DNA-Damage Response
EMT	Epithelial-Mesenchymal Transition
PI3K	Phoshoinositide 3-kinase
mTOR	Mammalian Target of Rapamycin
AR	Androgen Receptor
rRNA	Ribosomal RNA
tRNA	Transfer RNAs
snoRNA	small nucleolar RNA
snRNA	small-nuclear RNA
piRNA	piwi-interacting RNA
ncRNA	non-coding RNA
tRFs	tRNA-derived RNA fragments
pri-miRNA	primary-miRNA
pre-miRNA	precursor-miRNA
RISC	RNA-induced silencing complex

CLL	Chronic Lymphocytic Leukaemia
AAV	Adeno-Associated Virus
BSA	Bovine Serum Albumin
mAb	Monoclonal Antibody
TIAM1	T lymphoma invasion and metastasis 1
GRB2	Growth Factor Receptor-Bound Protein 2
Cas	Crk-Associated Substrate
FAK	Focal Adhesion Kinase
IGFR	Insulin-like Growth Factor Receptor
GAS6	Growth Arrest Specific 6
DI	Deionized Water
APTES	(3-Aminopropyl)triethoxysilane
EDC-HCl	N-(3-Dimethylaminopropyl)-N′-ethylcarbodiimide hydrochloride
PBS	Phosphate-buffered saline
NHS	*N*-Hydroxysuccinimide
FTIR	Fourier Transform Infrared Spectroscopy
DLS	Dynamic Light Scattering
PDI	Polydispersity Index
ESR	Electron Spin Resonance
MNPs	Magnetic Nanoparticles
BE	Binding Efficiency
ATCC	American Type Culture Collection
DMEM/F12	Dulbecco's Modified Eagle's Medium
FBS	Fetal Bovine Serum
EDTA	Ethylenediaminetetraacetic acid
HMEC	Human Mammary Epithelial Cells

cDNA	Complementary DNA
MTT	3-(4,5-dimethylthiazol-2-yl)-2,5-diphenyltetrazolium bromide
EMEM	Eagle's Minimum Essential Medium
MTS	(3-(4,5-dimethylthiazol-2-yl)-5-(3-carboxymethoxyphenyl)-2-(4-sulfophenyl)-2H-tetrazolium)
PMS	Phenazine Methosulfate
BCA	Bicinchoninic Acid
SDS-PAGE	Sodium Sodecyl Sulfate–Polyacrylamide Gel Electrophoresis
PVDF	Polyvinylidene Difluoride
HRP	Horseradish Peroxidase
ECL	Enhanced Chemiluminescence
SD	Standard Deviation
ANOVA	Analysis of Variance
TCGA	The Cancer Genome Atlas Program
EPR	Enhanced Permeability and Retention
RES	Reticuloendothelial System

1. INTRODUCTION

Cancer is an increasingly global problem that affects all human beings. BC is the most common cancer among women and it accounts for approximately 23% of all cancer patients [1, 2]. BC is an aggressive cancer type and has a high heterogeneous complex biological profile. BC is clinically categorized into four subtypes based upon molecular properties and presence of ER, PR and HER2. These are: basal-like (BL) or TNBC, HER2 overexpressing, luminal A (ER and/or PR positive and HER2 negative) and luminal B (ER and/or PR positive and HER2 positive) [3]. TNBC represents around 15-20% of all cases of BC and is identified by a lack of immunohistochemical expression of PR, ER and HER2. Due to this reason, hormonal therapies such as tamoxifen (targeting ER) and trastuzumab (targeting HER2) cannot be applied to the patients with TNBC [4]. Currently, there are several available treatment options for the TNBC patients including surgery, radiation therapy and chemotherapy [5]. However, TNBC is highly aggressive and heterogeneous disease with its different subclasses. Besides, the distant recurrence, early relapses and metastasis, and mortality rate in TNBC is significantly worse comparing to other subtypes [6]. In addition to its intratumoral heterogeneity, tumor protein 53 (TP53) gene is mutated in 84% of TNBC cases. These unfavorable characteristics of TNBC cause a poor clinical outcome and short overall survival in patients [7, 8]. Therefore, to identify the underlying molecular mechanism of TNBC and the specific targets, and to develop effective and promising therapies are essential to enhance the clinical outcome of TNBC patients [9-11].

miRNAs having 18-24 nucleotides are one of the members of small non-protein coding RNAs. Numerous evidences have demonstrated that miRNAs extensively play a critical role in the key features of cancer cells affecting variety of pathophysiological proccesses such as cell survival, differentiation, proliferation, migration, angiogenesis and invasion [12-14]. miRNAs interact with the 3'-UTRs of the target messenger RNAs (mRNAs) complementarily and simultaneously at post-transcriptional level, and this results in inhibition in mRNA degradation and/or of translation [15, 16]. Therefore, miRNAs have emerged as potential therapeutic targets in several cancer types including TNBC [17]. Thus far, various miRNAs have been identified based on their expression levels in cancer cells. For instance, miRNAs such as miR-155, miR-21 and miR17-92 are one of the overexpressed miRNAs, and they are considered as oncogenic miRNAs while miRNAs such as miR-16-1, miR-15a, miR34 are called as TS miRs with their low or lost

expressions in cancer tissues [18]. Within increasing interest in miRNA development over the years, several studies have revealed that miRNAs are also highly effective in BC progression, tumorigenesis, metastasis and angiogenesis [19-21]. In various cancer types such as glioma, lung, melanoma, pancreatic and breast cancer, the expression of miR-329 was determined to be deregulated and inversely correlated with pathological charachteristics [22-26]. However, the potential role and molecular mechanism of miR-329 as a miRNA therapeutic were not yet identified for TNBC.

A successful clinical application of miRNA therapy depends on safely delivery of miRNAs to the target area at a therapeutically efficacious concentration. The systemic use of unmodified or free miRNA results in insufficient therapeutic effect due to its rapid degradation in the blood. Therefore, carrier-based systems are necessary for miRNA delivery to safely and efficaciously accomplish its destination [27, 28]. An ideal delivery system should protect miRNA from degradation, facilitate cellular uptake, maintain miRNA at a constant concentration during the treatment, and should not induce an immunogenic response and side effects [29-31].

Over the years of studies, a large number of viral and non-viral vectors have been generated to be used as miRNA delivery systems [32]. Although viral vectors enable to evade the defence mechanism of the body, the attempts of their clinical use have failed since they induce the immune response [33]. Non-viral vectors exhibit low toxicity and immunogenicity, and they have been widely studied for gene transfection applications. Among the other non-viral delivery systems, SPIONs have drawn attention in a variety of biomedical applications including gene therapy. The unique features of SPIONs such as low toxicity, biocompatibility and biodegradability make them promising materials not only for cancer therapy but also in diagnosis via using magnetic resonance imaging (MRI) [34, 35]. By means of their magnetic characteristics SPIONs can be directed to tumor site by an external magnetic force and also used for hyperthermia applications [36]. Polysaccharide or protein based natural polymers such as chitosan, alginate, dextran, albumin, gelatin and synthetic polymers such as polyethylene glycol (PEG) and polyethylenimine (PEI) have been commonly preffered to cover the surface of the SPION in order to avoid aggregation of the colloidal suspension [37, 38].

The aim of this presented study is to develop magnetic nanoparticles for the delivery of miR-329 and to evaluate in vitro and in vivo antitumor efficacy of this novel therapeutic system in TNBC by identifying the underlying molecular mechanism of miR-329. This

work exhibited for the first time the potential of novel PLL/Ser-SPIONs as miRNA delivery system, and the tumor suppressive effects of miR-329 in progression of TNBC regulating eEF2K and AXL genes. The findings showed that PLL/Ser-SPIONs-miR-329 caused a drastic inhibition in tumor growth through inhibition of several oncogenic pathways. This work suggests PLL/Ser-SPIONs-based miR-329 therapy may be a promising therapeutic approach for TNBC therapy.

2. GENERAL INFORMATION

2.1. Breast Cancer

BC is the second most common cause of death among women and it is the primary cause of cancer-related deaths in women worldwide. Annually, 1 million women are diagnosed with BC around the world [39]. In 2012, this number was 1.7 million, and 521.900 women were reported to have died from BC [40]. Globally, the highest number of new BC cases occurred in 2015 [41]. In Turkey, BC is the most common type of cancer in women and the most deaths were observed in this type of cancer case [42]. According to Health Ministry data between the years 2007-2012, around 48.000 women are diagnosed with BC every year in Turkey [43].

The incidence of BC in women has been revealed to be one in eight and the risk of dying from BC throughout life is 3.4%. It was estimated that 30% of new cancer cases in women would be BC in 2017. In general, the overall survival rate of BC has increased over the last decade [44, 45]. This is based on a strong association between survival and diagnostic stage that is related to tumor size and metastasis. In the US, the 5-year survival rate between 2001 and 2007 was observed as 98.6% and 83.8% for localized and regional stages, respectively, whereas for distant stage disease it was recorded as 23.3%. Similar results were obtained from other countries for BC cases [46].

BC can be grouped as invasive or non-invasive followed by the stage and grade in the routine clinical practice. Classification is made according to the location of the abnormal tissues in the patient, the histological features of the breast tissue, and the clinical symptoms of the patient [47]. Most BCs are invasive. Paget's disease, colloid (mucinous) carcinoma, invasive lobular carcinoma, infiltrating ductal carcinoma, tubular carcinoma, inflammatory carcinoma, medullary carcinoma are grouped as invasive BC. Non-invasive BCs do not spread to surrounding tissues and they remain localized. In situ ductal carcinoma and in situ lobular carcinoma are the two main types of non-invasive BC. BCs can spread to the different parts of the body through the bloodstream and lymph nodes, and thus may become metastatic [48].

2.1.1. Breast Cancer Subtypes

BC has a high degree of inter- and intratumoral heterogeneity, and is a very complex disease. For that reason, to identify pathological, clinical and molecular factors, and to

categorize BC to its subtypes at molecular level is essential to select the treatment modalities and to evince the best outcomes in patients. Histological stratification of BCs on the basis of the expression of PR, ER and HER2 receptors has been a pioneer in the categorizing and prognosis of BCs [49, 50].

ER is a transcription factor and steroid hormone receptor and, is expressed in nearly 70% of invasive BCs. When prompted by estrogen, ER activates the oncogenic pathways in BC cells. The PR (streroid hormone) expression is also a sign of ERα signaling. Another molecular target, HER2 is a transmembrane receptor tyrosine kinase (RTK) classified in the family of epidermal growth factor receptor. HER2 is overexpressed in almost 20% of BCs and shown as HER+. These three proteins are also targets of specific therapeutics such as tamoxifen (used for hormonal therapy) and HER2-targeted therapies [49]. Although histological stratification is yet used as a standard practice in treatment, it is tried to unravel the complexities in subgroups of BC with technological advances [3].

BCs are classified into four major subtypes (BL, HER2 enriched, luminal A and luminal B) according to the expression levels of PR, HER2 and ER (Table 2.1) [3, 51, 52]. Each of these subtypes is significantly associated with clinical outcomes, disease progression, histological features and therapeutic response [53]. Ki-67 is a protein and it has a role as a cellular marker for proliferation. Based on some researchers, it has been accepted to be the fourth molecular marker for the classification. However, although the Ki-67 index is effective as a prognostic and predictive biomarker, it is not yet used in the clinical treatment of BC due to the lack of standard procedures [52, 54]. The genes expressed in the luminal epithelial layer of the mammary gland is called luminal A and luminal B cancers. Approximately 70% of BC are hormone receptor positive, and one or both of ER and PR are expressed in this type of BC [55]. Luminal A cancers possess only low Ki67, HER2− and ER+ and/or PR+. These types of tumors are often identified as low-grade, and they respond to the hormonal therapies such as tamoxifen (ER modulator) and aromatase inhibitors and therefore, they commonly show the best results among all subtypes [56, 57]. Luminal B tumors which are known as more aggressive, overexpress all three main receptors; HER2+ and ER+ and/or PR+ or HER2– and ER+ and/or PR+, high Ki67. Luminal B tumor can be cured via hormonal therapies, however, because it oftenly relapses, the its clinical responses are poor [58, 59]. HER2 enriched tumors are aggressive in nature and represent 20% of all BC cases. This tumor overexpresses only HER2 [60]. For ER+ or PR+ BCs, to inhibit ER signaling,

endocrine agents can be used as a primary systemic treatment. Trastuzumab and pertuzumab as HER2 antibodies, and lapatinib and neratinib as small-molecule tyrosine kinase inhibitors can be applied to the patients with HER2+ BC [61, 62].

Table 2.1. Molecular subtypes of breast cancer [63]

Molecular Subtypes	*Profile of Biomarkers*	*Prevalence (%)*
Luminal A	ER+ and/or PR+, HER2–, low Ki67	42-59
Luminal B	ER+ and/or PR+, HER2+, or, ER+ and/or PR+, HER2–, high Ki67	6-19
HER2 enriched	ER–, PR–, HER2+	7-12
BL/Triple Negative	ER–, PR–, HER2–	14-20

The type of cancer based on a distinct gene-determining structure in the basal cells that regulate the breast canals is BL BC [64]. BL tumors have ER-negative character and are distinct from ER-positive tumors in a molecular way. TNBCs are similar to BL cancers at approximately 70%, but both terms are not synonymous because they are clinically and histopathologically dissimilar [65].

2.2. Triple Negative Breast Cancer

TNBC is characterized by the lack of HER2 overexpression or gene amplification, and no expression of ER and PR [66]. TNBCs account for about 15 to 20% of all cases of BC and they are associated with high mortality worldwide. Compared to the other types, TNBC is a highly aggressive neoplasm with a strong association with distant recurrence, visceral metastasis and death [67]. It is more common in women under 40 age and among Hispanic or African-American women [4, 68]. Risk of distant relapse of TNBCs is high in the first 3 to 5 years after diagnosis. While the survival rate of first 5 year in TNBC is 70%, it is estimated to be 80% in other subtypes. However, the specific molecular pathophysiology of TNBCs is not yet fully understood [4, 69]. Approximately 20% of patients with TNBC have a BC gene mutation in BRCA1 [70]. Around 70% of TNBCs are in the BL subtype class, and most BL cancers are TN. BL 1, BL 2, immunomodulatory (IM), luminal androgen receptor (LAR), mesenchymal stem-like (MSL), mesenchymal-like (M) and unstable (UNS) are the seven subtypes of TNBC that were identified in a

genomic analysis. Among other types, BL is relevant to the best prognosis. The type of cancer that has a BRCA mutation is usually included in the basal subtype class and tends to be triple negative. Tumors without BRCA1/2 mutations but showing the characteristics of BRCA pathway deficiency are defined as BRCAness [71].

TNBCs are more aggressive types and defined as higher-grade tumors. They mostly found as invasive ductal carcinomas. Moreover, having a large tumor size, lymph node involvement at diagnosis, high proliferative capacity, poor differentiation and high chemosensitivity are the main characteristics of TNBCs. One of the features that distinguish these tumors from other BC subtypes is that they spread to the lungs and brain instead of bone and soft tissues [72-74].

2.2.1. Treatment Options for TNBC

Hormonal or trastuzumab-based therapy cannot be applied to the patients with TNBC due to absence of molecular receptors such as PR, ER and HER2. In addition, the heterogeneity of the disease has been always a challenge for TNBC therapy. Therefore, the only treatment methods available for TNBC are surgery and chemotherapy, either individually or in combination, and radiation therapy. New therapeutic drugs are also being developed which target specific receptors [39].

2.2.1.1. Surgery

TNBC patients are younger than other BC patients, and have higher-grade and aggressive tumors. This does not affect the choice of the type of surgical treatment. There are many studies showing that the possibility of TNBC patients that may choose lumpectomy or mastectomy procedures for surgery [39]. Lumpectomy is a type of surgery to remove only a portion of breast having cancer or abnormal tissue. It is also called as breast-conserving surgery (BCS). On the contrary, mastectomy is a surgical removal of one or both breasts completely to treat breast cancer patients.

The best local treatment for TNBC is surgical excision. In MRI, TNBC usually appears as a unifocal mass lesion. Local and regional recurrence risks of TNBC patients have been reviewed in several reports. It has been shown in some studies that the rate of local recurrence in TNBC is higher than the HER2-negative and hormone receptor-positive subtypes [75]. On the contrary, other reports showed that the rate of local recurrence in

TNBC was lower than the non-basal or non-TNBC subtypes. Furthermore, in TNBC, the regional or locoregional recurrence risk is higher than the other BC subtypes. Despite the fact that the local or regional relapse powerfully effects the quality of life of patients, their impact on outcomes remains unclear [76].

2.2.1.2. Radiation Therapy

As for patients with other BC subgroups, TNBC patients have traditionally been given radiotherapy after mastectomy or BCS. However, there is still controversy [77]. Since TNBC is a highly aggressive and rapidly growing cancer type, radiotherapy after BCS at early stage (T1-2N0) may not have the same effect like mastectomy as in any other BC types [78]. In spite of this, there are also studies showing that the local recurrence risk is reduced and overall survival is increased in TNBC patients receiving radiation therapy after surgery compared to those not receiving radiation therapy [79, 80].

2.2.1.3. Chemotherapy

TNBC is a biologically aggressive cancer type. Although the patients with TNBC respond to the chemotherapy in a better way comparing to the other BC types, its more aggressive character in the metastatic environment lead to poor prognosis [81]. The treatment modalities used for TNBC targets are: taxanes, platinum compunds and anthracycline containing regimens. [82]. Numerous works indicated the advantage of combining new chemotherapy agents with conventional chemotherapeutics such as anthracycline, antimetabolites, platinum agents, new microtubule stabilizing agents and taxanes [83]. Taxanes are the important agents that have activity in TNBC but have not shown a specific impact compared to non-TNBC [84]. Although all alternatives are offered for first-line therapy in TNBC, the generality are the taxanes. A platinum-based regimen, single agent capecitabine, gemcitabine and vinorelbine, and combination of capecitabine and vinorelbine are often used as second-line treatment options. Platinum-based regimens that are mostly recommended for first-line treatment option and the second-lines are carboplatin plus gemcitabine, carboplatin plus paclitaxel and cisplatin plus gemcitabine [39].

TNBC patients with high visceral metastasis rates have an average survival time of seven to thirteen months, and tend to have restricted chemotherapy response. Choosing the

therapeutically active reagents that are likely to provide a significant benefit is essential [85]. Since TNBC is highly heterogeneous, molecular biomarkers need to be identified to foresee the response to specific chemotherapeutics. Thus, the available chemotherapy alternatives and their forward combination strategies with targeted treatments can be developed [86].

2.2.1.4. Targeted Therapy

Approximately 70% of the TNBCs were demonstrated to be BL via identification of gene expression. Nevertheless, a remarkable amount of BL tumors can express HER2, PR or ER and at a minimum another basal molecular receptor [87]. Thus, TNBCs have various mRNA expressions-based subtypes, and they represent a specific histopathological subtype (Table 2.2). Morphology, signaling profiles and discrepancies in mutational phenotype among tumors provide TNBC to be clinically heterogeneous [88, 89].

Basically, there are seven subtypes of TNBC based on the data of gene expression profiling obtained from twenty-one BC data sets [91]. BL1, BL2, LAR, M, MSL and IM are included into these subclasses. These subclasses show different therapeutic responses. In addition, they are also well correlated with pathological complete response (pCR) rates thereafter neoadjuvant chemotherapuetic approach [92].

BL1 tumors have high Ki67 expression and contain DNA-damage response (DDR) and cell cycle genes. These tumors are sensitive to, and respond well to, taxanes (paclitaxel or docetaxel) and antimitotic agents such as DNA-damaging agent cisplatin. The genes of metabolic signaling, proliferation and survival-mediated RTKs are highly found genes in BL2 tumors. M and MSL tumors are in the group rich in expression of growth factor signaling pathway and epithelial-mesenchymal transition (EMT) elements. SRC family kinase and phoshoinositide 3-kinase (PI3K)/mammalian target of rapamycin (mTOR) inhibitors are potential therapeutic agents for these subclasses [91]. LAR tumors are characterized by being enriched for androgen receptor (AR) signaling, steroid synthesis and hormone-regulated signaling pathways. Combination of PI3K and AR (anti-androgen, bicalutamide) targets is effective in this subclass in preclinical models [93]. Lastly, the IM subclass is characterized for T cell functions and immune response-mediated cell signaling with antigen presence. Molecular targeting is very important in TNBC, and

resistance to targeted therapies has to be taken into consideration for an effective TNBC treatment [53].

Table 2.2. Genomic TNBC subtypes and therapeutic targets [40, 53, 90]

TNBC Subtypes	Genetic Abnormalities	Potential Therapeutic Target
BL 1	Proliferation drivers: cell cycle, cell division, DNA damage response (ATR-BRCA pathway)	PARP inhibitors Cisplatin
BL 2	Growth factor and metabolic signal pathways (MET, EGFR, Wnt/β-catenin)	mTOR, inhibitors Growth factor inhibitors
LAR	Hormonal-mediated signaling-androgen receptor gene Luminal gene expression pattern	Anti androgen therapy PI3K inhibitors
IM	Immune cell processes	PDI/PDLI inhibitorsa
M	Cell differentiation Cell motility Growth factor signaling EMT	mTOR inhibitors Growth factor inhibitors Src inhibitors
MSL	Low proliferation Angiogenesis genes	Growth factor inhibitors, mTOR inhibitors, PI3K inhibitors, Antiangiogenic therapy Src antagonist
(UNS)	DNA damage responses and cell proliferation	PARP inhibitors Cisplatin

2.3. Small non-coding RNA

With recent studies, it is known that the percentage of the non-protein coding part of human DNA is 98%. Over the years, researchers regarded to this 98% compartment of the human genome as "junk DNA". Besides that, there was a prevalent idea that the junk was not thrown away, but was stacked away to be used potentially. [94, 95]. Considering DNA discovery milestones, the following developments have been groundbreaking: by J. F. Miescher, the first nucleic acid isolation and specification in 1869, the hypothesis of 'a gene, an enzyme' by E. Tatum and G. Beadle in 1941, the DNA structure description in 1953 by J. Watson and F. Crick, and the completion of the human genome sequencing in 2001. However, with the ENCODE project in 2012, in which the 'junk DNA' was deeply investigated, researchers proved that at a minium 80% part of the human genome is effective in a biological way [96]. Cis/trans regulatory elements, pseudogens, repeat sequences, telomeres and introns have been shown to be section of the junk DNA. Thus, a proper portion of this DNA is transcribed into ncRNA containing functional RNA molecules. Highly abundant transfer RNAs (tRNAs), ribosomal RNAs (rRNAs), small nucleolar RNAs (snoRNAs), microRNAs (miRNAs), siRNAs, small-nuclear RNAs (snRNAs), piwi-interacting RNA (piRNAs) and long ncRNAs are the structures that are included in this class of RNA molecules. In a report, Palazzo and the co-workers forecasted that ncRNAs are comprised of 99% of the total RNA [97]. ncRNAs can be categorized based on their function or length (18–200 nt are small; more than 200 nt are long ncRNA). rRNAs, tRNAs, snoRNAs and snRNAs are called as housekeeping ncRNAs. rRNAs and tRNAs have essential role in mRNA translation, snoRNAs involved in rRNA modification whereas snRNA in splicing [98, 99]. According to the results of studies in the last twenty years, regulatory ncRNA molecules have been shown to play in almost all biological pathways. It has been reported that deregulation of miRNAs, piRNA and tRNA-derived RNA fragments (tRFs), e.g. is associated with many metabolic diseases including cancer [100, 101].

2.3.1. miRNA

Lee, Feinbaum and Ambros described a small ncRNA that regulates mRNA translation through complimentary RNA-RNA interaction for the first time in early 1993 in Caenorhabditis elegans [102]. This molecule is the most frequently studied subclass of

small ncRNA, and it is currently known as miRNA. miRNAs are highly conserved in most eukaryotes and composed of 18–24 nucleotide sequences [103, 104]. These single-stranded RNA molecules take part in the regulation of several gene expressions in eukaryotes [15]. The number of human miRNAs that has been identified so far is more than 2500, and they are available in the miRNA database (miRBase) [105]. About half of the miRNAs are found in delicate genomic regions which induce the cancer risk [106]. It was revealed that miRNAs enable to target numerous of genes (for each miRNA family, on average ∼500) and to regulate more than 30% of fundamental gene expressions [107-109]. These genes are involved in several essential biological processes that are programmed cell death, proliferation, survival, differentiation and invasion [108, 110].

2.3.1.1. Biogenesis of miRNA

miRNAs are highly conserved molecules via evolution, and they are large subtypes of interference RNAs. The target genes of these molecules are regulated in post-transcriptional level by mRNA translation inhibition or mRNA induction degradation as a result of binding of miRNAs to the 3′-UTR of the target mRNAs. This mechanism initiates with transcription of primary-miRNAs (pri-miRNAs) from the protein-coding genes by the activation of type II RNA polymerase enzyme. Pri-miRNAs have a cap at the 5′ end and a poly-A tail at the 3′ end, and they are also like hairpin/stem-loop structures. These pri-miRNAs are transformed to precursor-miRNA (pre-miRNA) by an enzymatic complex that is consisted of RNAse III (called as Drosha) and DGCR8 (a double-strand binding protein). Then, by nuclear receptor exportin 5 activity, pre-miRNA is transferred to the cytoplasm. Double-strand RNA molecule having passenger/guide strands and containing 18-24 base pair is generated by Dicer enzyme action. After the passenger strand is cleavaged, guide strand and argonaute proteins form a complex called the RNA-induced silencing complex (RISC). This complex binds complementarily to the interested mRNA's 3′-UTR side. To occur a perfect binding, the miRNA and the related mRNA sequences should be completely complementary. By this way, the clevage of the target mRNA will occur. If not so, the translation process will be inhibited. Additionally, each miRNA may have more than one target mRNA transcripts. [28, 111, 112].

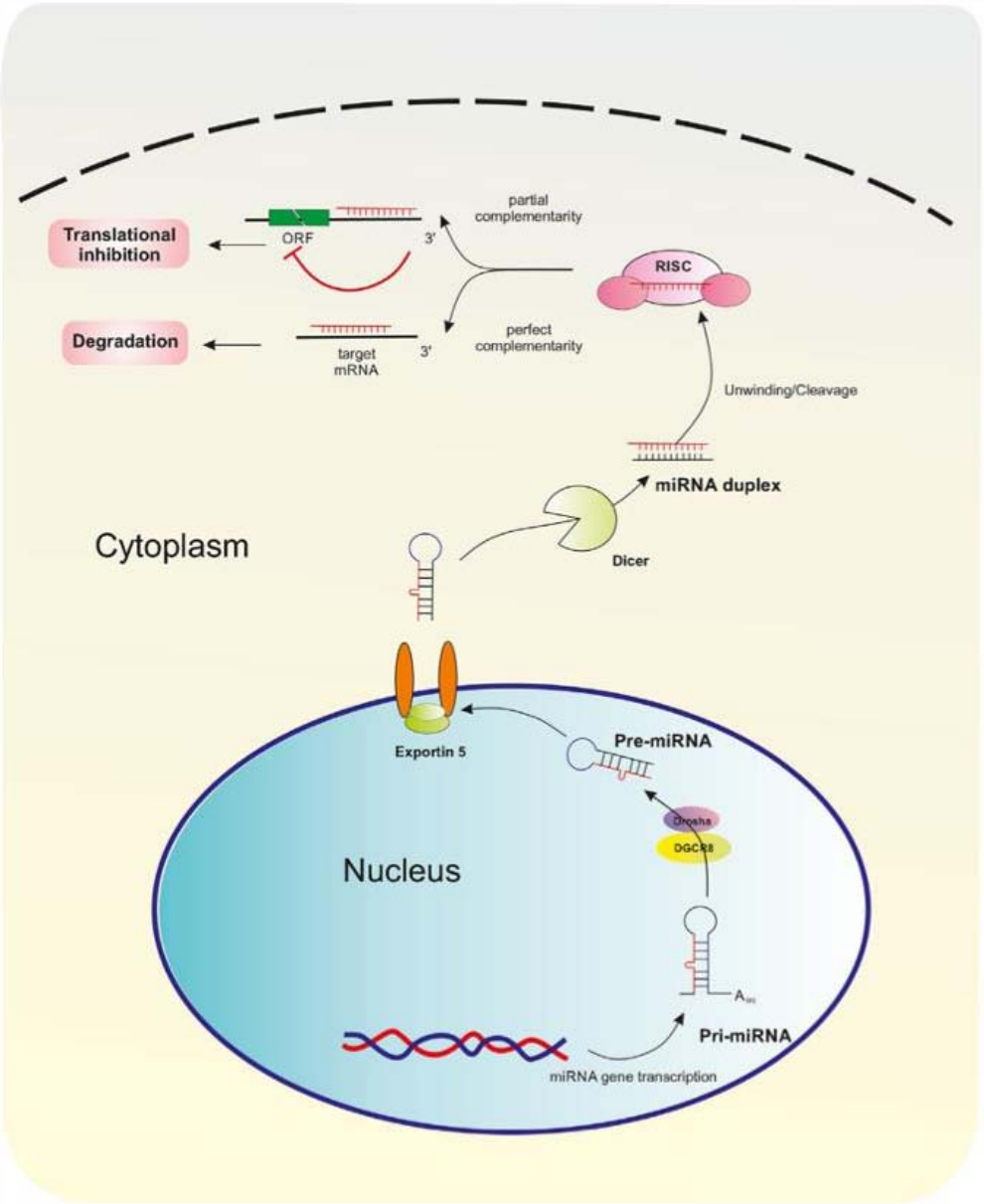

Figure 2.1. The biological mechanism of miRNA [28]

2.3.1.2. The Function of miRNA in Cancer

miRNAs possess significant function in large number of cellular pathways such as differentiation, proliferation, development, cell cycle and apoptosis. Based on a study, it is revealed that miRNAs are commonly found at regions of amplification or heterozygous loss, delicate region, or break-point sites in human cancer [113]. miRNAs can be epigenetically silenced by the activation of histone hypoacetylation or DNA promoter hypermethylation in addition to the genetic and structural alterations. This has been

previously described in hematological malignancies and solid tumors [114, 115]. Data of miRNA expression resulted in that abnormal expression of miRNA is a prevalent event in many tumors [116]. It was concluded by the studies that initiation and progression of many cancer types were related to deregulation of miRNAs [117]. Considering deregulated miRNAs affect the basic features of cancer progression, miRNAs can have functions either as oncogenes (oncogenic miRNAs or oncomiRs) or TS (TS miRNAs). In several cancers, some miRNAs may have both characteristics [12, 118, 119]. The relation between cancer and miRNAs was demonstrated for the first time in a study by Calin and his colleagues. Their group discovered that miR-15 and miR-16 acted as TSs. The miRNAs were deleted and downregulated at 13q14 region in 69% of chronic lymphocytic leukaemia (CLL) patients analyzed [120]. The tumor suppression activities of miR-15 and miR-16 were also proved by further analyses [121]. Various other tumor suppressors including let-7 [122] and miR-34 [123] were also identified.

2.3.1.3. Approaches of miRNA Therapeutics in Cancer

There are two main reasons for using miRNAs as a novel therapeutic approach in the treatment of cancer. First one is the difference of miRNA expression between tumor and normal tissues. Second one is by targeting miRNA expression the cancer phenotype can be altered [124]. The new developments in the field of genetic gain- or- loss-of-function of specific miRNAs and the in vivo results of pharmacological modulation of miRNAs, have made miRNAs promising targets as new generation therapeutics, recently. In miRNA-based therapeutic applications, miRNAs can enable to target more than one gene. This makes them superior comparing to other approaches and allows them to be highly potent in regulating certain cellular process and pathways related to normal and cancerous cell [106]. In most vertebrate species, miRNAs have short sequences and are found as highly conserved. By this means, miRNAs can be easily targeted for therapeutic strategies. Additionally, this also allows the same miRNA compound to be used for preclinical studies and in clinical trials [125, 126].

2.3.1.4. miRNA Replacement Therapy

The function of TS miRNAs is to induce oncogenic protein-coding gene degradation by targeting it. The cancer cells express low level of TS miRNAs and

this plays a role in carcinogenesis or progression of cancer. Therefore, miRNA replacement therapy has rapidly become a novel and promising therapeutic approach for the treatment of cancer [127, 128]. In miRNA replacement strategy, the synthetic oligonucleotides having the same structure and properties with the selected TS miRNA, known as miRNA mimics, are introduced to the cells to overcome the down regulation or loss of this TS miRNA. miRNA mimics are double-strand molecules. As they are administered into the cells, they are converted to a single-strand molecule and regulate their protein-coding genes in the miRNA-like manner. Therefore, miRNA mimics are synthesized possessing several chemical modifications to enhance their cellular internalization and stability [129, 130].

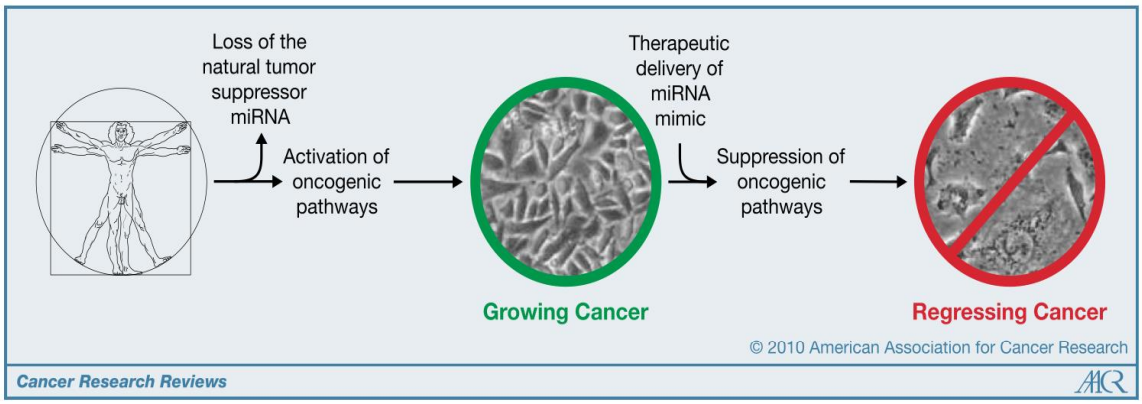

Figure 2.2. miRNA replacement therapy in cancer [128].

2.3.1.5. Challenges in Therapuetic Targeting of miRNAs

The difficulties in cellular uptake and specific in vivo delivery of efficient amount of synthetic miRNA limit the success of the target inhibition by miRNA. Due to rapid degradation of unmodified or "naked" miRNA by cellular or serum nucleases, stability of miRNA therapeutics in tissues and body fluids reduces [131]. In addition, when miRNA is given to systemic administration, it can be easily removed by immune system and excreted by renal filtration. The negative charge of miRNA restricts its cellular internalization since cell membrane is also negatively charged. Since miRNA is a water-soluble molecule, cell penetration becomes difficult by passive diffusion [132]. It was previously reported that the percentage of the uptaken injected dose by the cells is only approximately 0.7% [133]. These drawbacks must be taken into consideration before using miRNA for its maximum therapeutic potential.

2.3.1.6. miRNA Delivery Systems

Because of all these drawbacks in naked miRNA delivery in systemic circulation mentioned above, a delivery system is necessary for an effective treatment [134]. An ideal miRNA delivery system should enable to (a) protect miRNA from nuclease degradation and from being excreted by renal filtration in systemic circulation; (b) accumulate in the target tissue; (c) pass cellular membrane via endocytosis; (d) escape from endosome and (e) release safely its therapeutic cargo [135, 136]. At the same time, this delivery system should be non-toxic, non-immunogenic, biocompatible and biodegradable [137]. Viral vectors and non-viral vectors are the common carriers to deliver the miRNA.

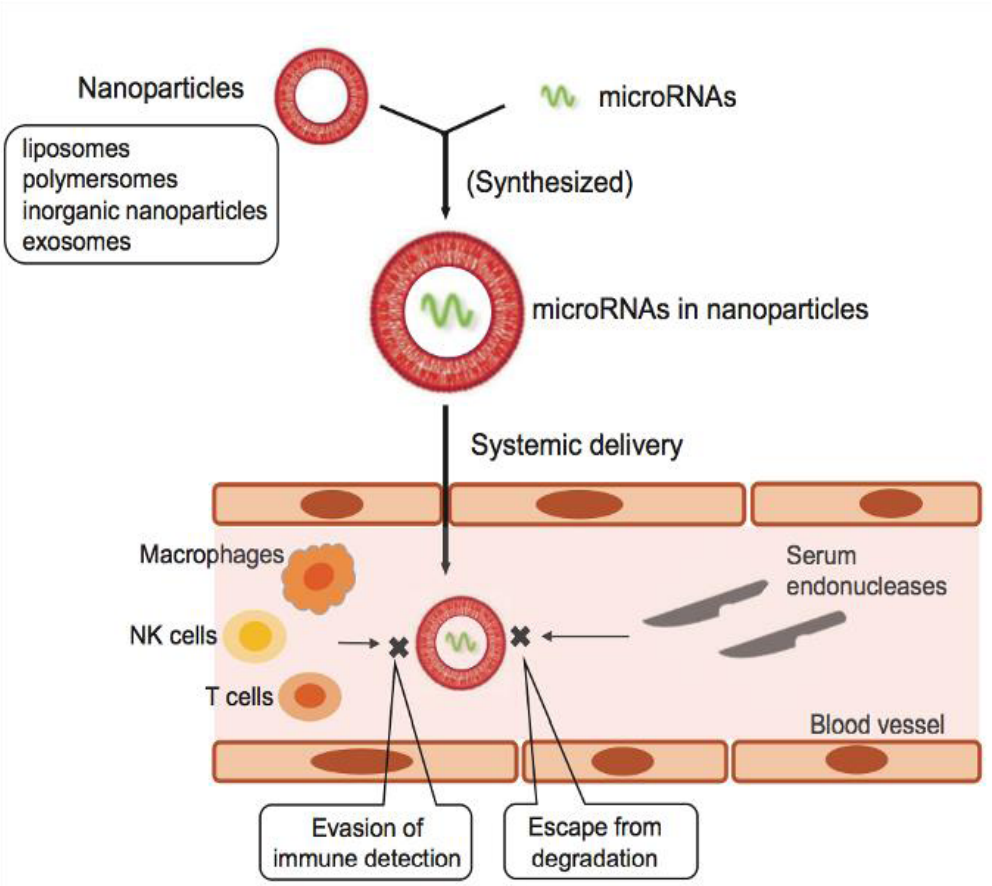

Figure 2.3. miRNA delivery via nanoparticles [118].

2.3.1.6.1. Viral Delivery Systems

Viral vectors are one of the first delivery systems for nucleic acid delivery to the target cells. Many researchers have been using miRNA encoding and genetically modified

viruses including lentiviruses [138-140], adenoviruses [141, 142], and adeno-associated viruses (AAVs) [143-145] in several gene silencing approaches [146]. These viruses have high ability to effectively transfer the genetic material into the nucleus of the target cells. Owing to their high transduction efficiency, in almost 70% of the clinical trials in gene therapy, the application of the viral vectors was shown [33]. However, using viral vectors limits their clinical applications by being expensive and causing mutagenesis (especially lentiviruses) and immunogenicity (especially adenoviruses) [147-149].

2.3.1.6.2. Non-viral Delivery Systems

The drawbacks of the viral vectors make the non-viral ones as alternative delivery systems, although transfection of the non-viral ones is not efficient as the viral ones. Non-viral vectors have low immunogenicity and cost-effective process with large-scale synthesis. Although a non-viral delivery system is highly potent in vitro, when it comes to in vivo because of the problems such as toxicity concerns, non-specific uptake, low pharmacokinetic profiles and immune responses, this system is generally failed [150]. Therefore, for clinical use, there is an urgent need to develop proper miRNA delivery systems that can be able to overcome all known issues that previously reported. The vectors based on lipids, polymers and inorganic particles are the most used non-viral vectors for in vivo applications [151, 152]. These nano-delivery vehicles can be easily functionalized with targeting ligands and by (PEG)ylation to enable specific delivery and to increase safe duration time in serum and body fluids, respectively [33]. To design an effective nanoparticle delivery systems, size and surface charge characteristics of the nanoparticles should be consired [153]. Size is important because the mono-nuclear phagocyte system can entrap the nano-delivery vehicles larger than 100 nm while the renal filtration process can eliminate the ones smaller than 5-6 nm [154]. The optimum and ideal size that nanoparticles should have has been discussed in years by several groups. Bedi et al. [155] reported that size range between 10-50 nm is the most proper one whereas according to Wang et al. [154] nanodelivery systems shoud be 10-100 nm. Since cellular uptake and transfection efficiency are high with the nanoparticles having a size smaller than 100 nm, some reseraches also suggested that ideal nanoparticle size range should be 20-100 nm [137, 153]. In addition to this, it was also indicated in a study conducted by Hirota and Terada that the cellular uptake depends on the cell type, and especially for cancer cells, nanoparticles possessing 50 nm are preferred [156]. At least most of the

researchers agree that an ideal delivery system should be no larger than 200 nm for a maximum cellular uptake [157-160].

Another parameter for an efficient delivery system that is important for cellular internalization is surface charge. The zeta potential value indicates the surface charges of the particles. It shows the measurement of the magnitude of electrostatic repulsive interaction between particles. Particles with higher zeta potential value exhibit greater stability [161]. Positively charged delivery systems are favored since they can be able to pass more through the negatively charged cellular membrane via electrostatic interactions in compared to negatively charged ones [160]. A varitery of nanoparticle delivery systems were developed and characterized for biomedical applications. Figure 2.4 shows several miRNA delivery systems.

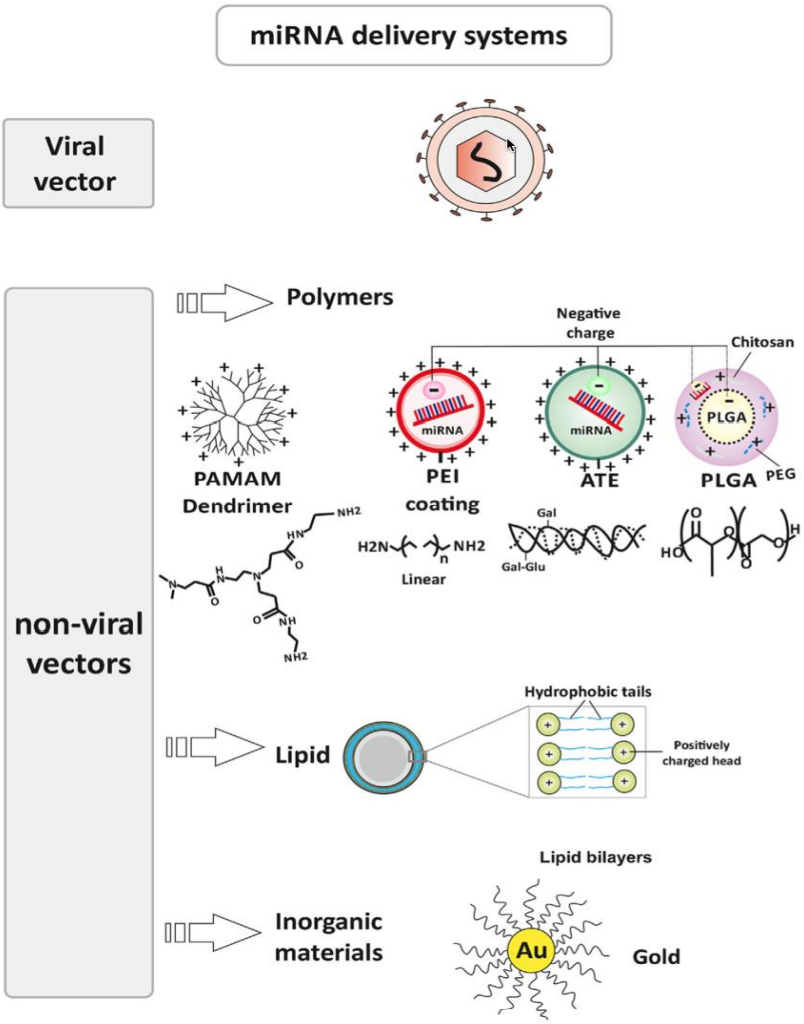

Figure 2.4. Various vector types for miRNA transfection [28]

2.4. Superparamagnetic Iron Oxide Nanoparticles

SPIONs are promising materials in cancer therapy and diagnosis among other nanoparticle types with their superparamagnetic and surface modification characteristics. IONs having the size range between 1-20 nm tend to become superparamagnetic with a single domain [162]. When the magnetic field is removed, SPIONs do not show ferromagnetic properties on the contrary to multiple-domain ferromagnetic structures which keep their magnetism although the magnetic field is switched off [163]. In recent years, the multifunctional features of SPIONs have provided them to be used in several application areas of cancer therapeutics such as MRI [164], drug and gene delivery [165, 166] and hyperthermia [167]. In addition to this, with their biocompatible and biodegradable properties, SPIONs are also used in magnetofection [168] and cell separation [169]. SPIONs are found mostly in magnetite form, Fe_3O_4, and they are converted to maghemite, γ-Fe_2O_3, when they are interacted with oxygen. In body, the metabolism of SPIONs is easy. By proteins such as ferritin, transferritin and hemosiderin they can be transported, and for later use, they can be stored in iron reserves of the body. The best advantage of SPIONs for targeted therapies is that they can be directed to the targeted area by applying an external magnetic field. This enables to avoid undesired side effects, a decrease in drug wastage, and a reduction in the drug release frequency [170]. The surface of SPIONs can be functionalized with several peptides, antibodies, receptors or ligands for specific targeting and to release their therapeutic payload as a controlled release manner [171].

Besides being non-toxic and stable at physiological pH for biomedical applications, for especially cancer studies SPIONs should have :

- High magnetization
- Small size and optimized surface charge values
- Proper surface coating to avoid from aggregation and possible toxicity
- Capability to react with various functional groups, receptors and drugs or genes
- High ability of targeting and drug delivery
- Increased high life
- Contrast enhancement characteristics for malignant cell and tissue imaging
- Potential to respond to magnetic field, heat or pH [165, 172].

2.4.1. Surface Modifications of SPIONs

SPIONs without any modification tend to aggregate, and by this way lose their superparamagnetical behavoirs in biological solutions. In addition, these large sized aggregates may block the capillary of the body when injected. Therefore, modifying the surface of SPIONs is essential. In general, to form stable colloids stabilizing the SPIONs by electrostatic or steric repulsion, organic or inorganic molecules are used. For in vivo use of SPIONs, the surface coating is also important to enhance the biocompability. There are researches showing that after cellular uptake of bare SPIONs caused cell death whereas the cytotoxicity reduced when SPIONs were coated with bovine serum albumin (BSA), pullulan or dextran [173, 174]. For targeting specific cells or tissues or for binding to therapeutic drug or genes, functionalization is also crucial. Biomolecules like peptides, monoclonal antibodies (mAbs), enzymes or oligonucleotides can be used to attach to the specific functional groups on the coating material [175].

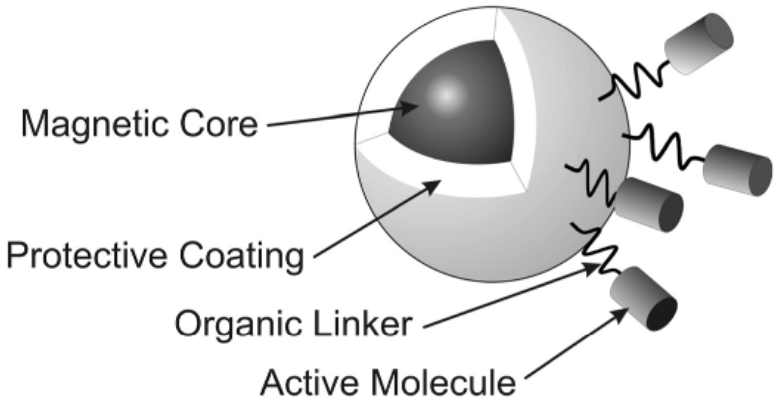

Figure 2.5. A design of the iron oxide nanoparticle for biomedical applications [176]

A functional ION contains several constituents: a magnetically responsive core, coating material, and organic linker/active molecule. The active molecule varies according to the specific application to be used. Figure 2.5 exhibits a typical schema of ION for biomedical applications [176].

2.5. miR-329

The location of miR-329 is on 14q32.3. It has been revealed by numerous studies that variety of cancer types including glioma [23, 177], cervical [178-180], melanoma [22], neuroblastoma [181], osteosarcoma [182], head and neck squamous cell carcinoma [183], gastric cancer [184, 185], colorectal [186-188], thyroid cancer [189], pancreatic cancer [25], bile duct cancer [190] or cholangiocarcinoma [191], hepatocellular cancer (HCC) [192], non-small cell lung cancer [193] and breast cancer [26, 194] exhibit dysregulated miR-329 expressing profile and it is inversely correlated with pathological characteristics. Thus far, these reports indicated that miR-329 suppressed cancer development by targeting several genes that contribute cancer progression mechanisms. For instance, in gastric cancer, T lymphoma invasion and metastasis 1 (TIAM1) gene was identified as a potential target for miR-329 [184]. In pancreatic cancer, miR-329 mediates anticancer activity regulating growth factor receptor-bound protein 2 (GRB2)/pERK signaling pathway [25]. In 2013, Wang et al. showed an inhibition in angiogenesis by miR-329 activity through interaction with CD146, which is an entdothelial biomarker [195]. Thus far, the function of miR-329 was investigated only in PR/ER(+) and HER2(-) BC by a previous work [26]. In the study, p130Cas/BC anti-estrogen resistance 1, which belongs to the Cas (Crk-associated substrate) family of adaptor proteins was demonstrated to be as a direct target for miR-329 in MCF-7 cells. p130Cas is a key molecule in tyrosine kinase-based signaling, and thereby it is related with migration, cell cycle, adhesion, apoptosis, cancer progression and development. The study concluded that forced expression of miR-329 suppressed the proliferation/migration/invasion of the cells and the tumor growth in mice by inhibiting p130Cas activity. Since in BC, overexpression of p130Cas is related to resistance to tamoxifen and poor prognosis, suppressing p130Cas by miR-329 not only may be a promising therapeutic approach but also may be a good option for combination with tamoxifen. However, the role and the mechanism of miR-329 in TNBC was not elucidated thus far and they still remain unclear.

2.6. eEF2K

eEF2K is an atypical, Ca^{2+}/calmodulin-dependent protein, and belongs to the α-kinase family. eEF2K regulates protein synthesis by phosphorylating and inactivating eEF2 (at Thr 56), that provides the ribosome go through the mRNAs at the elongation step of

protein synthesis process [196-198]. The activation of eEF2K occurs in hypoxia, nutrient deprivation, energy depletion conditions that may be observed in poorly-vascularised tumors. A number of studies indicate that eEF2K promotes cancer cell survival under such stress conditions and exhibits cytoprotective effects. Under normal conditions, eEF2K is not essential for cells and this makes eEF2K as a potential target for solid tumors treatment [199]. Cancer cells require high levels of protein synthesis and metabolic energy to enable the cells to grow and proliferate rapidly. However, since tumors have limited nutrient, the cells thereby adapt to nutrient deprivation for survival. In many cancers, tumor cells highly express eEF2K, and this makes eEF2K as an advantageous molecule for cancer cells to survive [199]. eEF2K is related to poor patient survival, and known to overexpressed in several solid cancers such as glioblastoma, colon and pancreatic cancer [200-203]. In recent studies, eEF2K was demonstrated to highly overexpressed in TNBC and to promote TNBC cell proliferation, migration, invasion [204]. It was also reported that eEF2K is involved in TNBC progression and tumorigenesis by regulating c-myc, cyclin D1, PI3K/Akt, Src/Focal Adhesion Kinase (FAK) and insulin-like growth factor receptor (IGFR) signaling pathways. In addition, eEF2K plays an important role in chemotherapy resistance in TNBC cells since eEF2K inhibition by siRNA led to sensitize tumors to doxorubicin [205, 206]. Therefore, strategies regulating eEF2K activity may contribute to develop novel treatment options for TNBC since therapeutic suppression of eEF2K results in tumor growth inhibition.

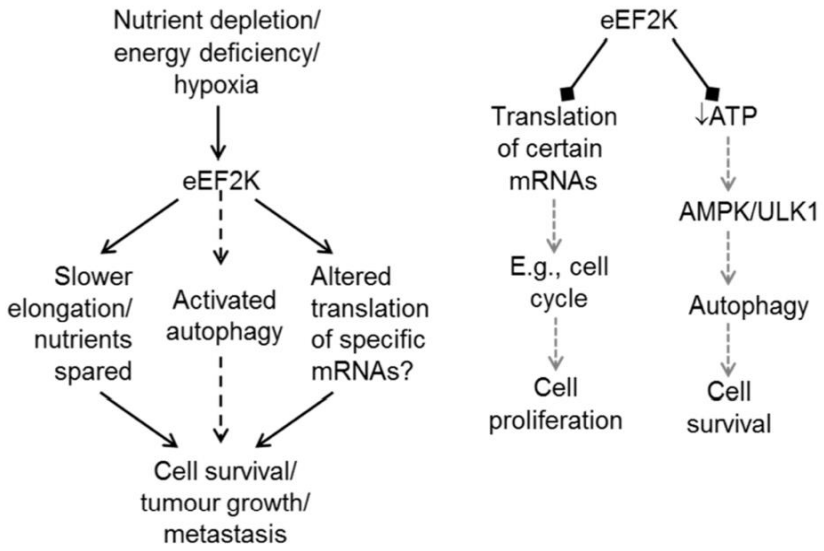

Figure 2.6. The functions of eEF2K in cancer cells [199]

2.7. AXL

AXL is a member of the RTK family which is called TAM (TYRO3, AXL, MER). It was first identified in cells isolated from patients with chronic myelogenous leukemia [207]. Growth arrest specific 6 (GAS6) is the ligand of AXL, and their interaction gives rise to dimerization of TAM receptors and to activate a variety of cellular processes that regulate cell proliferation, survival, migration, invasion, autophagy, drug resistance and angiogenesis [208-212]. Important functions in cancer cells and high expression levels in many cancers including ovarian [213], prostate [214], lung [215], pancreas [210] and breast [212] allow AXL to be considered as oncogenic. Particularly, a remarkable relation was reported between AXL protein and tumor stage in BC patients [216]. In a study conducted in 2011, Mackiewicz and co-workers indicated that the expression of miR-34a was 3-fold low in MDA-MB-231 cells (TNBC cells) than ER(+) MCF-7 cells and HER2(+) SK-BR-3 breast cancer cells. They identified AXL as a target mRNA of miR-34a by using multiple miRNA/target prediction algorithms and confirmed binding of miR-34a to the 3'UTR of AXL by luciferase reporter assays. The studies of miR-34a overexpression in TNBC cells resulted in an inhibited level of AXL and thereby cell migration. An inverse correlation was also obtained between miR-34a and AXL expression in TNBC cell lines and patients [217]. Taken all together, targeting strategies against AXL in patients with TNBC holds great promise to achieve an effective outcome.

3. MATERIALS AND METHODS

3.1. Production of PLL Modified Sericin-Coated SPIONs

3.1.1. Purification of Sericin From Silk Cocoons

2 g of Bombyx mori cocoons and 50 ml of 0.1 M sodium carbonate (Na_2CO_3) (Sigma-Aldrich) were mixed. The solution was boiled by autoclaving for 20 min at 110°C. After that, the solution part was taken and left in dialysis membrane (12 kDa) (Sigma-Aldrich) for 24 h. Next day, the solution was centrifuged at 14000 rpm for 30 min two times and the impurities that were deposited at the bottom were removed each time. Thus, sericin solution was obtained [218].

3.1.2. Production of SPIONs

SPIONs were produced by a modified procedure using a co-precipitation method [219-221]. First of all, all glass materials were incubated in aqua regia (65% nitric acid (HNO_3) (Merck) and 37% hydrochloric acid (HCl (Merck) at a molar ratio of 1:3 for 1 h and washed with deionized water (DI) prior to use. 800 ml of DI water was boiled and stirred for 1 h to remove all dissolved oxygen, and this oxygen-free water was used during the entire synthesis. The molar ratio of iron II chloride tetrahydrate ($FeCl_2.4H_2O$) (Merck) and iron III chloride hexahydrate ($FeCl_3.6H_2O$) (Merck) that were used was 1:2. 1.26 g and 3.24 g of these chemicals were weighed, respectively, and both were dissolved in 10 ml boiled DI water, separately. Then, two solutions were added simultaneously to the flask containing 70 ml of boiling DI water. The mixture was stirred for 5 min on a magnetic stirrer and heated to 85°C. Ammonia (NH_3) solution (Merck) was then added dropwise to the boiling solution until the pH of the solution reached to 9.3-9.4. The color of the solution turned to black which indicated the co-precipitation reaction had started. To complete the reaction, the solution in the flask was refluxed at 90°C for 1 h. Then, to remove the excess NH_3, the supernatant part of the iron oxide solution was decanted using a strong magnet, and the particles were washed two times with DI water. 30 ml of 2 M HNO_3 solution was added onto the pellet, and the mixture was stirred for 10 min. Then, the supernatant was removed, and 90 ml of DI water was added onto the pellet. The resulting solution was dialysed for two days against a 0.01 M HNO_3 solution. The obtained SPION solution was then passed through nitrogen gas, and stored at 4°C until use. For further size-size distributions and zeta potential measurement analyses, the solution was homogenized for 10 min, and SPIONs were diluted in DI water to eliminate aggregation.

3.1.3. Modifying SPIONs with APTES

20 ml of SPION solution as forementioned was placed in a flask, and to this solution 2.2 ml of (3-Aminopropyl)triethoxysilane (APTES) (Sigma-Aldrich) was added dropwise having a final concentration of APTES in the mixture as 10% (v/v). The resulting solution was then refluxed at 120°C for 3 h under vigorous magnetic stirring. Then, APTES-modified SPIONs were collected by washing with DI water [222]. Thus, amine-functionalized SPIONs were synthesized.

3.1.4. Production of Sericin-SPIONs

To activate the –COOH groups of sericin, 20 µl of 50 mM N-(3-Dimethylaminopropyl)-N′-ethylcarbodiimide hydrochloride (EDC-HCl) (Applichem Biochemica GmbH) (prepared in 1 ml phosphate-buffered saline (PBS, PAN Biotech)) and 20 µl of 15 mM *N*-Hydroxysuccinimide (NHS) (Sigma-Aldrich) (prepared in 1 ml PBS) were added to 2 ml sericin solution which mentioned as above. At room temperature, the obtained solution was stirred for 30 min. Then, 1 ml APTES-modified SPION solution was added dropwise to the sericin solution and the mixture was stirred for 1 h. The resulting suspension was centrifuged at 12000 rpm for 15 min to remove the unreacted compounds [223]. Sericin-coated SPIONs were thus obtained.

3.1.5. Production of PLL Modified Sericin-SPIONs

Sericin-coated SPIONs were modified with PLL to gain positive moieties prior to miRNA interaction. For this, 500 µl PLL solution (0.1% in H_2O, Sigma-Aldrich) was added to the nanoparticles and the mixture was left for stirring for 2 h on a rotator at room temperature. The resulting suspension was centrifuged at 12000 rpm for 15 min to remove the unreacted compounds. PLL/Sericin-coated SPIONs were thus obtained.

3.2. Physicochemical Characterizations

3.2.1. FTIR Analysis

Physicochemical characterization analyses of all synthesized samples were performed using a Nicolet iS 50 Fourier Transform Infrared Spectroscopy (FTIR). All spectra from 500 to 4000 cm^{-1} wave number range in transmission mode were recorded with a 4 cm^{-1} resolution.

3.2.2. Dynamic Light Scattering (DLS) and Morphological Characterizations

Size-size distributions and polydispersity index (PDI) of the nanoparticles were analyzed by DLS using a Zetasizer (Malvern 3000, UK). Surface charge of the nanoparticles was also measured by using a Zetasizer. Prior to analysis, nanoparticles were diluted with DI water, and all measurements were carried out at 25°C in triplicate. TEM (JEOL JEM-1220) was used to determine the precise morphology of the nanoparticles.

3.2.3. Determination of Magnetic Properties of The Nanoparticles

Magnetic properties of SPIONs and PLL/Ser-SPIONs were determined using electron spin resonance (ESR) method via a Bruker EMX 131 X-band ESR spectrometer. The samples were placed between the poles of the electromagnet, whose cavity was homogeneous and whose value could change linearly, forming an external magnetic field. ESR spectra was drawn as the first derivative of the absorption curve by keeping the microwave frequency constant at 9.3 GHz and changing the magnetic field.

3.3. In vitro Degradation and Stability of The Nanoparticles

Produced PLL/Ser-SPIONs (MNPs-magnetic nanoparticles) were also tested for their in vitro degradation profiles. For this purpose, the nanoparticles were placed into 15 ml tubes with PBS (pH:7.4 and pH:5.5) and lysozyme (0.07 mg/ml), and they were incubated at 37°C with gentle shaking (100 rpm) for two weeks. The turbidity of the nanoparticles was measured at certain time points using a Lovibond Checkit turbidity meter (Tintometer, Germany). The lysozyme degradation was reflected as percentage of mass remaining in nanoparticles [224]. The mass remaining (%) was calculated by comparing the measurements of initial turbidity and the turbidity at a certain time.

To investigate the stability of the nanoparticles, Ser-SPIONs and PLL/Ser-SPIONs were placed into 15 ml tubes with PBS at 7.4, and storaged at 4°C. The turbidity measurements of the nanoparticles were carried out for one month. All measurements were performed in triplicate.

3.4. Determination of Binding Efficiency (%)

For the binding studies of MNPs and miR-329, firstly 100 μg/ml of MNPs in RNAse-free water and miR-329 (hsa-329-3p, Qiagen) at different concentrations (25 nM, 50 nM and 100 nM) in nuclease-free water were prepared. The solutions were gently mixed and incubated at room temperature for 1 h. After incubation, the MNPs-miR 329

suspensions were centrifuged 3 times at 12000 rpm for 10 min. Supernatants were collected after each centrifuge step to meausure the amount of unbound miRNA. Collected samples were further analyzed via a fluorometric method using Quant-iT™ RiboGreen® RNA Assay Kit (Thermo Fisher Scientific) as described below.

The binding efficiency (BE) (%) were calculated according to the following equations:

$$BE(\%) = \frac{(the\ amount\ of\ added\ miRNA - the\ amounf\ of\ free\ miRNA\ in\ supernatant)}{the\ amount\ of\ added\ miRNA} \text{x}100$$

3.5. In vitro Release Kinetics

In vitro release behaviour of miR-329 from MNPs was investigated. MNPs-miR 329 samples were prepared as described above, and placed in mini-centrifuge tubes in PBS solution (pH 7.4). The tubes were put in a water bath shaker at 37°C. At certain time intervals, 100 µl of nanoparticle-miR suspensions were collected and same amount of PBS was added onto the samples each time. Collected samples were further analyzed via a fluorometric method using Quant-iT™ RiboGreen® RNA Assay Kit as described below.

3.5.1. Quant-iT™ RiboGreen® RNA Assay

To calculate miRNA binding efficiency and to determine miRNA release kinetics, Quant-iT™ RiboGreen® RNA Assay Kit was used according to the manufacturer's instructions. The Ribogreen fluorescent dye in the kit content allows to bind only RNA samples, and this structure can be able to be measured by spectrofluorometry. The supernatants, collected from the assays for the determination of binding efficiency and in vitro release kinetics, were mixed with the Ribogreen fluorescent dye. The RNA standards, another kit content, were prepared, and these solutions were also mixed with the dye. The fluorometric intensity of the all samples was measured by a spectrofluorometer (TECAN, Switzerland) in 96-well plates for fluorescence-based assays (black walled, clear bottom) (Invitrogen). Calibration curve was generated based on the fluorometric intensity versus the concentrations of the standards. The amount of unbound and released miRNA in the samples was calculated by using the equation obtained from this calibration curve. The

measurements were conducted at 478 nm excitation wavelenght and 520 nm emission wavelenght.

3.6. Intracellular Localization of The MNPs

Intracellular uptake and localization of miR-control loaded MNPs were investigated using a JEM 1010 TEM (JEOL, Peabody, MA, USA). For this purpose, MDA-MB-231 cells (1×10^5 cells/well) were growth in 6-well plates. Next day, miR-control and MNPs were interacted and added to the wells. Then, the cells were incubated for another 24 h. The cells were then gently washed three times with PBS and were fixed. Images were taken using AMT Imaging System (Advanced Microscopy Techniques Corp, USA).

3.7. Confocal Microscopy Analysis

Confocal microscopy analysis was performed in order to monitorize the cellular uptake of the MNPs. MDA-MB-231 cells (5×10^4 cells/ml) were growth in the chambers of Nunc™ Lab-Tek™ Chambered Coverglass (Thermo Fisher Scientific) for 24 h. MNPs were interacted with AllStars Negative siRNA labeled with Alexa Flour 555 and AllStars Negative siRNA without any labeling (Qiagen), for 1 h at dark and room temperature. Then, the cells and the MNPs were incubated for 3 h at 37°C in 5% CO_2-containing incubator. At the end of 3 h, the cells were gently washed three times with PBS. Hoechst 33342 solution (Thermo Fisher Scientific) mixed with cell culture media was added onto cells. After 30 min of incubation, cell images were taken by a Nikon Eclipse T*i* Confocal Microscope. HiPerFect, a commercially available transfection reagent (Qiagen), treated cells were also used as a positive control.

3.8. Preparation of The Cells

TNBC cell lines; MDA-MB-231, MDA-MB-436 and BT-20 (American Type Culture Collection (ATCC) were cultured in Dulbecco's Modified Eagle's Medium (DMEM/F12) (Corning) supplemented with 10% Fetal Bovine Serum (FBS) (Corning) and 1% penicillin/streptomycin (Corning) in 75 cm^3 sterile flasks. The culture was maintained in sterile conditions at 37°C in 5% CO_2-containing incubator. Proliferation of cells on flask surface was examined microscopically every 24 hours for fungal and bacterial contamination. When the cells had 80-90% confluency, they were passaged by treatment with Trypsin-Ethylenediaminetetraacetic acid (EDTA) (0.25%, phenol red, Thermo-Fisher).

3.9. Transfection of The Cells with miRNA Mimics and siRNAs

Hsa-miR-329-3p mimic (5'-AACACACCUGGUUAACCUCUUU-3'), miRNA mimic negative control (Ambion, Life Technologies) and EF2K siRNA, AXL siRNA, negative control siRNA (Sigma-Aldrich) were received as lyophilized and diluted with nuclease-free water (Qiagen) reaching a final stock concentration of 50 μM and 100 μM for miRNAs and siRNAs, respectively. HiPerFect, a transfection reagent consisting of blend of cationic and neutral lipids, was used as a positive control. Prior to cell transfection, miR-329, miR-control, eEF2K and AXL siRNA, control siRNA and HiPerFect solutions at desired concentrations were separately prepared using FBS-free medium. Then, the solutions were mixed, gently pipetted and then incubated with either MNPs or HiPerFect solutions at room temperature. After 6 h of transfection, to each well FBS was added reaching a final percentage as 10% and the medium maintained until the analysis.

3.10. miRNA Reverse Transcription and qPCR Analyses

3.10.1. Total RNA Isolation

The expression levels of hsa-miR-329-3p in several non-treated breast cancer cells and in non-cancerous Human Mammary Epithelial Cells (HMEC) were determined. For qPRC anaylsis, first, total RNA of all samples was isolated. For this, cells of each sample were collected into mini centrifuge tubes adding 1 ml Trizol (Ambion, Life Technologies). 200 μl of chloroform (Fisher Scientific) was added and each tube was vigorously vortexed for 15 sec then incubated for 2 min at room temperature. The samples were then centrifuged at 8800 rpm at 4°C for 15 min. The upper phase of the solution was placed in a new tube and 500 μl of 100% isopropanol (Fisher Scientific) was added onto it. After mixing gently, the mixtures were incubated for 10 min at room temperature. Furthermore, the samples were centrifuged at 8800 rpm at 4°C for 10 min. Supernatants were removed and only RNA pellets were left in the tubes. The pellet was washed with 1 ml 75% ethanol (Decon Labs, Inc) and was vortexed briefly, then the sample was centrifuged at 6500 rpm for 5 min. Supernatant was removed and the pellet was left for air drying for 5-15 min. Moreover, 50 μl nuclease-free water (Thermo Fisher Scientific) was added onto the pellet and the sample was incubated at 60°C for 15 min. By this way, total RNA of each sample was isolated.

3.10.2. cDNA Synthesis

The purity and concentration of the obtained RNA were measured spectrophotometrically using a Nanodrop (NanoDrop 1000 Thermo Scientific). 1 µg from each sample was calculated accordingly. qScript microRNA cDNA Synthesis Kit (Quanta BioSciences) was used based on the supplier's instructions for converting RNA samples to complementary DNA (cDNA). For this, first, Poly(A) tailing reaction was followed as below:

Component	**Volume**
Poly(A) Tailing Buffer (5X)	2 µl
Poly(A) Polymerase	1 µl
RNA (1 µg)	up to 7 µl
Final Volume	10 µl

The components were added to a 0.2 ml PCR tube and the mixtures were vortexed gently and centrifuged briefly. The following reaction conditions were used as: 37°C for 60 min and 70°C for 5 min (T100 Thermal Cycler, Bio-Rad) Then, First-Strand cDNA synthesis reaction was setup as follows:

Component	**Volume**
Poly(A) Tailing Reaction	10 µl
microRNA cDNA ReactionaMix	9 µl
qScript Reverse Transcriptase	1 µl
Final Volume	20 µl

After gently vortexing and briefly centrifuging the tubes, the samples were allowed the reaction at following conditions: 42°C for 20 min and 85°C for 5 min. By this way, cDNA for each sample was obtained and the samples were diluted with 40 µl nuclease-free water prior to qRT-PCR.

3.10.3. RT-qPCR

Real-time SYBR Green RT-qPCR was carried out using PerfeCta microRNA Assay Kit (Quanta BioSciences) according to the supplier's directions. For each RT-qPCR reaction following components were added to 384-well PCR plates (Fisher Scientific):

Component	**Volume**
PerfeCta SYBR Green SuperMix (2X)	6.25 µl
PerfeCta microRNA Assay Primer (10 µM)	0.3 µl
PerfeCta Universal PCR Primer (10 µM)	0.3 µl
Nuclease-free water	1.65 µl
cDNA	4 µl
Final Volume	12.5 µl

The protocol conditions were followed as: Pre-incubation/activation: 95°C for 2 min, PCR (40 cycles) Denature: 95°C for 5 sec and Anneal: 60°C for 30 sec. The expression levels of miR-329 were normalized to the level of an endogenous control, U6 snRNA (Qiagen). The relative expression levels were determined using the comparative threshold cycle ($2^{-\Delta\Delta Ct}$) method via CFX384 Real Time System (Bio-Rad).

3.11. Cell Proliferation Assays

3.11.1. MTT Test

The biocompatibility of the nanoparticles on L929 cells was tested via 3-(4,5-dimethylthiazol-2-yl)-2,5-diphenyltetrazolium bromide (MTT) assay. For this, L929 cells were grown in Eagle's Minimum Essential Medium (EMEM) containing 10% FBS and

1% penicillin–streptomycin at 37°C and 5% CO_2 conditions. The cells were seeded in 96-well plates at a density of 1250 cells per well and incubated for 24 h. Next day, produced SPIONs, APTES-SPIONs, Ser-SPIONs and PLL/Ser-SPIONs were suspended in EMEM reaching a final concentration of 5 µg/ml, 25 µg/ml and 100 µg/ml. Cells were treated with the nanoparticles for 24 and 48 h. At the end of incubation times, the cell medium was removed and MTT solution (5 mg/ml in PBS) was added onto cells. After 4 h of incubation at 37°C and 5% CO_2, the well content was replaced with isopropanol-HCl mixture to dissolve the formazan crystals. Absorbance measurement of each well was conducted by reading the plates at 570 nm using ELISA reader (iMark Microplate Reader, Bio-Rad).

The cell viabilities were calculated based on the equation below:

$$\text{Cell viability (\%)} = \frac{A570\ (sample)}{A570\ (control)} \times 100$$

Each group's cell viability was normalized to the control, which is defined as 100%. Each sample group was tested in sextuplicate wells.

3.11.2. MTS Test

(3-(4,5-dimethylthiazol-2-yl)-5-(3-carboxymethoxyphenyl)-2-(4-sulfophenyl)-2H-tetrazolium) (MTS) cell proliferation assay was also conducted. This is a colorimetric test for quantification of viable cells. In this method, NAD(P)H-dependent dehydrogenase enzymes of viable cells reduce MTS tetrazolium compound in the presence of phenazine methosulfate (PMS) into a colored formazan product that has an absorbance maximum at 490 nm. For this assay, TNBC cells (1250 cells/well) were seeded into 96-well plates and incubated overnight. Next day, the cells treated with various concentrations of bare PLL/Ser-SPIONs and miR-329 (25 nM and 50 nM) loaded PLL/Ser-SPIONs or HiPerFect for 5 days. At the end of the incubation time, MTS and PMS (19:1 v/v) solutions were mixed well and 20 µl of the mixture was pipetted onto each well at dark. The absorbance of each well was measured using Elisa Reader.

3.11.3. Colony Formation Assay

The effect of bare nanoparticles (at various concentrations), miRNA mimics (using HiPerFect or MNPs) and siRNAs (using HiPerFect) on TNBC cell clonogenicity was

evaluated via colony formation assay. 300 cells/ml were seeded into 24-well plates and the plates were incubated for 2 days for cell attachment. The cells were transfected with the experimental groups and cultured for 12 days. After the incubation time, the colonies in each well were stained with crystal violet (Sigma-Aldrich) and subsequently washed with DI.

3.12. Wound Healing Assay

To evaluate motility and migration of the cells, a wound healing assay was conducted. TNBC cells at a density of 1.25×10^5 cells/well were seeded into 6-well plates. After 24 h incubation, the cells were interacted with 100 nM of miRNA mimics or siRNAs (using MNPs or HiPerFect) for 48 h. Then, the bottom of each well was stracted straightly using a 200 µl sterile pipette tip (time 0). After replacing the medium with the fresh one, cell images were taken using a phase contrast microscope (Nikon Eclipse TE-200-U). The cultures were maintened until time point of 24 h and 48 h, and the images were taken at those times as well.

3.13. Invasion Assay

The invasion assay was performed in order to analyze the invading capability of the cells after the miRNA mimics and siRNA treatments. For this purpose, first, TNBC cells (1.25×10^5 cells/well) were plated into 6-well plates for 24 h. The next day, the cells were treated with 100 nM of miRNA mimics and siRNAs (using MNPs or HiPerFect). At the end of 72 h, matrigel (Corning) and FBS-free medium (14:1 v/v) were mixed gently and added carefully onto 24-well transwell inserts (Falcon) avoiding making air bubbles. The mixture inside the inserts was left incubation for 6 hours to solidify. After 6 h, the excess of the matrigel in each insert was removed. Meanwhile, 8×10^4 cells of each experimental group were counted and mixed with FBS-free medium, then added to the upper chamber of the insert. 500 µl of 10% FBS containing medium was also added into each well interacting with the lower chamber of the inserts. The cells inside the inserts were incubated for 48 h in incubator. Furthermore, the cells were fixed and stained using Hema 3 Stain Set (Fisher Scientific). By using a cotton swab, the cells found in the upper chamber were removed. Invading cells in the lower chamber were counted using a light microscope (Nikon Eclipse TE-200-U).

3.14. Apoptosis Analysis

To evaluate the apoptosis effect of miR-329 on TNBC cells either using HiPerFect or MNPs as transfecting reagent, FITC Annexin V Apoptosis Detection Kit (BD Pharmingen) was used according to the supplier's directions. Briefly, MDA-MB-231 and MDA-MB-436 cells (5×10^4 cells/well) seeded into 6-well plates and incubated overnight. Cell were then transfected with HiPerFect-miR 329 and MNPs-miR 329 for 120 h. At the end of the treatments, cells were collected and washed three times with cold PBS by centrifuging at 1500 rpm for 5 min. Next, 1X Annexin V binding buffer, FITC Annexin V and PI (Propidium Iodide) staining solutions were added onto cell pellets and the mixtures were incubated at dark for 15 min at room temperature. Flow cytometry analysis was performed by using Beckman Coulter Gallios Cell Analyzer.

3.15. Western Blot Assay

For Western blot analysis, TNBC cells were seeded in six-well plates at a density of $5x10^4$ per well. The cells were treated with 100 nM of miRNA mimics or siRNAs (using MNPs or HiPerFect) for 120 h. At the end of the treatments, the cells were collected from the wells and were lysed in lysis and extraction buffer (Thermo Fisher Scientific), protease inhibitor (Sigma-Aldrich), phosphatase inhibitor (Sigma-Aldrich), and sodium fluoride (NaF) (Gibco Laboratories) solution. The mixtures were centrifuged at 13500 rpm for 15 min at 4°C, and the total protein of each samples was obtained by collecting the supernatants. Furthermore, protein amount of each sample was calculated using Pierce Bicinchoninic Acid (BCA) Protein Assay Kit (Thermo Fisher Scientific). The samples were prepared using lysis buffer and 4x Laemmli Sample Buffer (Bio-Rad) reaching a final protein amount of 60 µg. Prior to electrophoresis step, each sample was incubated at 100°C for denaturation. For protein separation, pre-stained protein ledder (Thermo Fisher Scientific) and all samples were subjected to sodium dodecyl sulfate–polyacrylamide gel electrophoresis (SDS-PAGE) with a 4-15% gradient protein gel (Bio-Rad) in running buffer and electro-transferred to polyvinylidene difluoride (PVDF) membranes (Immobilon-P, Milipore) in transfer buffer. Expression levels of the proteins to be analyzed were determined using antibodies for eEF2K, p-EF2, Src, Cyclin D1, (Cell Signaling Technology), AXL (R&D Systems), p-Src (Santa Cruz Biotechnology), p-FAK, FAK (BD Biosciences). Rabbit, mouse (Cell Signaling Technology) or goat (Santa Cruz Biotechnology) horseradish peroxidase (HRP)-conjugated secondary

antibodies were also used for the corresponding antibodies. GAPDH (Cell Signaling Technology) was used as a house-keeping protein. The visualization of the immunoblots was carried out by treating the membranes at dark with Western Lightning Plus Enhanced Chemiluminescence (ECL) Substrate (Perkin Elmer).

Several non-treated breast cancer cells; MCF-7, BT-474, SK-BR-3 (ATCC) and non-cancerous breast epithelial cells; MCF-10A (ATCC) were also subjected to western blot protocol as mentioned above to evaluate the expression levels of the specific proteins, eEF2K and AXL.

3.16. Animal Studies

Prior to in vivo miR-329 delivery, MNPs were suspended in nuclease-free water and gently mixed either with miR-control or miR-329 solutions at room temperature for 1 h and thus miR-loaded MNPs were prepared. Athymic nude female mice (4-5 weeks old) were procured from The University of Texas MD Anderson Cancer Center. The animal studies were performed with respect to an experimental procedure certified by MD Anderson Institutional Animal Care and Use Committee. MDA-MB-231 and MDA-MB-436 cells having a density of 2×10^6 cells/100 µl (20% matrigel + 80% FBS-free medium) were injected orthotopically into the right middle mammary fat pad of each mouse. In one to two weeks after cell injection, MNPs-miR 329 and MNPs-miR control treatments were initiated. Each mouse received miRNAs having a concentration of 8 µg/mouse (0.3 mg/kg), intraperitoneally, once a week in a volume of 200 µl for 4 weeks. Every week, tumor volumes were measured by using an electronic caliper. The following equation: tumor volume = $1/2 \times \text{width}^2 \times$ length was used for the calculation of the estimated tumor volumes. Mice were euthanized with CO_2 after 4 weeks of the treatments. Then, tumor tissues were removed and collected for further Western Blot analysis.

3.17. Statistical Analysis

All data were expressed as means ± standard deviations (SDs). Statistical significance between groups was determined via one-way Analysis of Variance (ANOVA) for multiple comparisons and the Student's t-test by using GraphPad Prism (version 8.0) software. $p < 0.05$ was considered as statistically significant.

4. RESULTS AND DISCUSSION

4.1. Size-size Distributions and Zeta Potential of The Nanoparticles

The hydrodynamic size, PDI and zeta potential characterizations of SPIONs, APTES-SPIONs, Ser-SPIONs and PLL/Ser-SPIONs were carried out by DLS. The results were summarized in Table 4.1. According to the obtained DLS results, SPIONs were synthesized at a size of approximately 15-20 nm. The average size of APTES-SPIONs was found as 22.5 nm. Sericin coating and PLL functionalization led to an increase in size of the nanoparticles which measured as 102.4 nm and 109.4 nm, respectively. Zeta potential of the nanoparticles were measured at pH 7.4 and also given in Table 4.1. As seen, without any modification, the zeta potential of SPIONs were obtained as 20.5 mV. After APTES modification, gaining $–NH_3$ moieties shifted this value to 33 mV. Sericin addition to the structure increased negative charges (-9.2 mV) of the samples because of the –COOH groups. To obtain cationic nanoparticles, PLL was used. As expected, PLL/Ser-SPIONs had a zeta potential of 15 mV. Moreover, obtained PDI results (range between 0.180–0.275) indicated that all nanoparticles had a good uniformity.

The size distributions, surface charge and PDI characteristics of miR-control attached PLL/Ser-SPIONs are also given in Table 4.1. As seen, after miR-control attachment, no significant changes were obtained in nanoparticle size. As expected, miRNA addition to the structure shifted the zeta potential value to negative charge which is -14.80 mV. This indicated that miRNAs were successfully attached to PLL/Ser-SPIONs.

Table 4.1. DLS characterizations of the nanoparticles

	Hydrodynamic size (nm)	PDI	Zeta Potential (mV)
SPIONs	17.23 ± 1.65	0.180 ± 0.09	20.50 ± 0.90
APTES-SPIONs	22.47 ± 0.87	0.243 ± 0.06	33.03 ± 1.15
Ser-SPIONs	102.40 ± 1.32	0.164 ± 0.01	-9.20 ± 1.60
PLL/Ser-SPIONs	109.40 ± 0.87	0.276 ± 0.03	13.10 ± 0.44
miR-control-PLL/Ser-SPIONs	114.85 ± 0.21	0.227 ± 0.01	-14.80 ± 0.63

4.2. Morphological Characterizations of The Nanoparticles

TEM micrographs of the nanoparticles were shown in Figure 4.1. As seen in the images, all nanoparticles exhibit a spherical shape and have narrow size distribution. SPIONs and APTES-SPIONS had size of approximately 10 nm. (Figure 4.1 A and B). APTES modification did not change the morphology and the size of the SPIONs significantly. Figure 4.1 also demonstrates that an around 5 nm surface coating of sericin was observed for Ser-SPIONs. Core SPIONs were seen as black and coating were seen as light gray that indicates the coating (Figure 4.1 C). The diameter of Ser-SPIONs was observed as almost 20-30 nm. PLL addition to the structure did not significantly change in size and morphology of the nanoparticles. As seen in Figure 4.1, the size of PLL/Ser-SPIONs were observed as 25-30 nm.

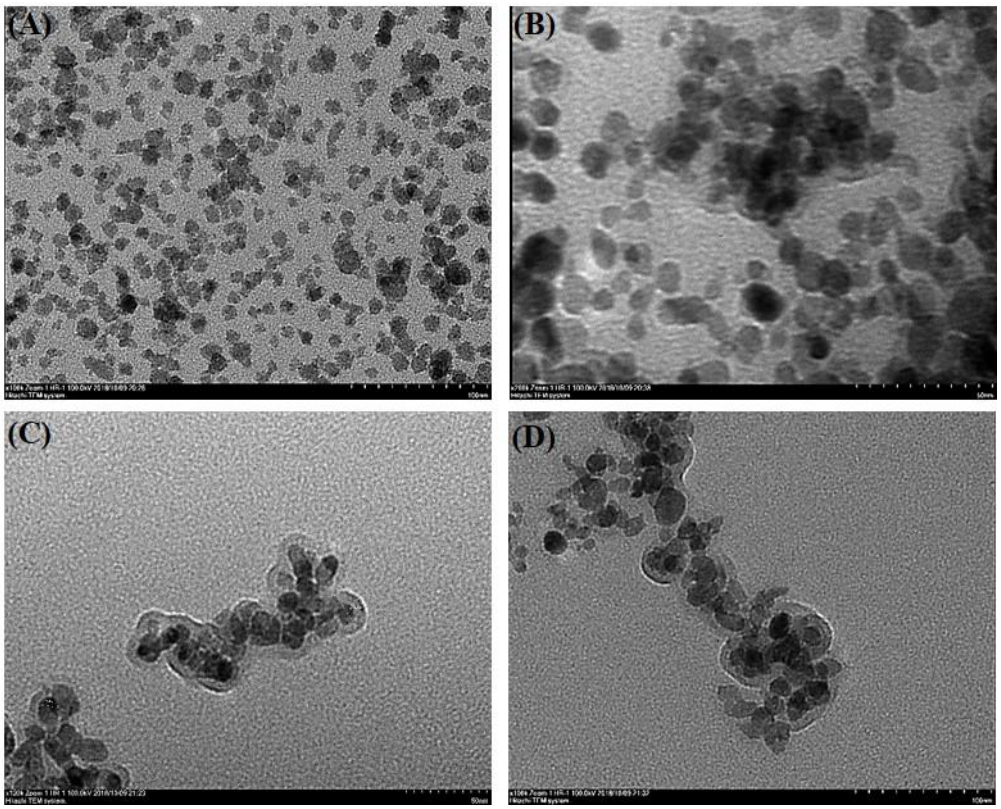

Figure 4.1. TEM images of the nanoparticles (A) SPIONs, (B) APTES-SPIONs, (C) Ser-SPIONs, (D) PLL/Ser-SPIONs

4.3. Physicochemical Characterizations of The Nanoparticles

4.3.1. FTIR analysis

Figure 4.2, 4.3 and 4.4 demonstrate the FTIR spectra of all samples. The results of sericin isolated from cacoon and commercially available sericin were compared and given in Figure 4.2. The absorption bands at about 1647 cm^{-1}, 1523 cm^{-1} and 1260 cm^{-1} were detected in both samples, which were the typical bands in sericin protein indicating amide I (1600-1700 cm^{-1}), amide II (1504-1582 cm^{-1}), and amide III (1200-1300 cm^{-1}), respectively. The band located at about 3271 cm^{-1} represented the stretching vibration of OH^{-} and was observed for both sericin structures. 2919 cm^{-1} and 2851 cm^{-1} C–H stretching bands were also observed for isolated sericin and commercial sericin, respectively [225-227]. These results confirm that sericin was successfully isolated from cocoons.

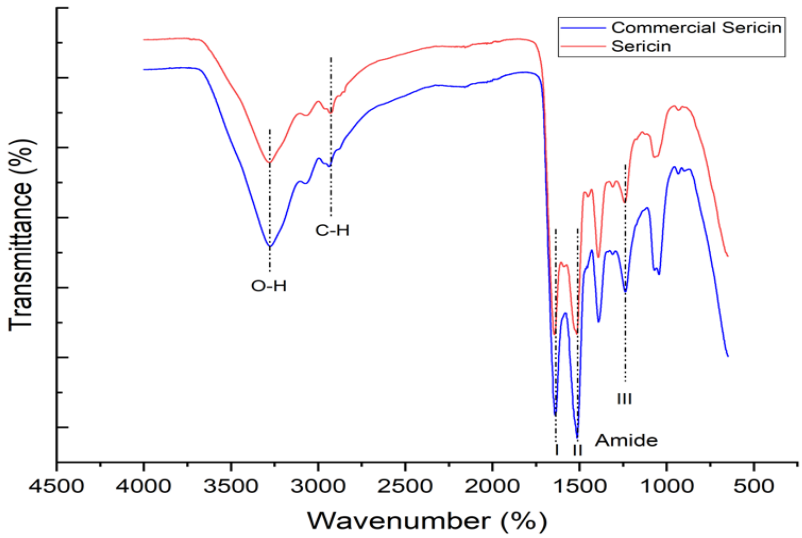

Figure 4.2. FTIR spectra of sericin isolated from silk and commercial sericin

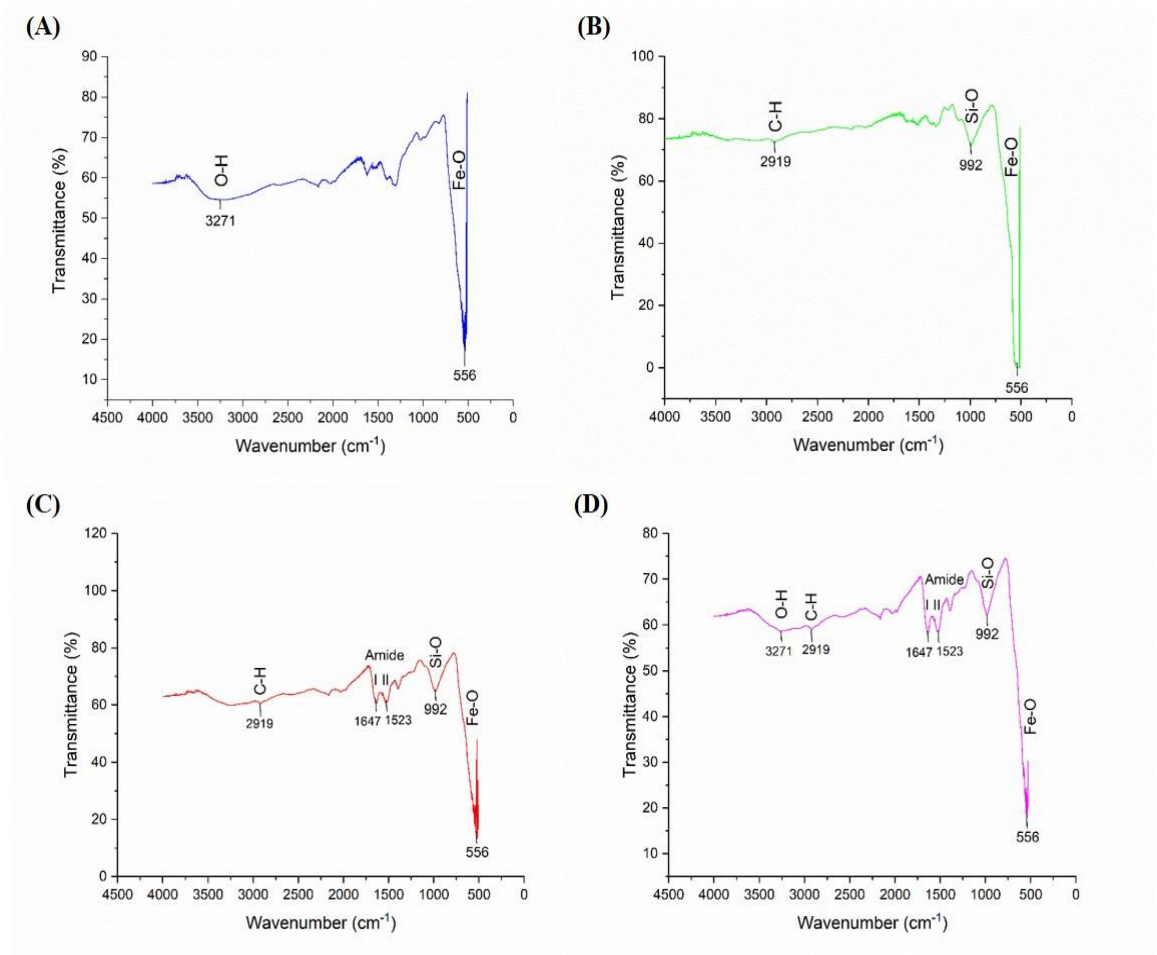

Figure 4.3. FTIR spectra of (A) SPIONs, (B) APTES-SPIONs, (C) Ser-SPIONs and (D) PLL/Ser-SPIONs

The FTIR spectra of SPIONs, APTES-SPIONs, Ser-SPIONs and PLL/Ser-SPIONs are also given individually in Figure 4.3 and all together in Figure 4.4. These all four structures have a strong absorption band almost at 560 cm^{-1} that indicates the Fe–O bond of bulk magnetite [228]. The characteristic peaks of OH groups on SPIONs based samples were at around 3200 cm^{-1}. When comparing SPIONs and APTES-SPIONs, the bands around 3000 cm^{-1} and 992 cm^{-1} representing C–H stretching and Si–O stretching vibrations, respectively, were clearly observed for APTES-SPIONs. This confirms the condensation between the alkoxysilane of APTES and the hydroxyl groups of the SPIONs surface [229, 230]. The addition of sericin and PLL to APTES-SPIONs structure is clearly obvious when amide I, amide II and amide III bands are obtained for Ser-SPIONs and PLL/Ser-SPIONs. All FTIR spectra results proved that all samples were synthesized successfully.

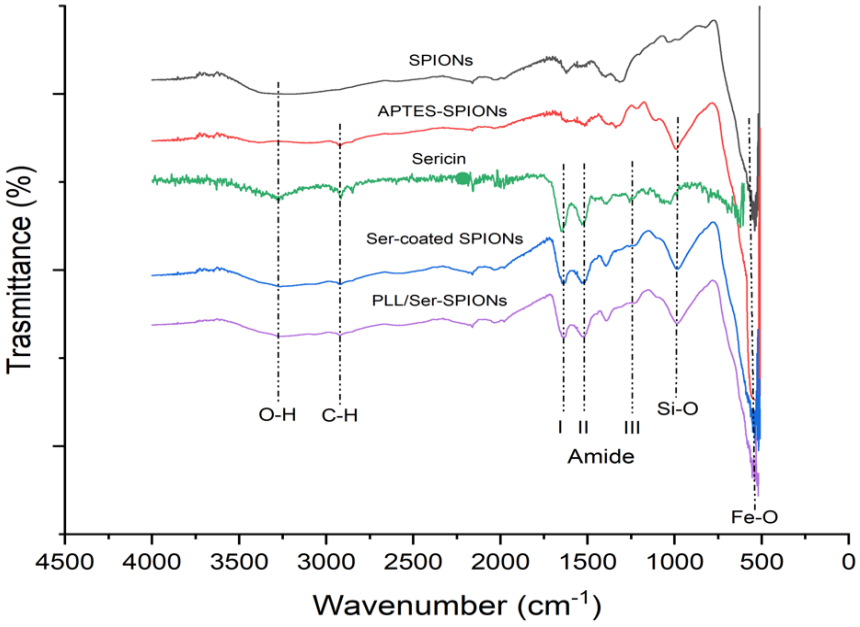

Figure 4.4. FTIR spectra of all structures synthesized

4.3.2. ESR Analysis of The Nanoparticles

The magnetic characterizations of the nanoparticles were conducted by ESR analysis. The obtained spectroscopic properties from ESR spectra are given in Figure 4.5, 4.6 and in Table 4.2. Molecules or parts of molecules with unpaired electrons are analyzed by ESR. Due to the fact that molecules with unpaired electrons display magnetic properties, it is possible to determine whether the materials prepared with this method have magnetic properties. As can be seen in Figure 4.5 and 4.6, the ESR spectra of SPIONs and PLL/Ser-SPIONs are in the form of an asymmetric resonance curve, respectively. Thus, it is confirmed that PLL/Ser-SPIONs synthesized in the studies exhibit magnetic properties.

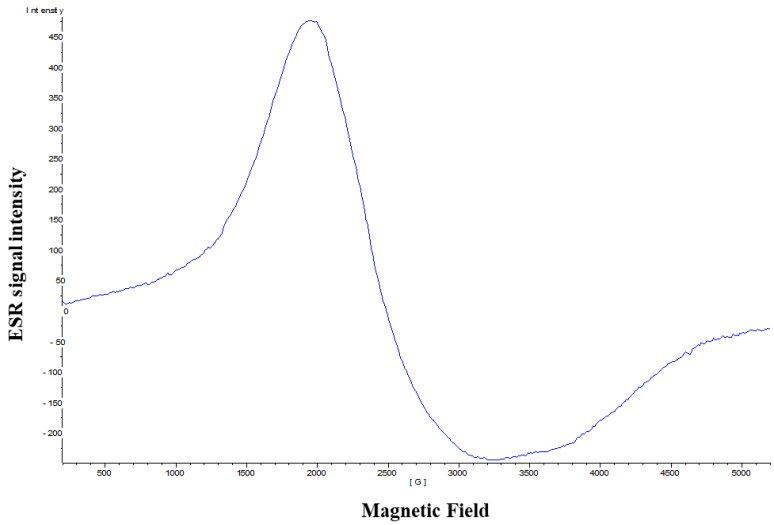

Figure 4.5. The ESR spectrum of SPIONs

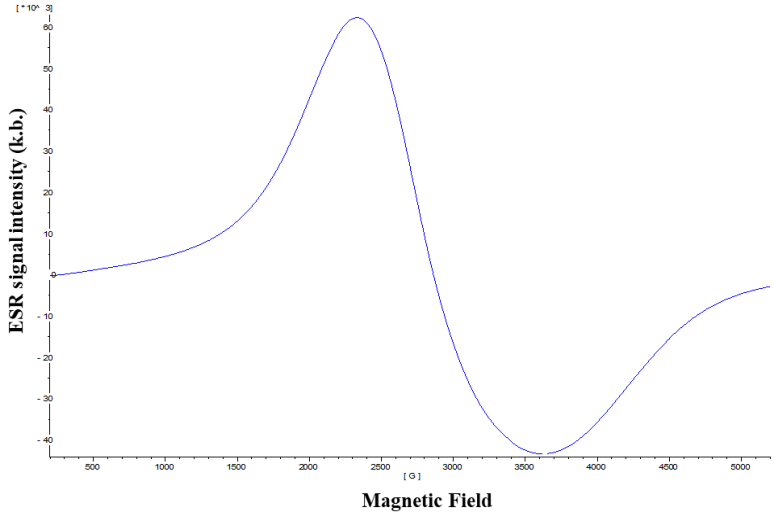

Figure 4.6. The ESR spectrum of PLL/Ser-SPIONs

(g) is the electroscopic splitting factor and for each substance it is a characteristic feature. This value for iron was found to be 1.940. According to the results in Table 4.2, the value of (g) obtained in the analysis complies with the literature.

Table 4.2. ESR characterizations of SPIONs and PLL/Ser-SPIONs

	Spectroscopic splitting factor (g)	Peak to peak linewidth (ΔH_{pp})
SPIONs	~2.785	~1360 G
PLL/Ser-SPIONs	~2.468	~1260 G

Table 4.2 also reveals that after coating and functionalizing SPIONs with sericin and PLL, the (g) factor decreased from 2.785 to 2.468. This indicates that the interaction decreases due to the introduction of the polymers between the magnetic units. Therefore, there is a decrease in signal strength.

4.4. In vitro Degradation and Stability of The Nanoparticles

To evaluate in vitro biodegradation behaviours of PLL/Ser-SPIONs at pH 5.5 and 7.4, the nanoparticles were incubated at 37^{o}C in PBS containing lysozyme. Nanoparticle degradation was measured based on the principle that intact nanoparticles exhibit high level of turbidity because of their wide amount of cross-linked structure. When enzymatic degradation initiates, the turbidity of the particles reduce [231, 232]. The turbidimetric measurements of the nanoparticles are given in Figure 4.7. The mass remainings (%) of the nanoparticles in 15 days were 85% and 83% incubated in pH 5.5 and 7.4, respectively. Non-significant difference was observed between both pH values.

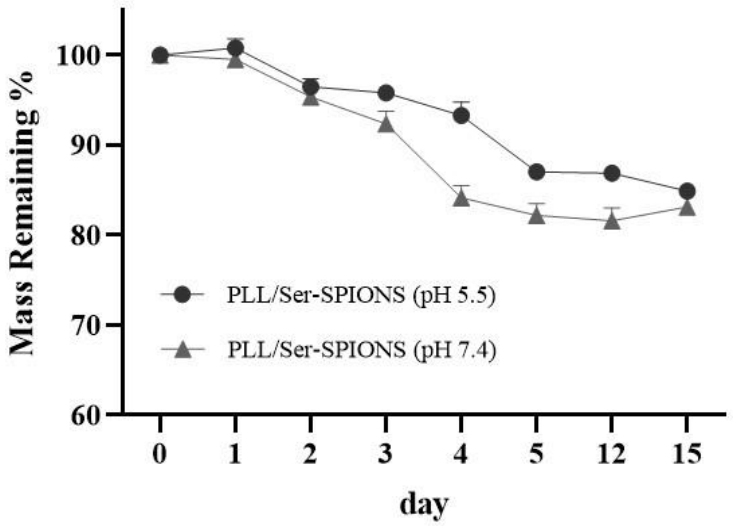

Figure 4.7. In vitro degradation profiles of PLL/Ser-SPIONs at pH 5.5 and 7.4

Although SPIONs are promising for several biomedical applications, number of drawbacks (aggregation, poor water solubility and oxidation) have to be solved for use in clinical applications. Various polymers are known to stabilize SPIONs and enhance their properties for further applications. However, in case of using excessively stabilized or non-degradable polymers, the therapeutic payload release will be limited. SPIONs can be colloidal stable and biodegradable, and can have high drug delivery capacity after incorporation with a biodegradable polymer [233]. Degradation of the nanoparticles allow the release of the encapsulated drug, however, controlled drug delivery is required to avoid burst release effect. According to the obtained results, PLL/Ser-SPIONs exhibited a controllable degradation profile, and fulfilled all the requirements for a proper drug delivery system.

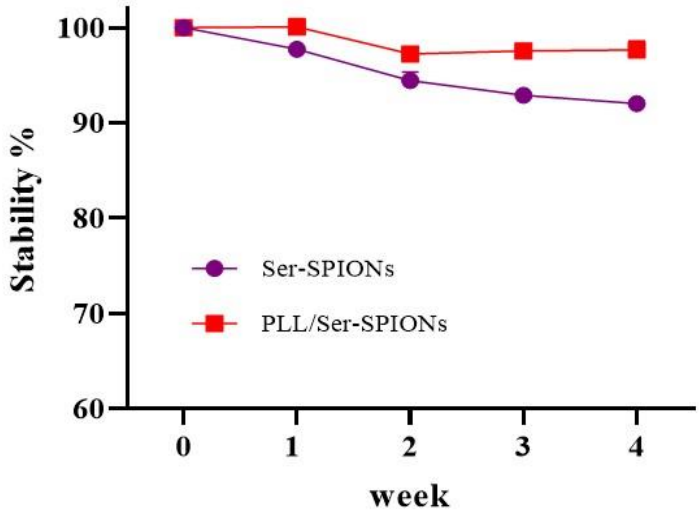

Figure 4.8. In vitro stability of Ser-SPIONs and PLL/Ser-SPIONs at 4°C

Storage stability of Ser-SPIONs and PLL/Ser-SPIONs was also examined by using a turbidimeter. As illustrated in Figure 4.8, after four weeks incubation of nanoparticles at 4°C in PBS, the percentage of intact nanoparticle content was found as 92% and 98% for Ser-SPIONs and PLL/Ser-SPIONs, respectively. These results suggest that PLL/Ser-SPIONs are more stable for long-term storage conditions.

4.5. Determination of Binding Efficiency (%)

PLL/Ser-SPIONs were interacted with miR-controls having concentrations of 25 nM, 50 nM and 100 nM, and the binding efficiencies (%) of each MNPs-miR control formulations were determined using a fluorometric method. 99.3%, 98.5% and 97.7% binding efficiencies were achieved when using 25 nM, 50 nM and 100 nM of miR-control, respectively. Zeta potential values of each sample were also analyzed. -11.34 mV and -12.75 mV zeta potentials were measured for 25 nM and 50 nM miR-control loaded PLL/Ser-SPIONs, respectively. For 100 nM miR-control, this value was determined as -14.80 mV as previously given in Table 4.1. This confirms increasing amount of miRNA led to a concentration dependent decrease in zeta potential of miRNA loaded nanoparticles. As a result, miRNAs were successfully loaded to the surface of the MNPs with high binding ability.

4.6. In vitro Release Kinetics

The in vitro release of miR-329 from PLL/Ser-SPIONs was evaluated for 7 days in PBS (pH 7.4) at 37°C. miR-329 at different concentrations (25 nM-50 nM-100 nM) were interacted with the nanoparticles. The results are demonstrated in Figure 4.9. As illustrated, in the first 4 h, the nanoparticles exhibited a burst miRNA release which was 15%, 44% and 55% for 25 nM, 50 nM and 100 nM miRNA concentrations, respectively. The reason of the quick release may occur due to the attachment of the miR-329 on the surface of the nanoparticles. After 24 h, 27%, 53% and 59% of miRNA was released from each 25 nM, 50 nM and 100 nM miR-329 loaded PLL/Ser-SPIONs, respectively. In the following hours, miR-329 loaded nanoparticles showed a slow and sustained release profile that contributes to prolonging the effectiveness of the miRNA.

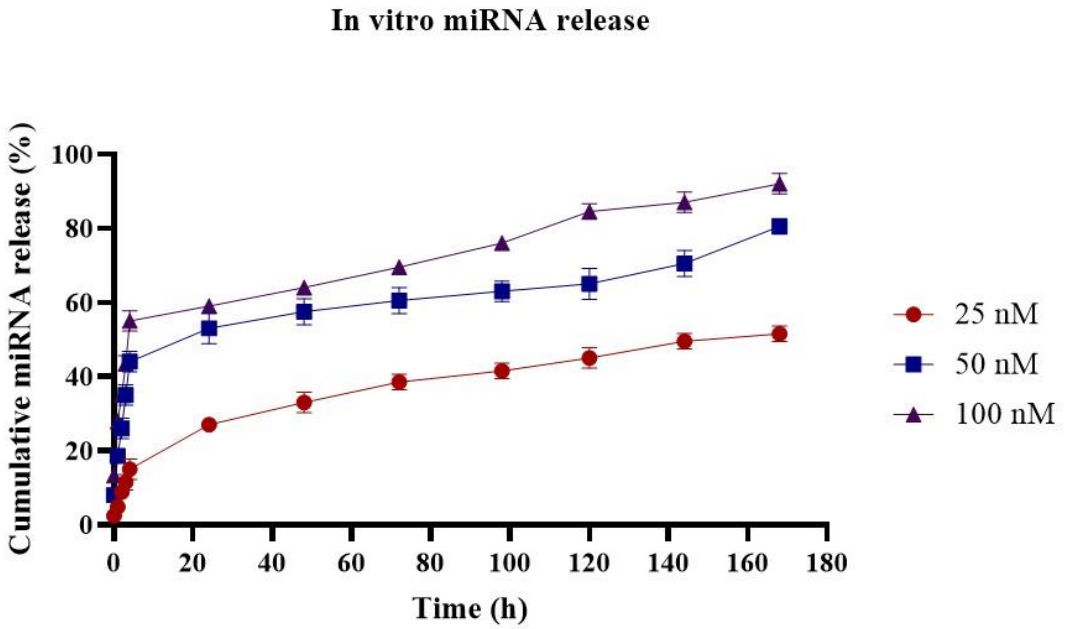

Figure 4.9. The in vitro release profile of miRNA-loaded PLL/Ser-SPIONs at pH 7.4

4.7. Cytotoxicity and Colony Formation Assays for Bare Nanoparticles

To investigate the cytotoxicity of nanoparticles on L929 cells, MTT assay was performed. The effects of concentration (5 µg/ml, 25 µg/ml and 100 µg/ml) and incubation time (24 and 48 h) were tested for all produced nanoparticles. The results are given in Figure 4.10. The results demonstrated that almost no cytotoxicity was observed after 24 h of the treatment. When the cells were treated with the highest dose of the nanoparticles (100

μg/ml) for 48 h, the percentages of cell viabilities were 89%, 90%, 96% and 93% for SPIONs, APTES-SPIONs, Ser-SPIONs and PLL/Ser-SPIONs, respectively.

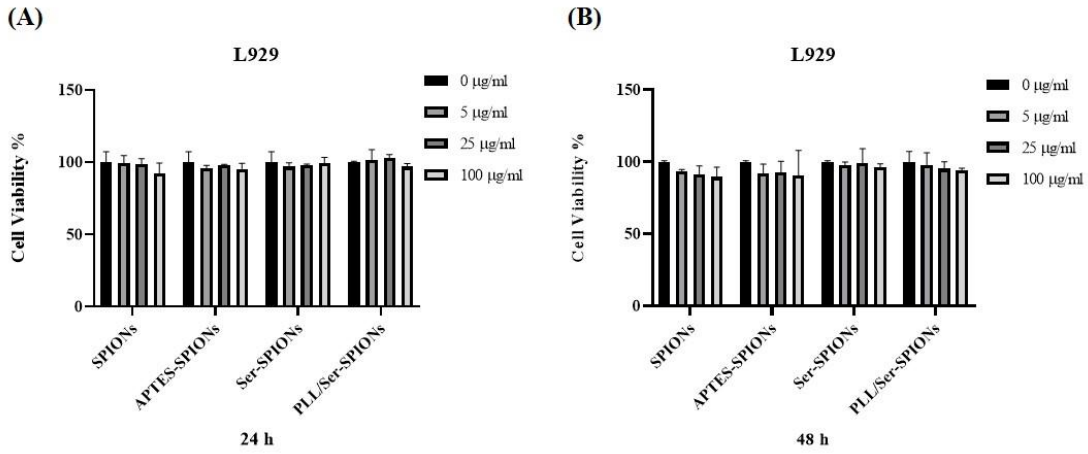

Figure 4.10. Cytotoxicity of all nanoparticles against L929 cells for (A) 24 h and (B) 48 h of incubation

The cytotoxicity of PLL/Ser-SPIONs was also evaluated againts TNBC cells. The nanoparticles possessing various concentrations (5 μg/ml, 25 μg/ml, 50 μg/ml and 100 μg/ml) were interacted with the cells for 5 days. As it is seen in Figure 4.11, almost no significant toxicity was obtained for all concentrations. Only when using the highest concentration of PLL/Ser-SPIONs (100 μg/ml), in MDA-MB-231 cells 16% of toxicity was observed. In addition, the percentages of the cell viability were found as 88% and 89% by using 100 μg/ml nanoparticles in BT-20 and MDA-MB-436 cells, respectively.

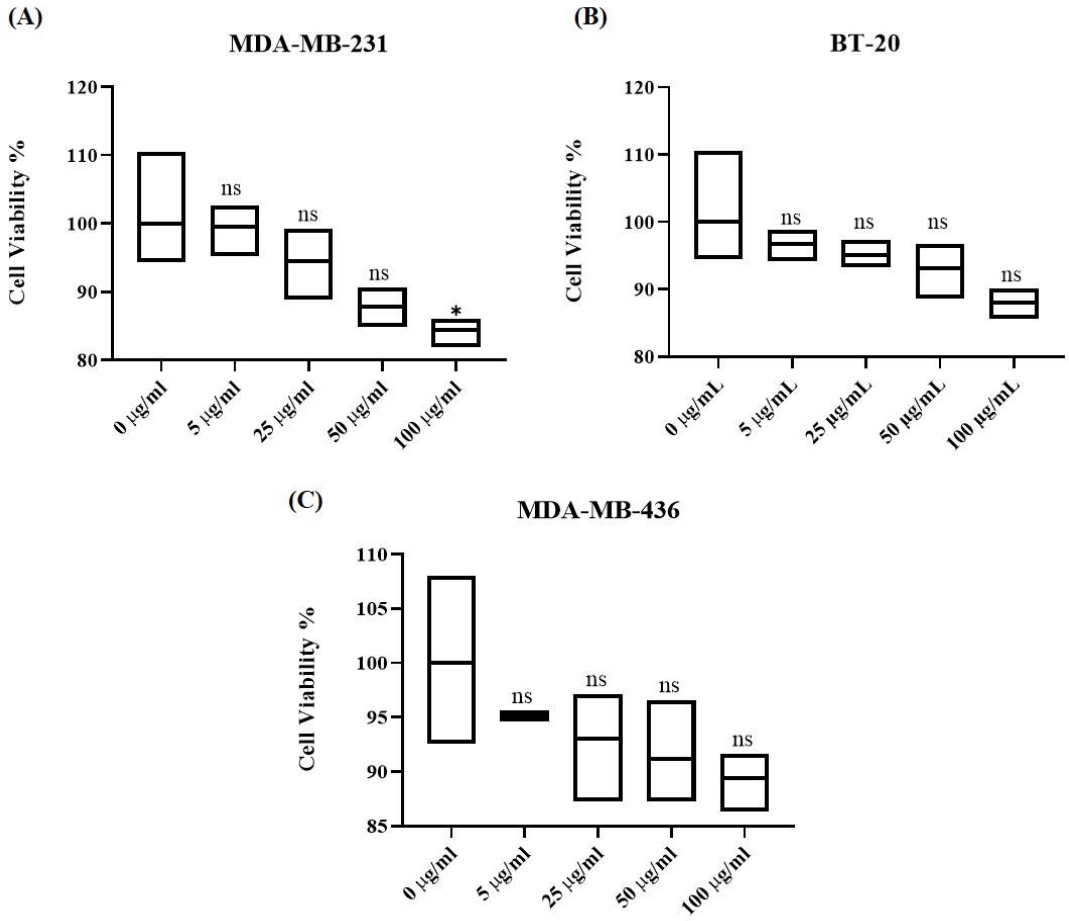

Figure 4.11. Cytotoxicity of PLL/Ser-SPIONs against (A) MDA-MB-231, (B) BT-20 and (C) MDA-MB-436 cells after 5 days of incubation

MTT and MTS analyses concluded that all nanoparticles were biocompatible and safe against to non-cancerous and cancer cells.

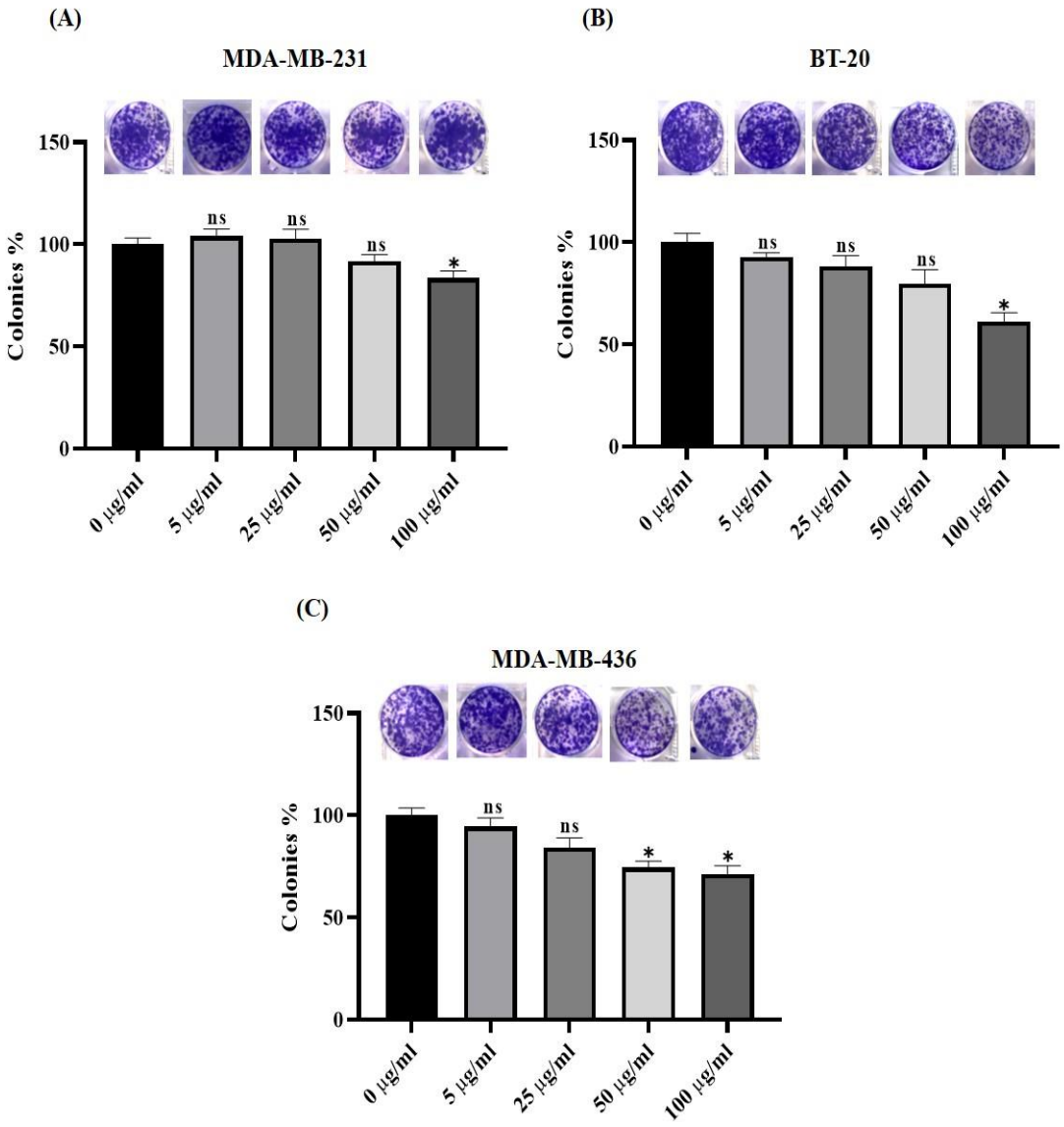

Figure 4.12. The effect of PLL/Ser-SPIONs on colony formation in (A) MDA-MB-231, (B) BT-20 and (C) MDA-MB-436 cells after 12 days of incubation

The effect of PLL/Ser-SPIONs at various concentrations on colony formation in TNBC cells was examined. The results are given in Figure 4.12. It was observed that all cells exhibited concentration-dependent colony formation ability. For MDA-MB-231, BT-20 and MDA-MB-436 cells, only the cells treated with 100 µg/ml of nanoparticles had a significant decrease in colony formation ability (83%, 61% and 71%, respectively). Since five times less number of cells were seeded into the plates for colony formation assay, and due to the long incubation time with the nanoparticles comparing to MTS assay,

cells were observed to be more sensitive against to the highest doses of the nanoparticles in the colony formation experiment.

4.8. Intracellular Localization of The Nanoparticles

To evaluate the uptake of produced MNPs-miR control by MDA-MB-231 cells, TEM analysis was conducted. According to the results, incubating the cells with MNPs-miR control for 24 h led to a successful localization in cell cytoplasm (represented by red arrows). TEM images were given in Figure 4.13. In addition, it is also clear after 24 h of incubation, most of the particles were localized in the cytoplasm comparing to extracellular environment. In Figure 4.13 A, one red arrow shows the MNPs-miR control found in the extracellular environment.

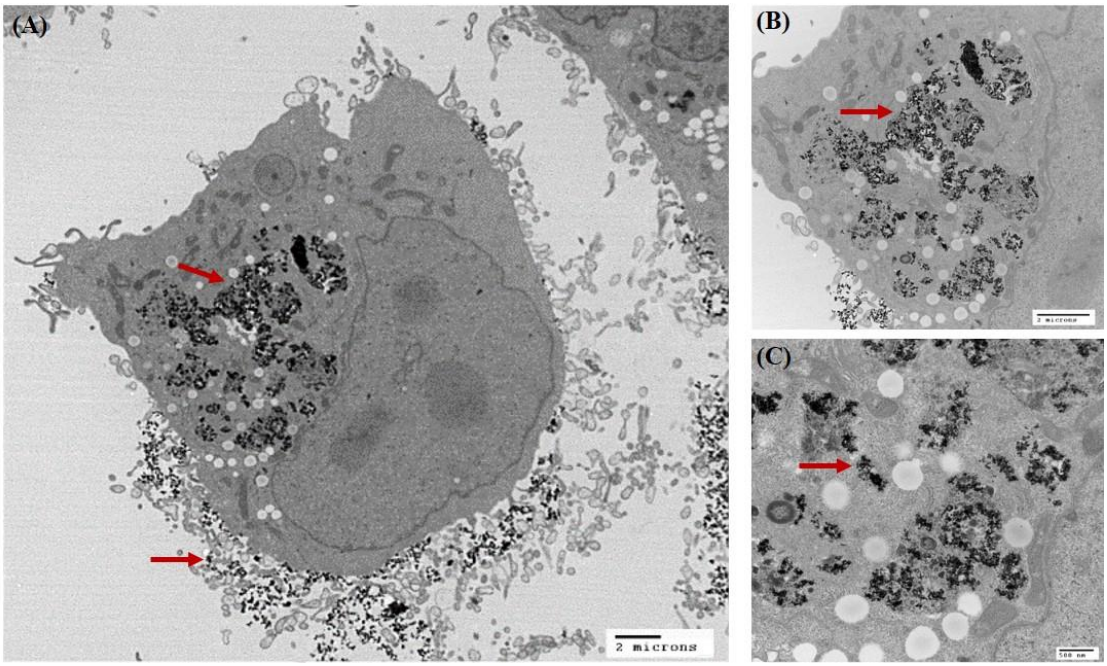

Figure 4.13. TEM images for intracellular localization of MNPs-miR control at (A) 4000x (B) 10000x and (C) 25000x magnifications

4.9. Confocal Microscopy

To investigate the delivery of small ncRNA (miRNA or siRNA) by the MNPs via confocal microscopy analysis, MNPs were interacted with control siRNA-Alexa Flour 555 prior to the assay. As it is shown in Figure 4.14, treatment of MNPs-control siRNA with MDA-MB-231 cells for 4 h resulted in high uptake of the particles. Same experiment was also performed for HiPerFect that was used as a positive control. The results were given in

Figure 4.15. These obtained results indicated that MNPs are as good as a commercially available transfection reagent for small ncRNA (miRNA or siRNA) delivery.

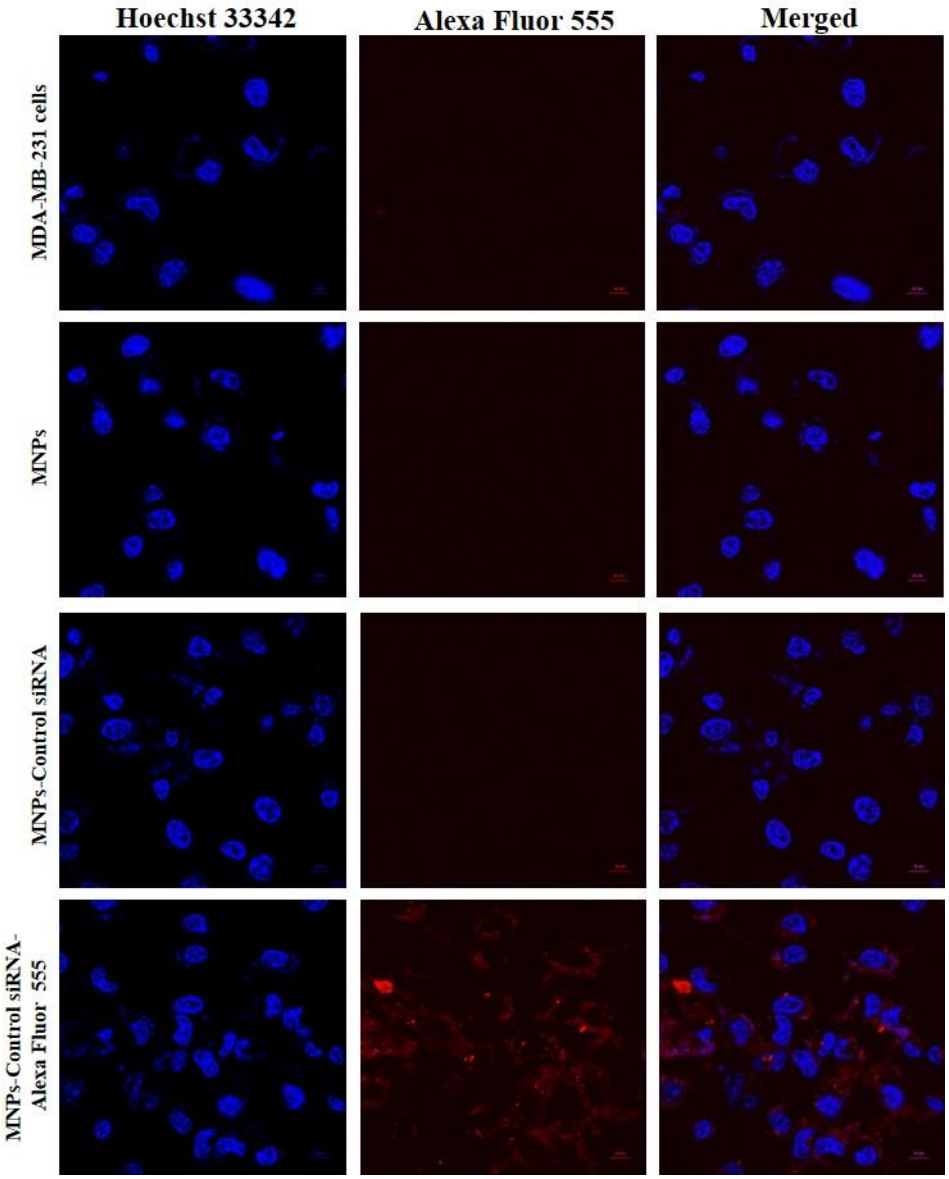

Figure 4.14. Cellular uptake of the nanoparticles by MDA-MB-231 cells

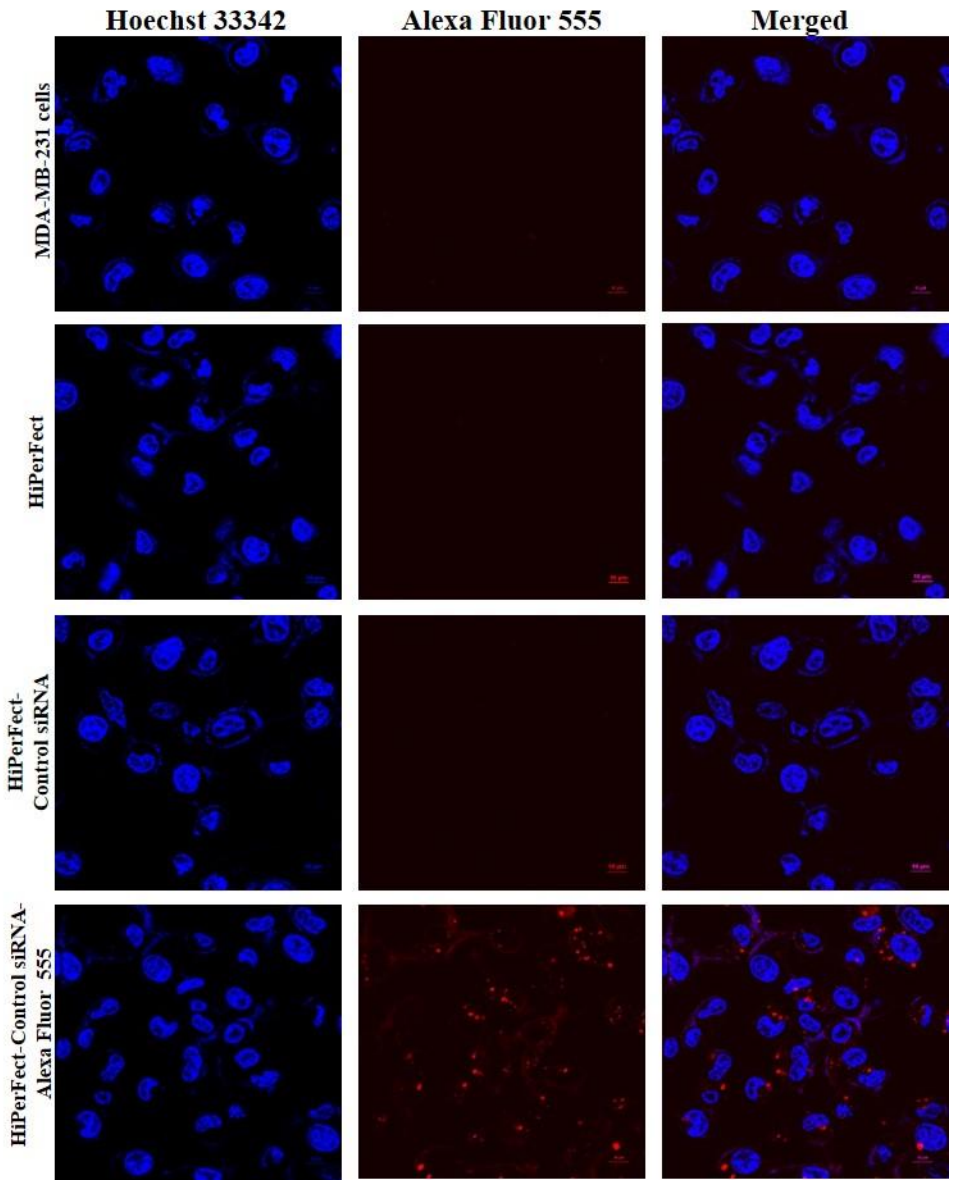

Figure 4.15. Cellular uptake of HiPerFect by MDA-MB-231 cells

4.10. The miR-329 Expression in Patient Data

The relation between miR-329 expression levels and the patients with BC was also investigated. As it is seen in Figure 4.16, in healthy individuals, the miR-329 expression is higher than the BC patients confirming the tumor suppressor effect of miR-329 (Figure 4.16 A). In addition, remarkably, it was observed that the expression of miR-329 is lower in TNBC compared to other BC subtypes. Low/or lost miR-329 level in TNBC indicates its importance among other types of BC (Figure 4.16 B).

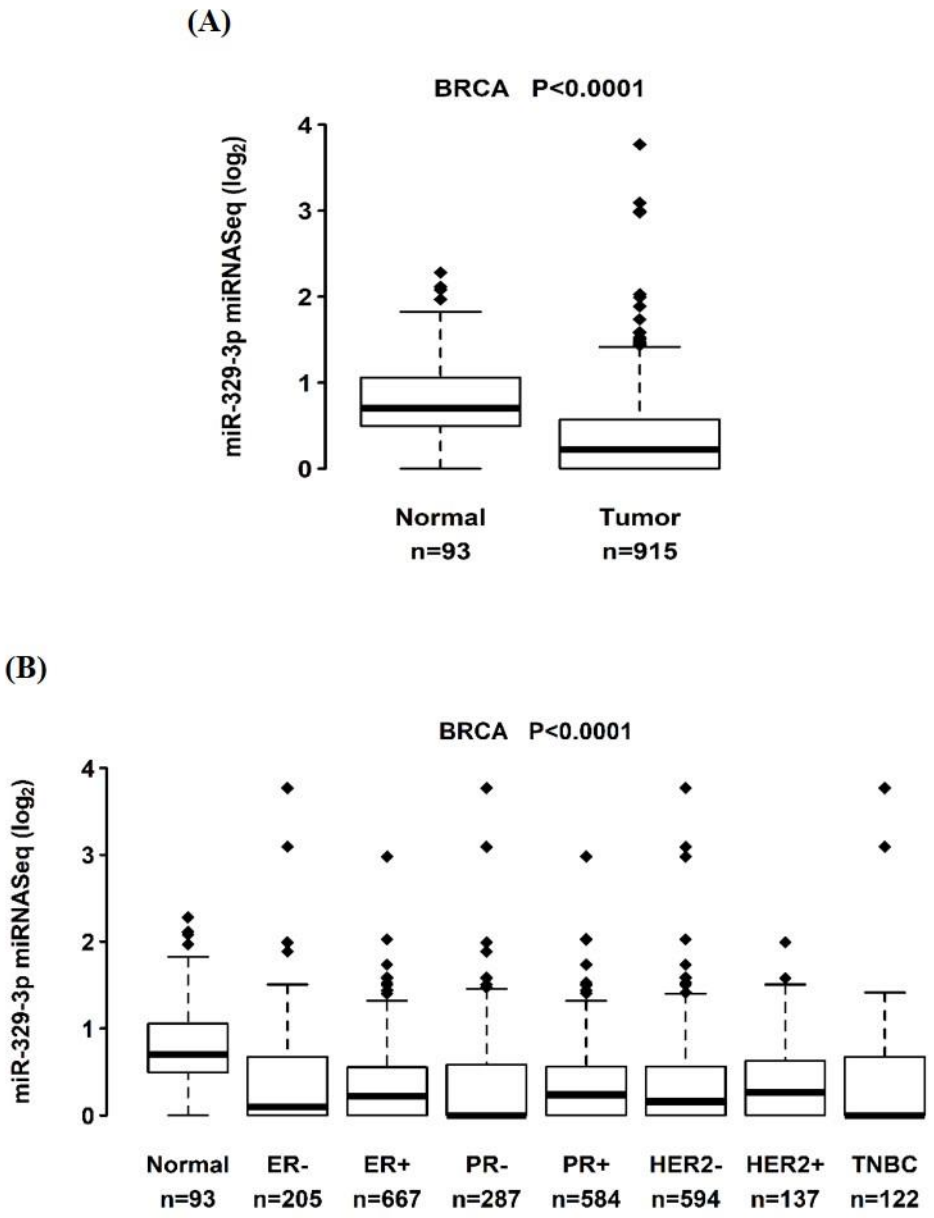

Figure 4.16. (A) Comparison of miR-329 expression between normal tissues and patients with BC, (B) Comparison of miR-329 expression levels in normal tissues and patients with various BC types

4.11. Kaplan-Meier Analysis

To reveal the clinical significance of miR-329, The Cancer Genome Atlas Program (TCGA) database was also analyzed. The results are given in Figure 4.17. As determined by Kaplan-Meier analysis, it was obtained that the patients having reduced expression of miR-329 (shown as blue color in Figure) is related to poor overall survival in patients with

TNBC (p = 0.055). Vice versa, significantly higher miR-329 expression (shown as red color in Figure) results in higher overall survival rate in patiens confirming the tumor suppressing effect of miR-329 in TNBC.

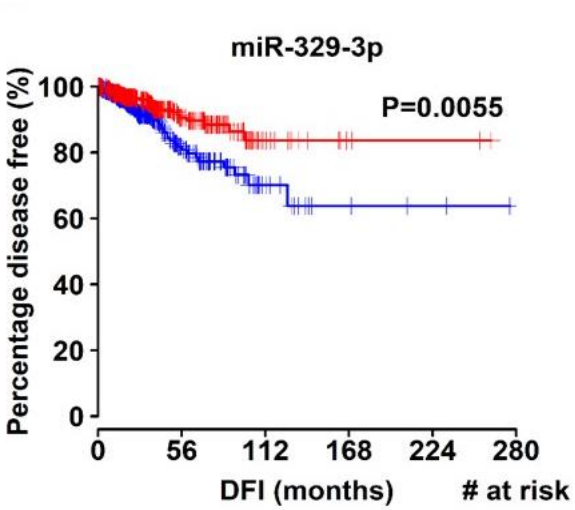

Figure 4.17. Kaplan-Meier analysis of miR-329 expression in patients with TNBC

4.12. RT-qPCR Analysis

The basal expression levels of miR-329 in various BC cells and non-cancerous breast cells (HMEC) were compared by RT-qPCR. According to the results, miR-329 expression was found to be higher in HMEC cells than all other BC cells (Figure 4.18). Moreover, it was also observed that miR-329 expression level was the lowest in MDA-MB-231, BT-20 and MDA-MB-436 cells. This explains the reason of using those cell lines in this study.

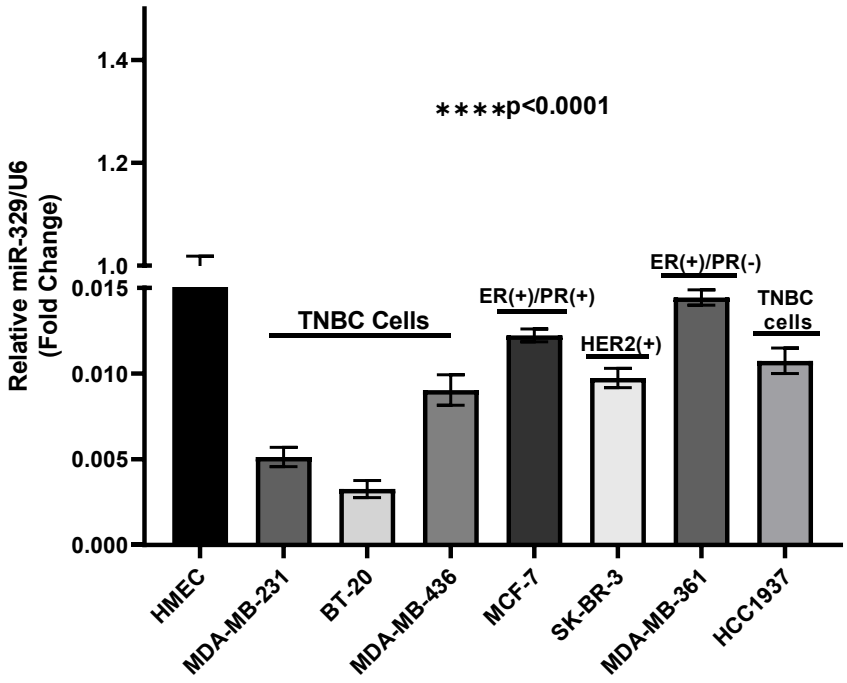

Figure 4.18. The basal expression levels of miR-329 in various BC cells and non-cancerous breast cells

4.13. The Protein Expression Levels of eEF2K and AXL in Multiple Cell Lines

The protein expression levels of eEF2K and AXL were investigated by Western Blot in several breast cancer cell lines including MDA-MB-231, BT-20, MDA-MB-436, MCF-7, BT-474 and SK-BR-3. As illustrated in in Figure 4.19, eEF2K and AXL are highly expressed in TNBC cells (MDA-MB-231, BT-20, MBA-MB-436). In addition, in non-cancerous breast cell epithelium MCF-10A cells, it was observed that there is no AXL expression (Figure 4.19 B). In a study performed by Bayraktar et al. the researchers reported that the protein expression level of eEF2K is significantly high in a variety of breast cancer cells and there is no eEF2K expression in MCF-10A cells [204].

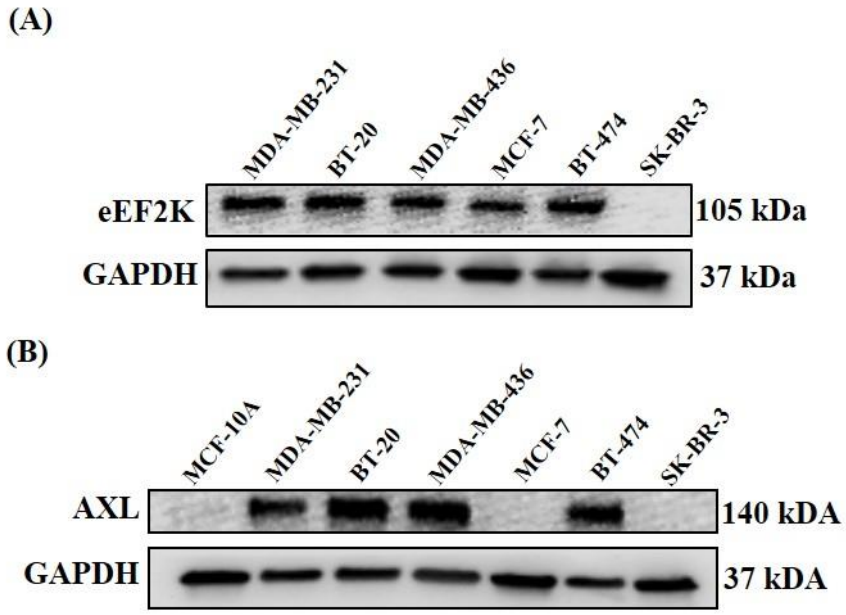

Figure 4.19. eEF2K and AXL protein expression levels in various breast cell lines

4.14. The Effect of Ectopic miR-329 Expression on eEF2K and AXL Protein Levels

To confirm the miRNA database analysis results showing that miR-329 has binding sites at 3'-UTR primes of eEF2K and AXL, and to identify the underlying molecular mechanisms of miR 329/eEF2K and miR-329/AXL axis, Western Blot assay was carried out. MDA-MB-231, BT-20 and MDA-MB-436 cells were transfected either with MNPs-miR control/miR 329 and HiPerFect-miR control/miR 329, and the total protein of each group was collected. HiPerFect was used as a positive control. According to the results (Figure 4.20), in all cell lines ectopic expression of miR-329 by using MNPs as a delivery agent remarkably inhibited the protein expression levels of eEF2K and AXL in comparison to MNPs-miR control treated cells. Similar results were also obtained using HiPerFect as a transfection agent. These findings reveal that miR-329 is a potential regulator of eEF2K and AXL expression in TNBC cells.

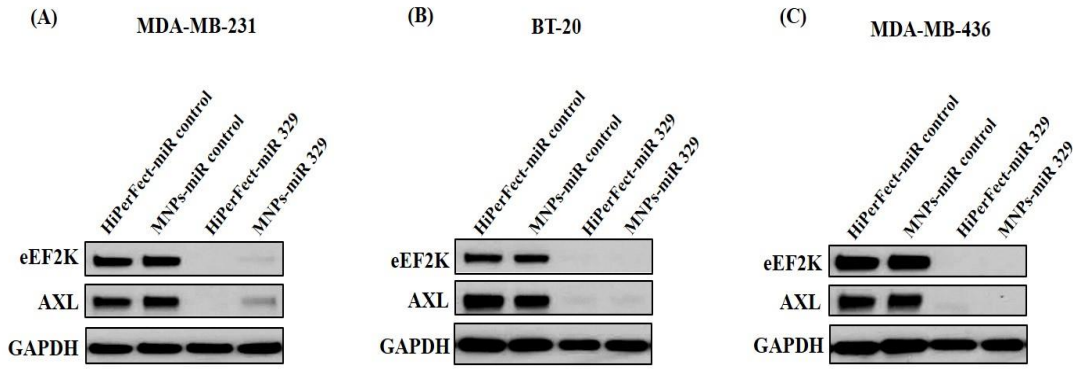

Figure 4.20. The protein expression levels of eEF2K and AXL after transfecting the cells with miR-329 using MNPs or HiPerFect in (A) MDA-MB-231, (B) BT-20 and (C) MDA-MB-436 cell lines

4.15. The Effect of Ectopic miR-329 Expression on Colony Formation and Cell Proliferation

MDA-MB-231, BT-20 and MDA-MB-436 cells were transfected either with and MNPs-miR 329 and HiPerFect-miR 329 to investigate the influence of miR-329 on colony formation ability. As illustrated in Figure 4.21, miR-329 treatment led to a significant reduction in colony formation compared to the miR-control treated cells. The colonies % were found to be as 4% (45% miR-control, ***$p < 0.001$), 11% (46% miR-control, ***$p < 0.001$) and 29% (87% miR-control, ****$p < 0.0001$) for MDA-MB-231, BT-20 and MDA-MB-436 cells, respectively, after MNPs-miR 329 transfection. The obtained results also revealed that the produced MNPs performed a similar ability as the commercial transfection reagent. When the cells were treated with HiperFect-miR 329, the percentage of the colonies was obtained as 7% (50% miR-control, ***$p < 0.001$), 13% (49% miR-control, ***$p < 0.001$) and 45% (90% miR-control, ***$p < 0.001$) for MDA-MB-231, BT-20 and MDA-MB-436 cells, respectively. Figure 4.21 also shows that for all cell lines, bare MNPs and HiperFect have non-significant effect on clonogenicity.

(A)

MDA-MB-231

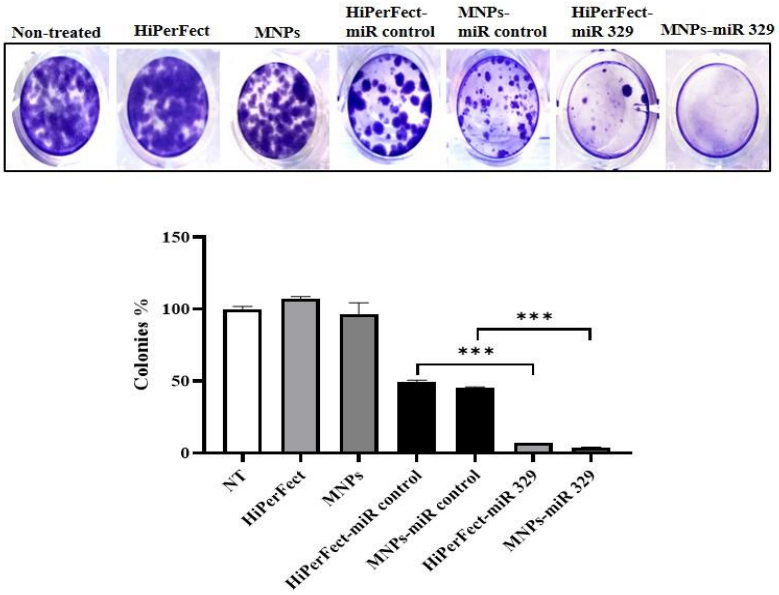

(B)

BT-20

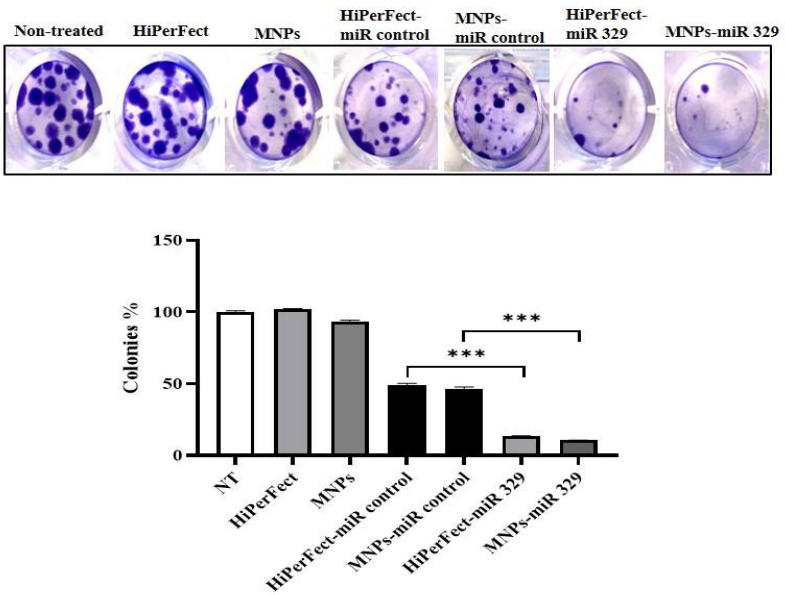

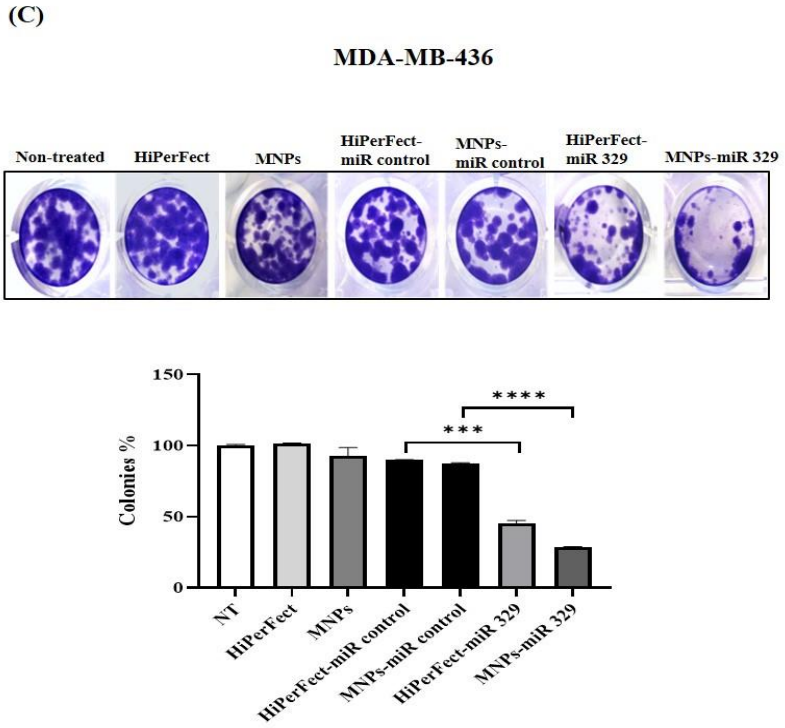

Figure 4.21. The effect of miR-329 expression on TNBC cell clonogenicity (A) MDA-MB-231, (B) BT-20 and (C) MDA-MB-436 cell lines

Further, the impact of miR-329 at 25 nM and 50 nM concentrations on TNBC cell proliferation was also determined via MTS assay. The results are given in Figure 4.22. A significant inhibition in cell growth was observed for all cell lines for both concentrations. In addition, as the amount of miR-329 increased for all cell lines, proliferation of the cells decreased. MNPs-miR 329 (50 nM) transfected MDA-MB-231 cells, BT-20 cells and MDA-MB-436 cells had 58% (**$p < 0.01$), 59% (***$p < 0.001$) and 68% (***$p < 0.001$) viability, respectively. In a similar manner, after transfecting the cells with HiperFect-miR 329, significantly decreased cell viability values were obtained as 58% (**$p < 0.05$), 53% (***$p < 0.001$) and 81% (***$p < 0.001$) for MDA-MB-231, BT-20 and MDA-MB-436 cells, respectively. All data were normalized against to their miR-controls. These results confirm the inhibiting effects of miR-329 expression in TNBC cells.

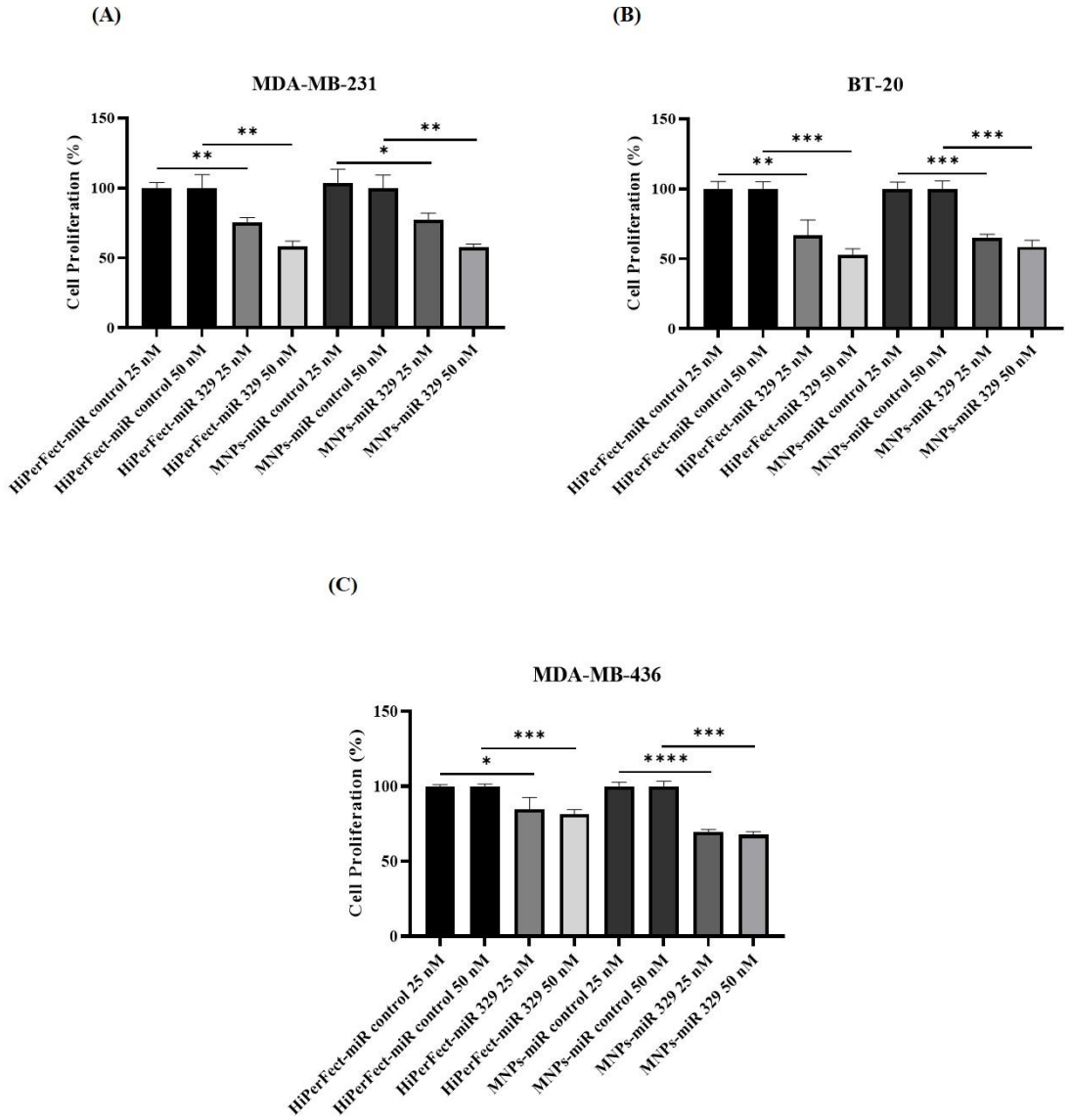

Figure 4.22. The effect of miR-329 (25 nM-50 nM) on TNBC cell proliferation (A) MDA-MB-231, (B) BT-20 and (C) MDA-MB-436 cell lines

4.16. The Effect of Ectopic miR-329 Expression on Cell Migration

To examine whether miR-329 expression suppresses MDA-MB-231, BT-20 and MDA-MB-436 cell migration, wound healing assay was performed. The obtained results showed that the number of migrated cells was significantly lower in miR-329 transfected cells either by using HiPerFect or MNPs comparing to miR-control treated groups. Figure 4.23 A demonstrates that after 48 h, in MDA-MB-231 cells, MNPs-miR 329 transfected cells

covered almost 57% of the space while MNPs-miR control treated cells covered 84% (****$p < 0.0001$). In BT-20 cells, after MNPs-miR 329 treatment, the cells covered 30% compared to its control (72%, ***$p < 0.001$) (Figure 4.23 B). Similarly in MDA-MB-436 cells, 58% of space was covered using MNPs-miR 329 compared to MNP-miR control (78%, **$p < 0.01$) (Figure 4.23 C). In addition, overexpression of miR-329 via HiperFect also reduced the number of the migrated cells for all cell lines. 63% (81% miR-control, ***$p < 0.001$), 43% (69% miR-control, ***$p < 0.001$) and 61% (77% miR-control, *$p < 0.05$) of the spaces were covered using HiPerFect-miR 329 in MDA-MB-231, BT-20 and MDA-MB-436 cells, respectively. Moreover, the results also revealed that bare MNPs had no effect on cell migration.

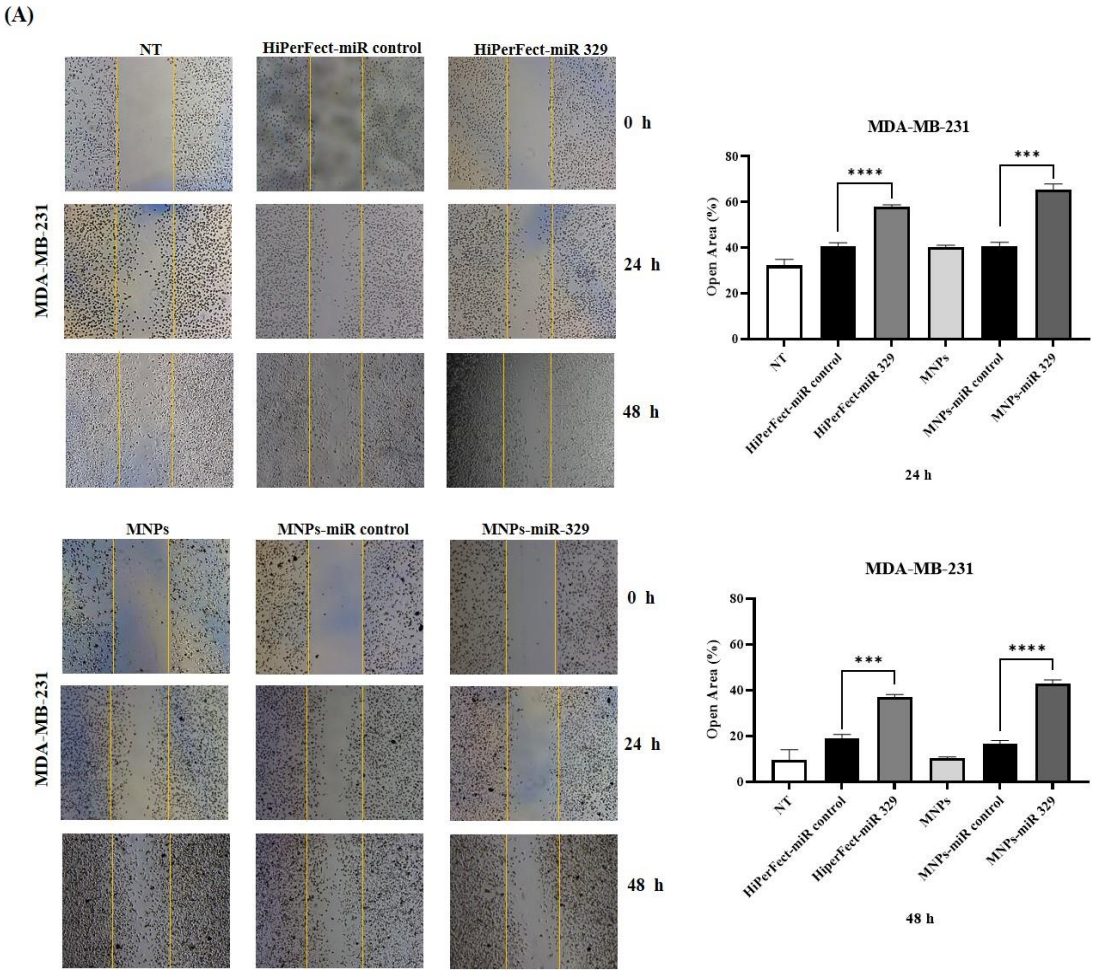

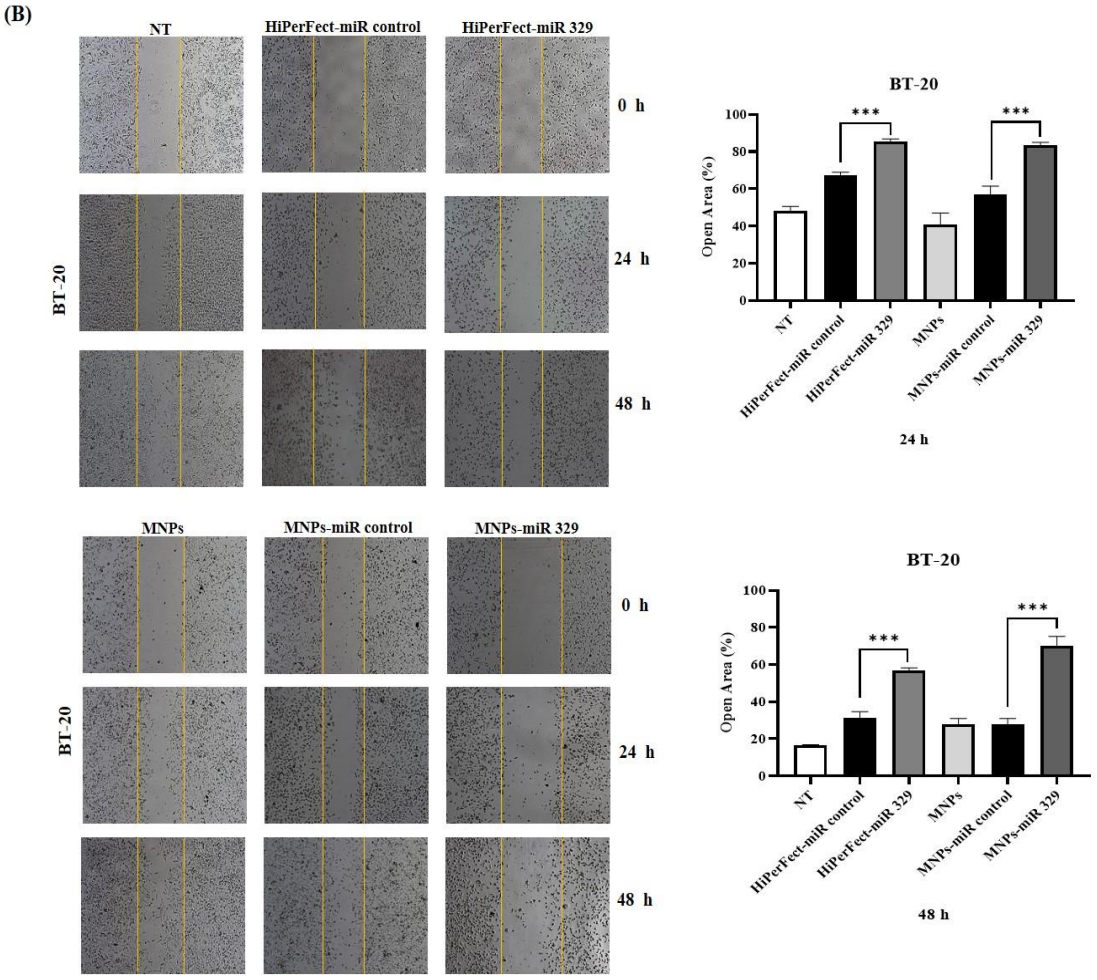
(B)
NT
HiPerFect-miR control
HiPerFect-miR 329
0 h
24 h
48 h
BT-20
MNPs
MNPs-miR control
MNPs-miR 329
BT-20
Open Area (%)
***
***
NT
HiPerFect-miR control
HiPerFect-miR 329
MNPs
MNPs-miR control
MNPs-miR 329
24 h
BT-20
Open Area (%)
***
***
48 h

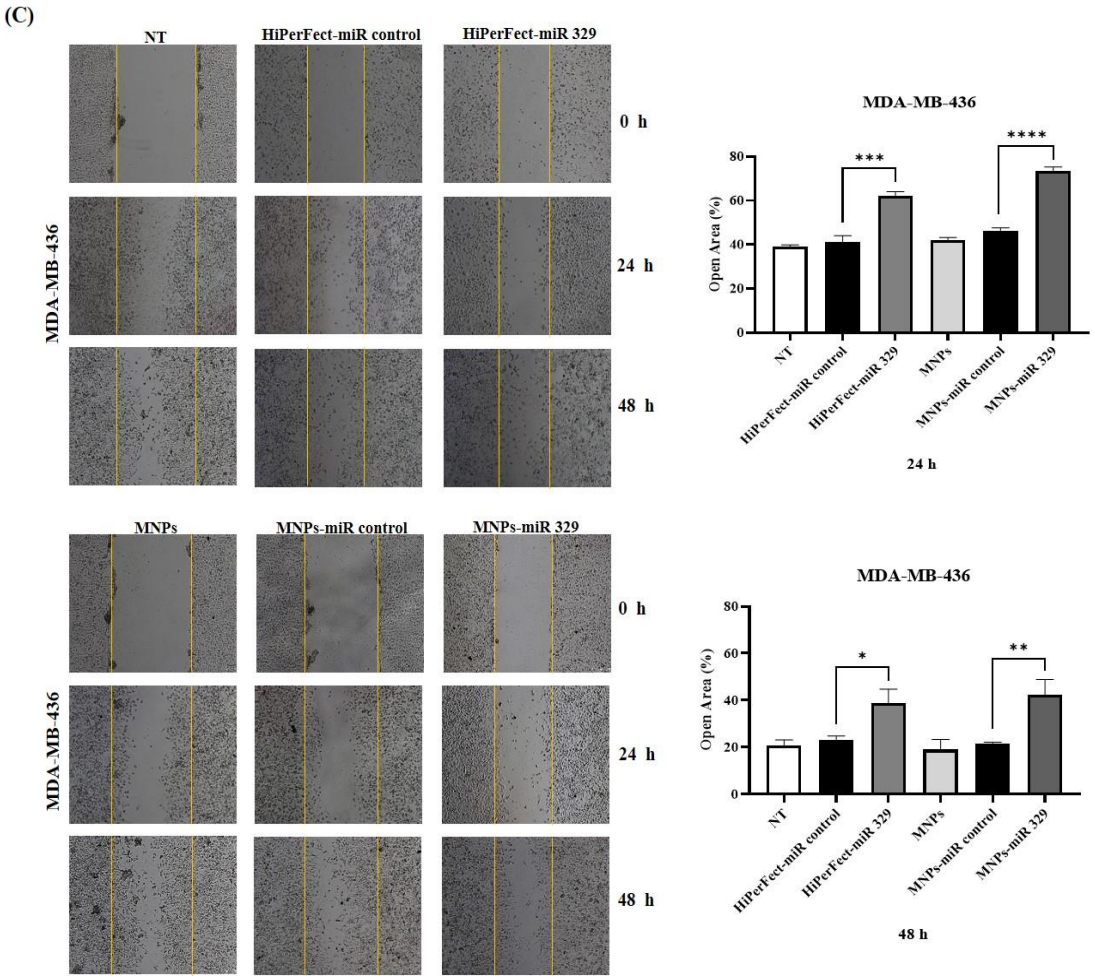

Figure 4.23. The effect of miR-329 expression on TNBC cell migration (A) MDA-MB-231, (B) BT-20 and (C) MDA-MB-436 cell lines

4.17. The Effect of Ectopic miR-329 Expression on Cell Invasion

In miR-329 treated TNBC cells, a significant decrease in the number of invasive cells was observed with either using HiPerFect or MNPs as a transfection reagent. The results are given in Figure 4.24. For MDA-MB-231 cell line, 48% of the cells invaded after HiPerFect-miR 329 treatment whereas 46% of the cells invaded after using MNPs-miR 329 compared to their controls, HiPerFect-miR control (97%, $^{****}p < 0.0001$) and MNPs-miR control (85%, $^{***}p < 0.001$), respectively. Similarly, for BT-20 cells, the percentage of invaded cells was found to be as 52% for HiPerFect-miR 329 treated group and 45% for MNPs-miR 329 treated group, in comparison with the control groups (99% and 90%, respectively, $^{***}p < 0.001$). The least number of invaded cells was obtained for MDA-MB-436 cells incubated with HiPerFect-miR 329 (30%) and MNPs-miR 329 (28%)

comparing to HiPerFect-miR control (96%, ***$p < 0.001$) and MNPs-miR control (73%, ***$p < 0.001$), respectively. Besides, the results also revealed that bare MNPs have no significant effect on cell invasion.

A)

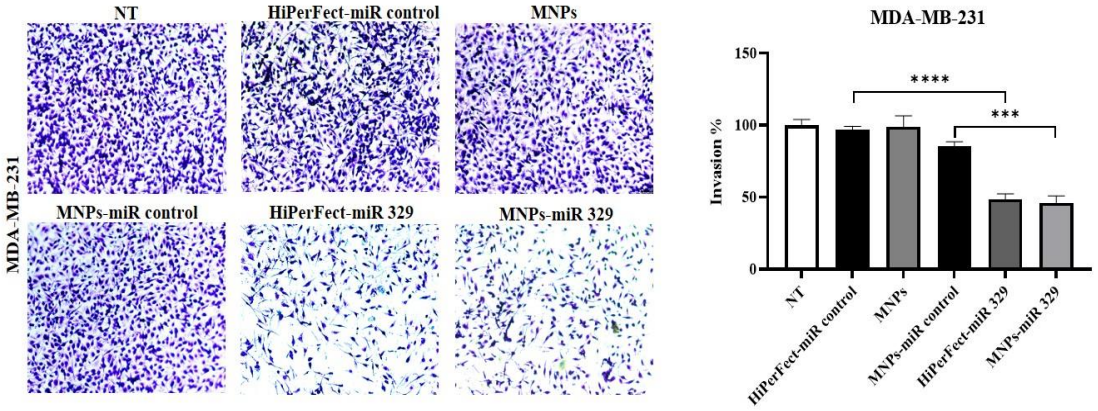

B)

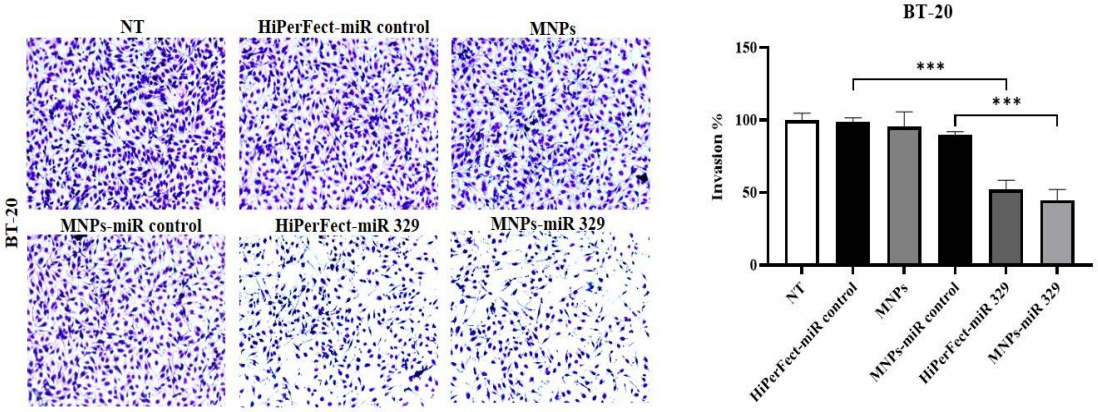

C)

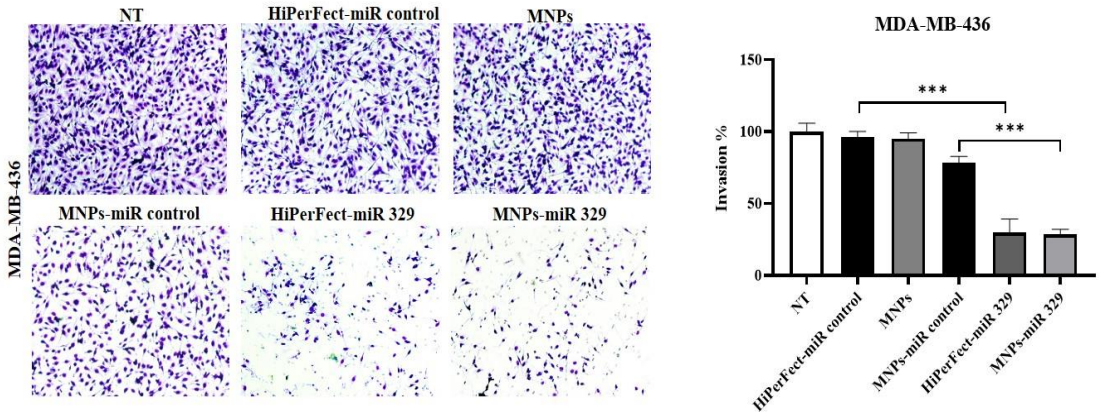

Figure 4.24. The effect of miR-329 expression on TNBC cell invasion (A) MDA-MB-231, (B) BT-20 and (C) MDA-MB-436 cell lines

4.18. The Effect of Ectopic miR-329 Expression on Apoptosis

Apoptosis analysis was carried out to elucidate the effects of miR-329 expression on apoptosis in MDA-MB-231 and MDA-MB-436 cells by using FITC Annexin V Apoptosis Detection Kit. The results are given in Figure 4.25 and 4.26. As it is seen, treating MDA-MB-231 and MDA-MB-436 cells with MNPs-miR 329 increased the number of apoptotic cells from 8% to 13% and from 5% to 10% comparing to the MNPs-miR control groups (*$p < 0.05$), respectively. Correlatively, using HiperFect as a miR-329 delivery reagent also resulted in an increased apoptosis rate for both cell lines. For example, in MDA-MB-231 cells, 14% apoptotic cells (comparing to HiPerFect-miR control (6%) **$p < 0.01$) were obtained while the percentage of the apoptotic cells was found to be 9% in MDA-MB-436 cells (comparing to HiPerFect-miR control (6%) *$p < 0.05$) after the treatments. These results revealed that miR-329 expression induced apoptosis rates for both used cell lines.

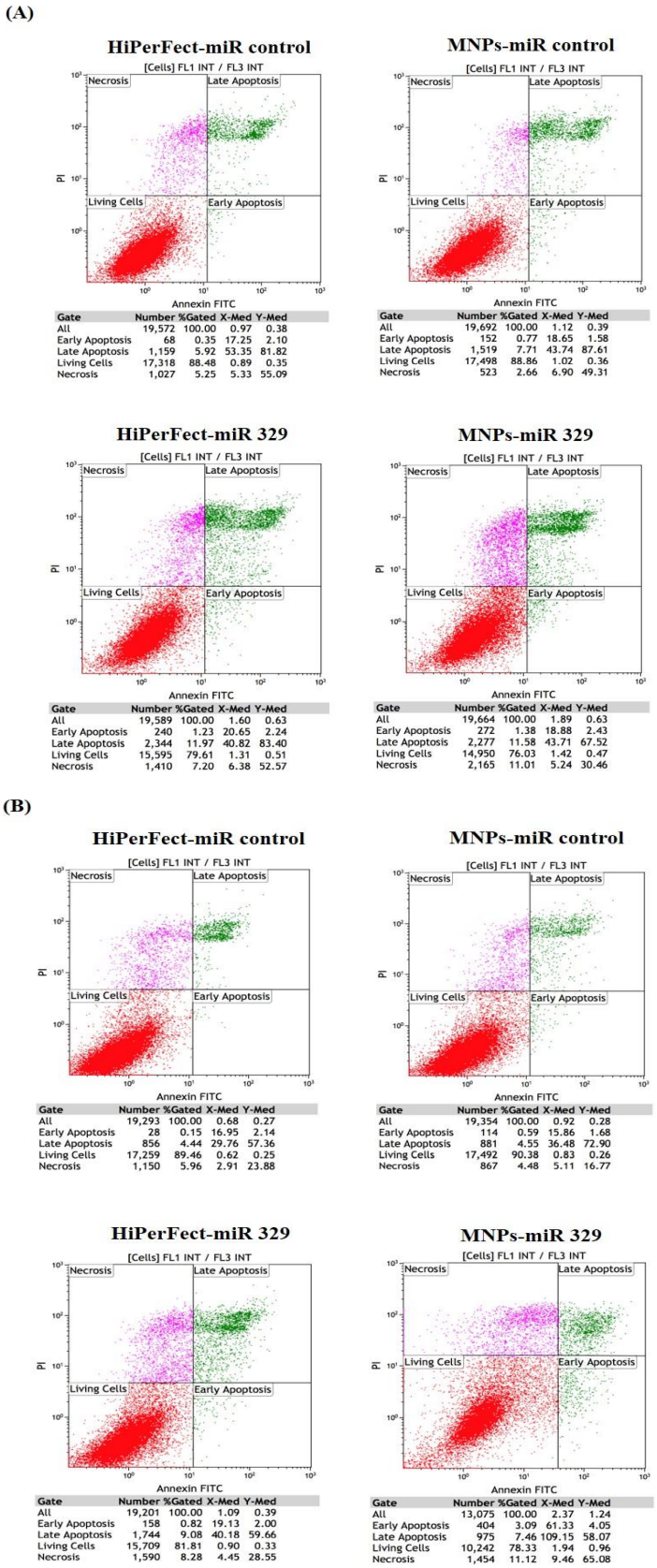

Figure 4.25. Flow cytometry results after treating the cells with miR-329 (A) MDA-MB-231 and (B) MDA-MB-436 cell lines

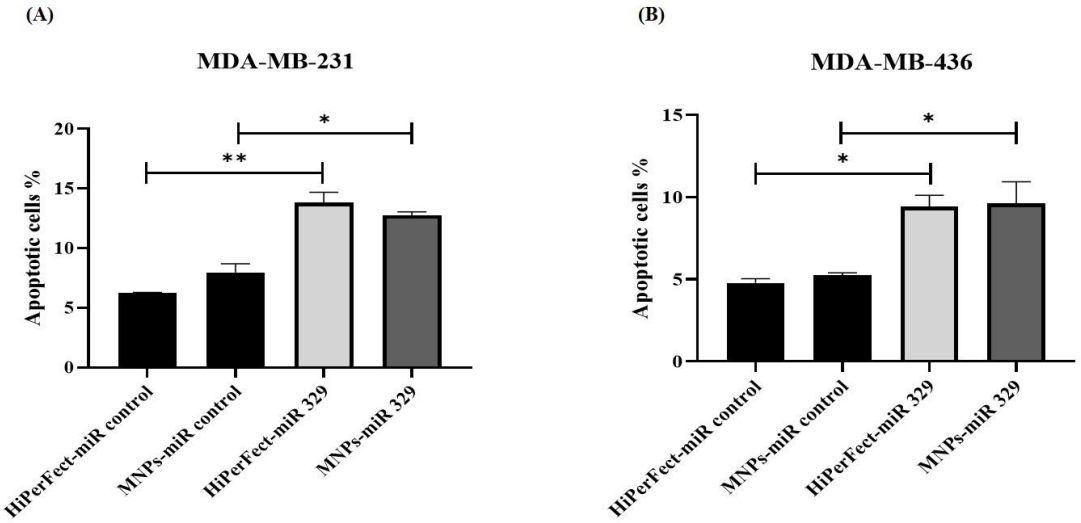

Figure 4.26. The apoptotic effect of ectopic miR-329 expression in TNBC cells (A) MDA-MB-231 and (B) MDA-MB-436 cell lines

4.19. The Effect of Ectopic miR-329 Expression on TNBC Cells at Molecular Level

In Figure 4.20, it was previously demonstrated that miR-329 delivery by MNPs and HiPerFect in all TNBC cells led to a drastic inhibition in eEF2K and AXL protein levels. Further, the affected downstream targets and signaling pathways were identified after miR-329 expression in MDA-MB-231, BT-20 and MDA-MB-436 cells. A remarkable decrease in TNBC cell migration and invasion was previously showed in Figure 4.23 and 4.24 as a result of the treatment with miR-329. To elucidate the inhibiting effect of miR-329 in migration and invasion at molecular level, Src and FAK protein levels in the cells were examined. Src is a protein that regulates migration, invasion, adhesion and proliferation in BC cells. FAK is a protein that auto phosphorylated on Tyr-397 and has a key role in migration and cell adhesion [204]. As demonstrated in Figure 4.27, a significant knockdown was observed in p-Src and p-FAK after miR-329 overexpression in TNBC cells while no changes were observed in total Src and total FAK. Moreover, the level of cyclin D1, which is involved in cell cycle and development/progression of cancer [204], was also dramatically inhibited after miR-329 treatment in all TNBC cells (Figure 4.27). Comparing the potential of MNPs and HiPerFect considering inhibition of target proteins, both nano-carrier systems exhibited almost same powerful effect.

(A)

MDA-MB-231

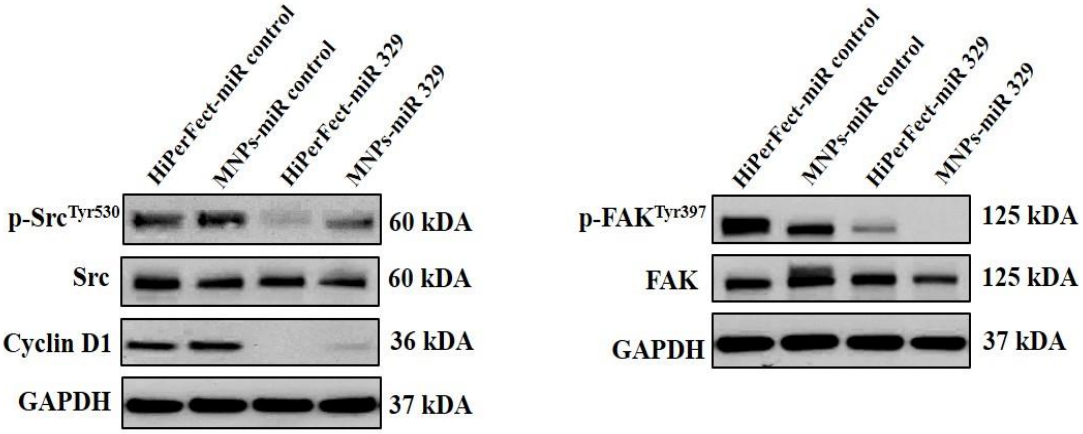

(B)

BT-20

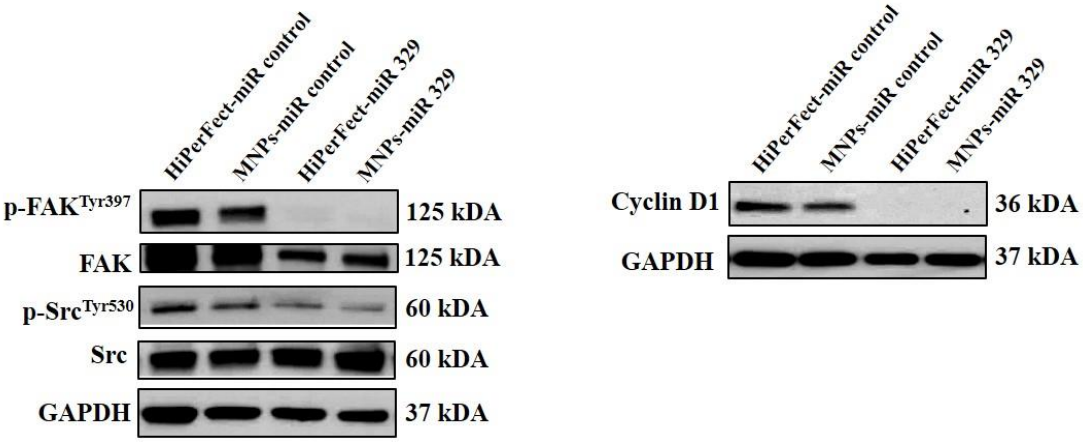

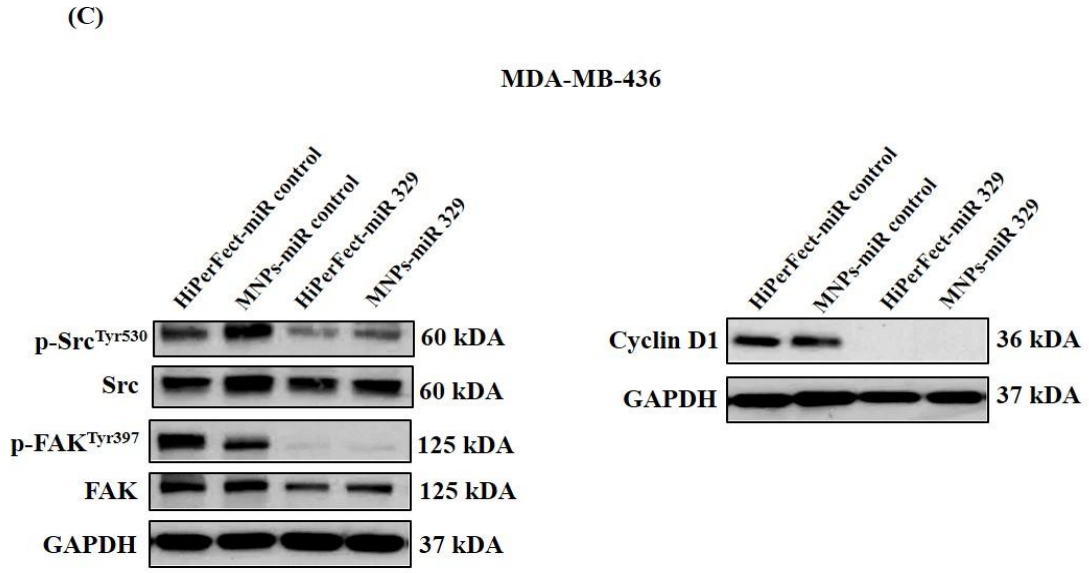

Figure 4.27. The effect of ectopic miR-329 expression on downstream targets and signaling pathways in TNBC cells (A) MDA-MB-231 and (B) BT-20 and (C) MDA-MB-436 cell lines

4.20. The Effect of Suppressed eEF2K and AXL Levels on Clonogenicity

To confirm the reduced cell proliferation, migration and invasion activity that miR-329 expression leads through eEF2K and AXL inhibition, the influence of eEF2K and AXL knockdown on cell proliferation, migration/invasion in TNBC cells was examined. For this purpose, MDA-MB-231, BT-20 and MDA-MB-436 cells were also treated with eEF2K siRNA, AXL siRNA and eEF2K+AXL siRNA by using only HiPerFect as a siRNA transfection reagent.

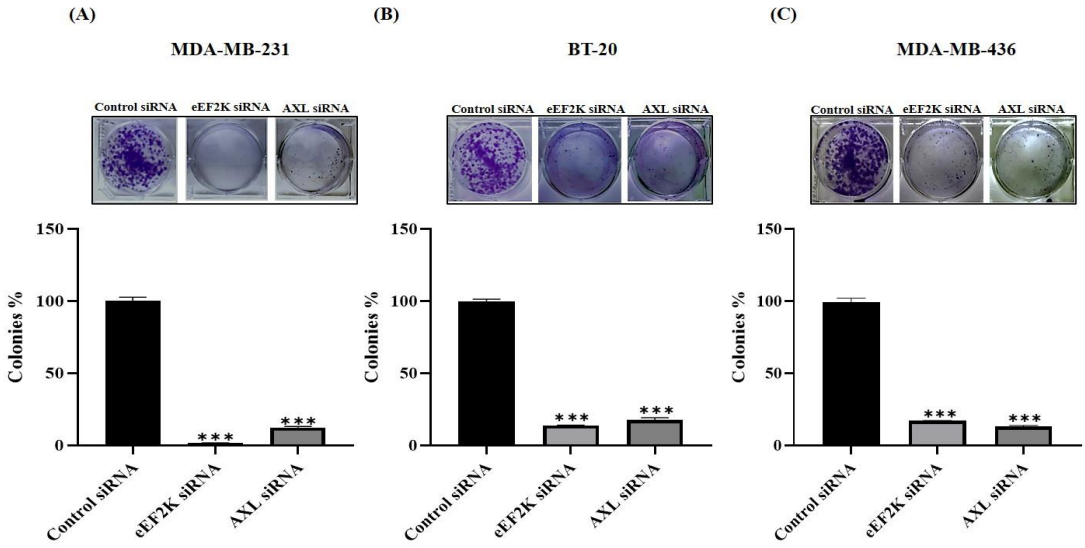

Figure 4.28. The effect of eEF2K and AXL inhibition on TNBC cell clonogenicity (A) MDA-MB-231, (B) BT-20 and (C) MDA-MB-436 cell lines

As it is seen in Figure 4.28 knockdown of eEF2K and AXL led to a significant reduction in colony formation of TNBC cells. In MDA-MB-231 cells 2% (***$p < 0.001$) and 12% (***$p < 0.001$) of colonies were formed when the cells interacted with eEF2K and AXL siRNA (in comparison to control-siRNA treated cells), respectively. Moreover, the percentages of the colonies formed in BT-20 and MDA-MB-436 cells were found to be as 14% (***$p < 0.001$) and 17% (***$p < 0.001$) for eEF2K siRNA treated cells. AXL downregulation by specific siRNA treatment exhibited a drastic inhibitory effect resulting in formation of colonies as 18% (***$p < 0.001$) and 13% (***$p < 0.001$) for BT-20 and MDA-MB-436 cells, respectively.

4.21. The Effects of eEF2K and AXL Knockdown on Cell Migration/Invasion

Migration and invasion activities were also analyzed in eEF2K and AXL siRNA treated TNBC cells. The wound healing assay results are given in Figure 4.29, 4.30 and 4.31. It was observed that the number of migrated cells was significantly reduced after silencing eEF2K and AXL in the cells. Figure 4.29 indicates that for MDA-MB-231 cells, 48%, 44% and 42% of the spaces were covered after eEF2K, AXL and eEF2K+AXL siRNA treatments, respectively, comparing to the control-siRNA treated cells (****$p < 0.0001$).

Figure 4.30 shows that these values were found to be as 67%, 42% and 48% in eEF2K, AXL and eEF2K+AXL siRNA treated BT-20 cells, respectively, (****$p < 0.0001$). In addition, in MDA-MB-436 cells silencing eEF2K, AXL and eEF2K+AXL led to cells to cover the 52%, 49% and 33% of the spaces, respectively, (****$p < 0.0001$) (Figure 4.31).

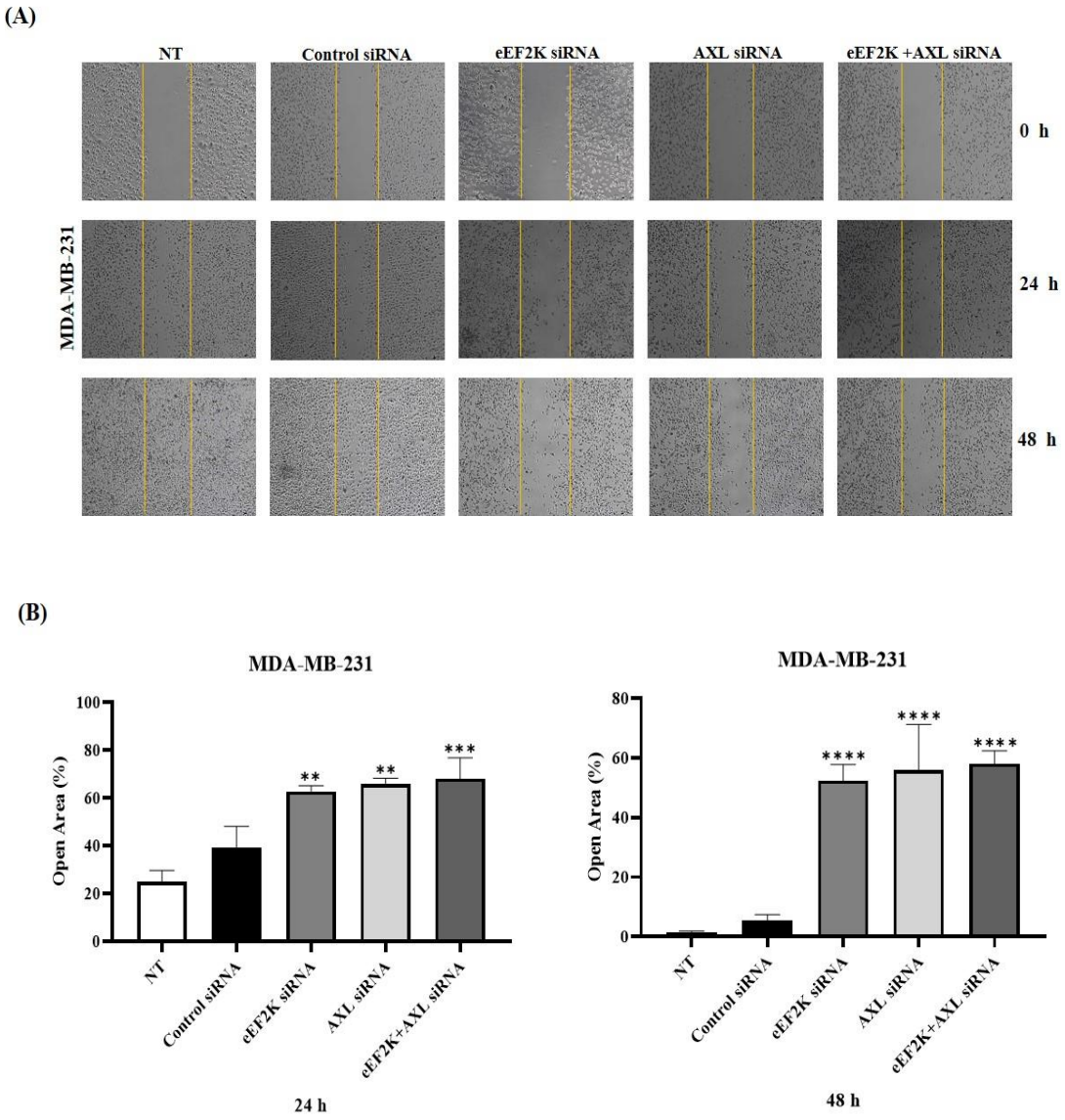

Figure 4.29. The effect of eEF2K and AXL knockdown on MDA-MB-231 cell migration (A) Cell images after 0 h, 24 h and 48 h (B) Open area (%) of the space for 24 h and 48 h

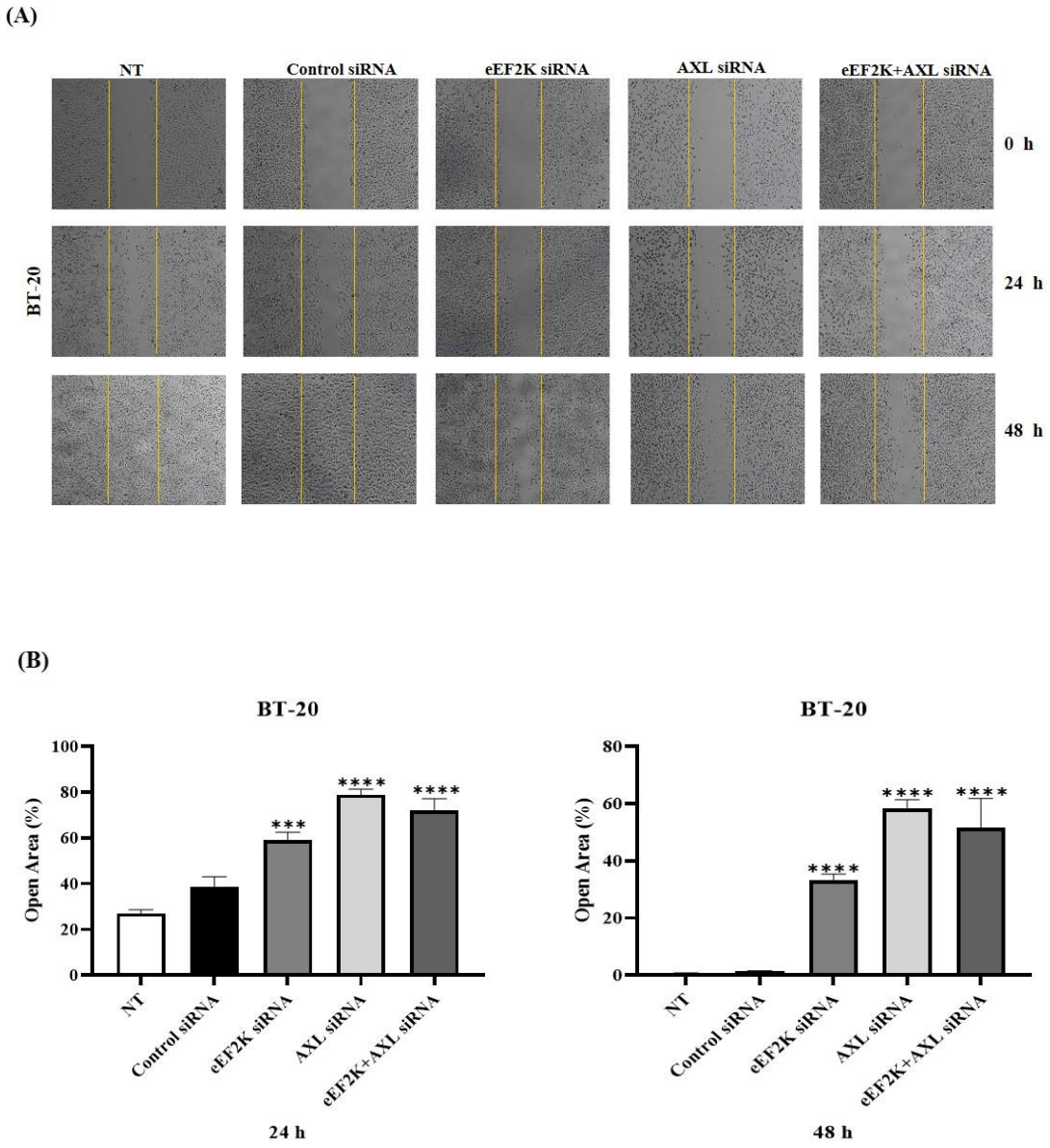

Figure 4.30. The effect of eEF2K and AXL knockdown on BT-20 cell migration (A) Cell images after 0 h, 24 h and 48 h (B) Open area (%) of the space for 24 h and 48 h

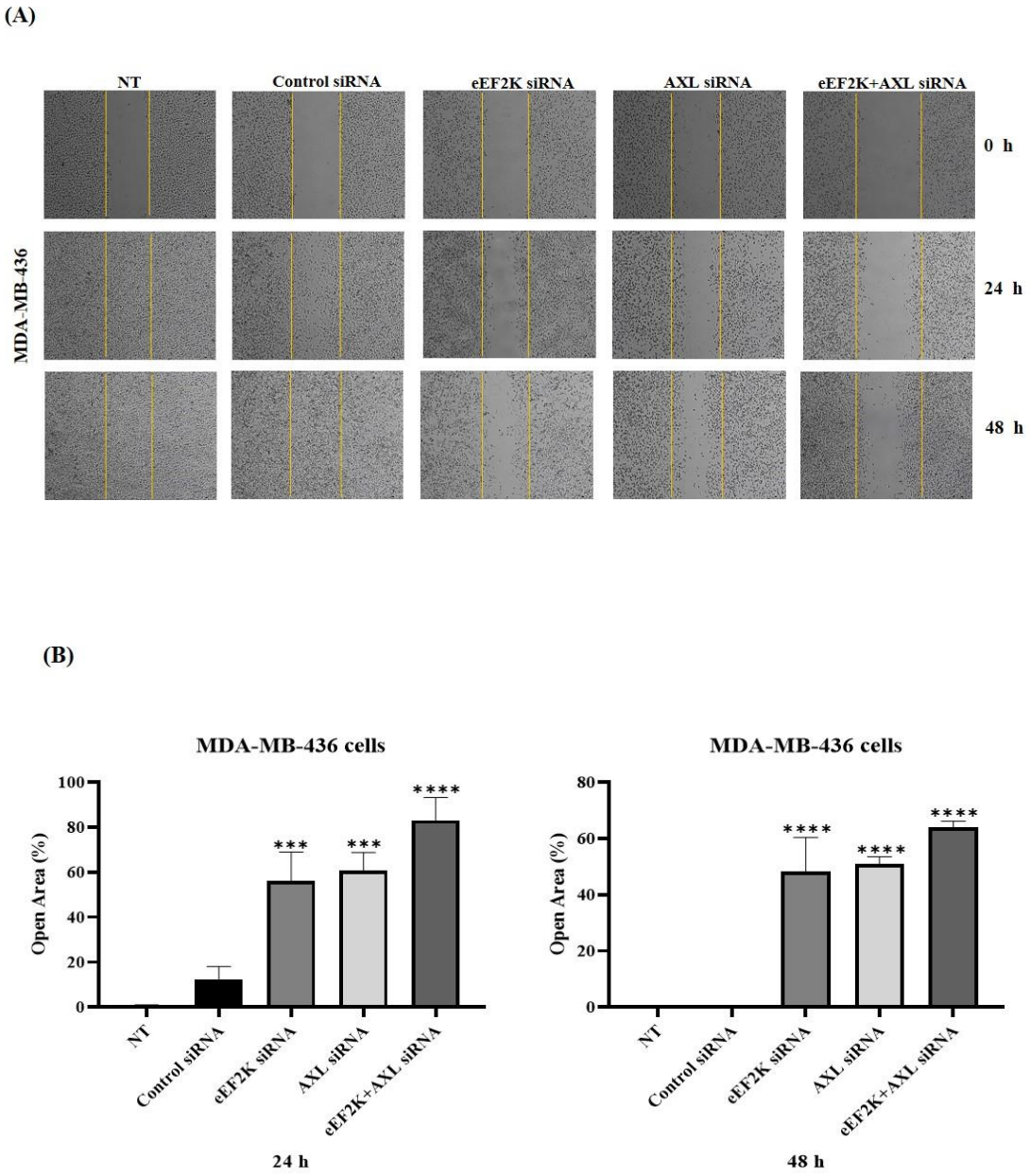

Figure 4.31. The effect of eEF2K and AXL knockdown on MDA-MB-436 cell migration (A) Cell images after 0 h, 24 h and 48 h (B) Open area (%) of the space for 24 h and 48 h

(A)

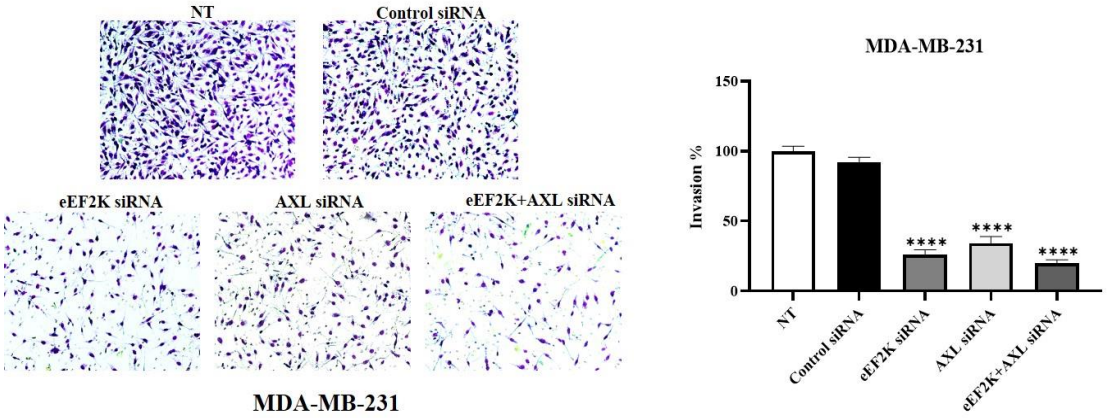

(B)

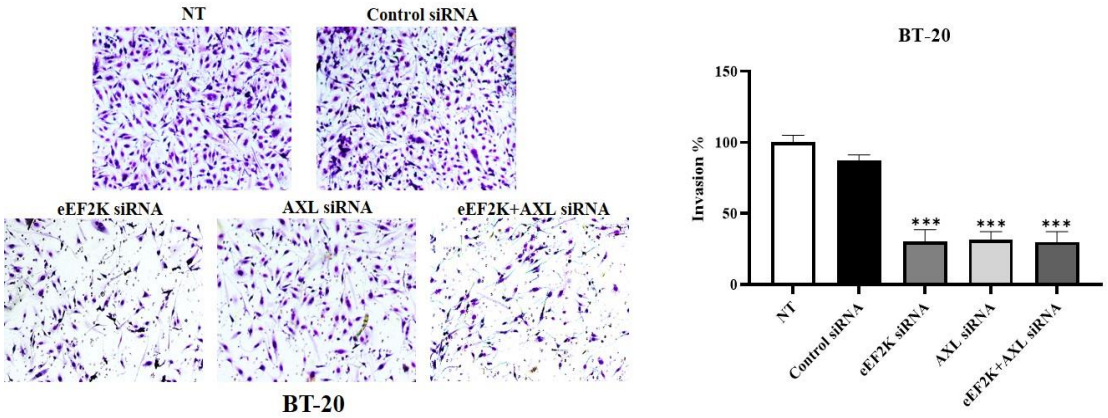

(C)

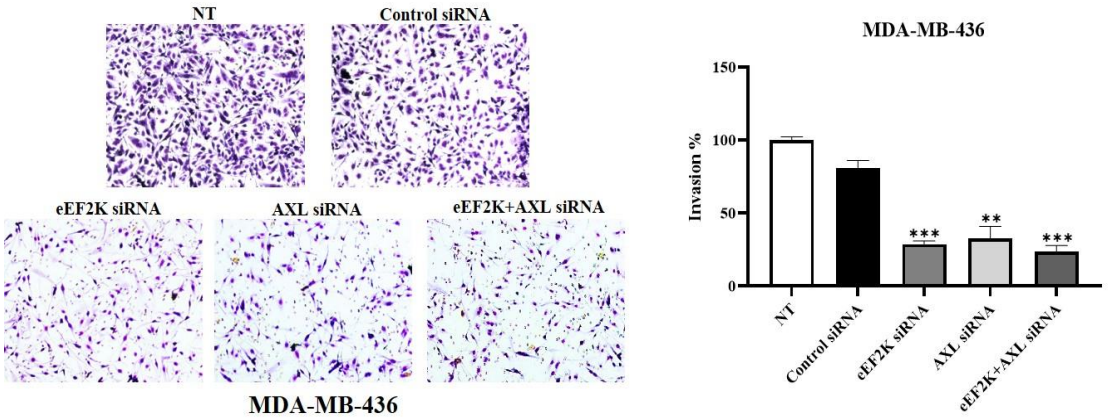

Figure 4.32. The effect of eEF2K and AXL knockdown on TNBC cell invasion (A) MDA-MB-231, (B) BT-20 and (C) MDA-MB-436 cell lines

In Figure 4.32, it was demonstrated that when the cells were interacted eEF2K, AXL and eEF2K+AXL siRNA, the number of invaded cells were dramatically decreased. After knockdown of eEF2K, AXL and eEF2K+AXL in MDA-MB-231 cell line, 26%, 34% and 20% of the cells invaded, respectively, compared to control-siRNA (****$p < 0.0001$) (Figure 4.32 A). Similar results were obtained considering the percentage of the invaded cells for BT-20 (30%, 31% and 30%) after eEF2K, AXL and eEF2K+AXL siRNA treatments, respectively, comparing to control-siRNA (***$p < 0.001$) (Figure 4.32 B) and for MDA-MB-436 cells (29%, 33% and 24%) after eEF2K siRNA (***$p < 0.001$), AXL siRNA (**$p < 0.01$) and eEF2K+AXL siRNA (***$p < 0.001$) treatments, respectively, comparing to control-siRNA. (Figure 4.32 C).

The results demonstrated in Figures 4.28, 4.29, 4.30, 4.31 and 4.32 reveal that silencing eEF2K and AXL leads to a remarkable reduction in colony formation, migration and invasion of TNBC cells. Inhibition of eEF2K and AXL recapitulates the effects of miR-329 confirming that the effects of miR-329 ectopic expression are mediated through eEF2K and AXL downregulation.

4.22. The Effect of eEF2K and AXL Knockdown on TNBC Cells at Molecular Level

To confirm that the effect of miR-329 in cells at molecular level is as a result of its targeting and inhibiting ability to eEF2K and AXL, the cells were also transfected with eEF2K and AXL siRNA, and the samples were analyzed by Western Blot assay. Figure 4.33 demonstrates that silencing eEF2K and AXL by specific siRNAs markedly downregulated the expression levels of eEF2K, AXL, p-Src, p-FAK and Cyclin D1 compared to the cells treated with control-siRNA. The expression levels of total Src and FAK did not change. Observing similar molecular effects after miR-329 mimic or eEF2K/AXL siRNA treatments in TNBC cells confirms that miR-329 recapitulates the effects of eEF2K and AXL downregulation.

(A)

MDA-MB-231

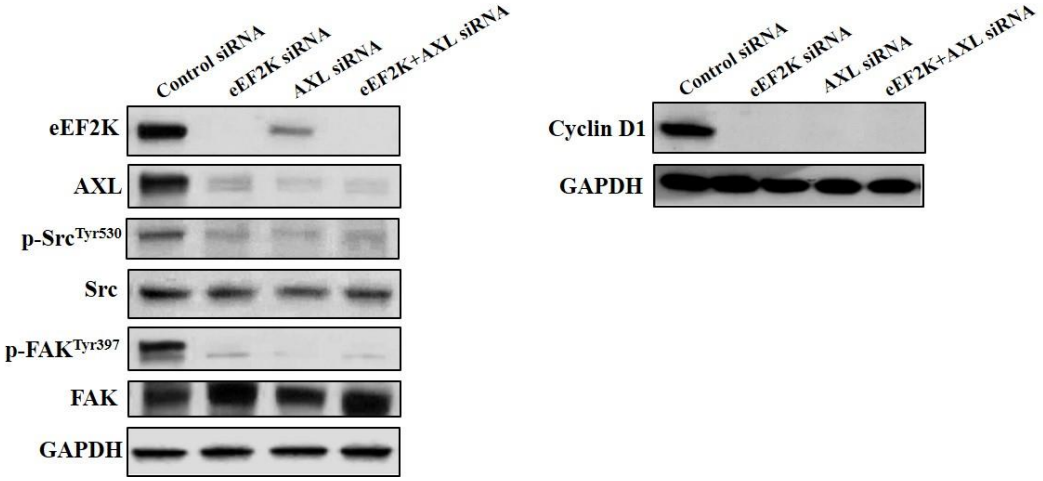

(B)

BT-20

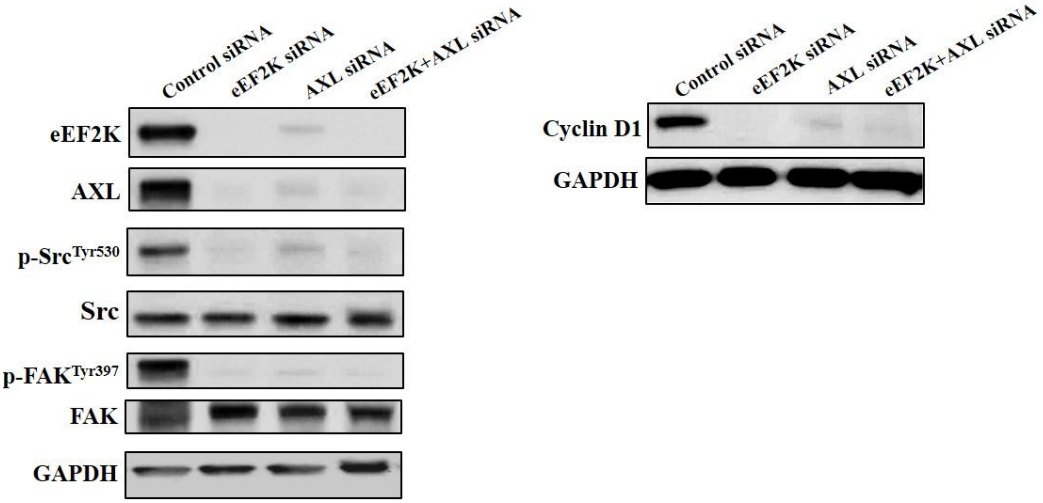

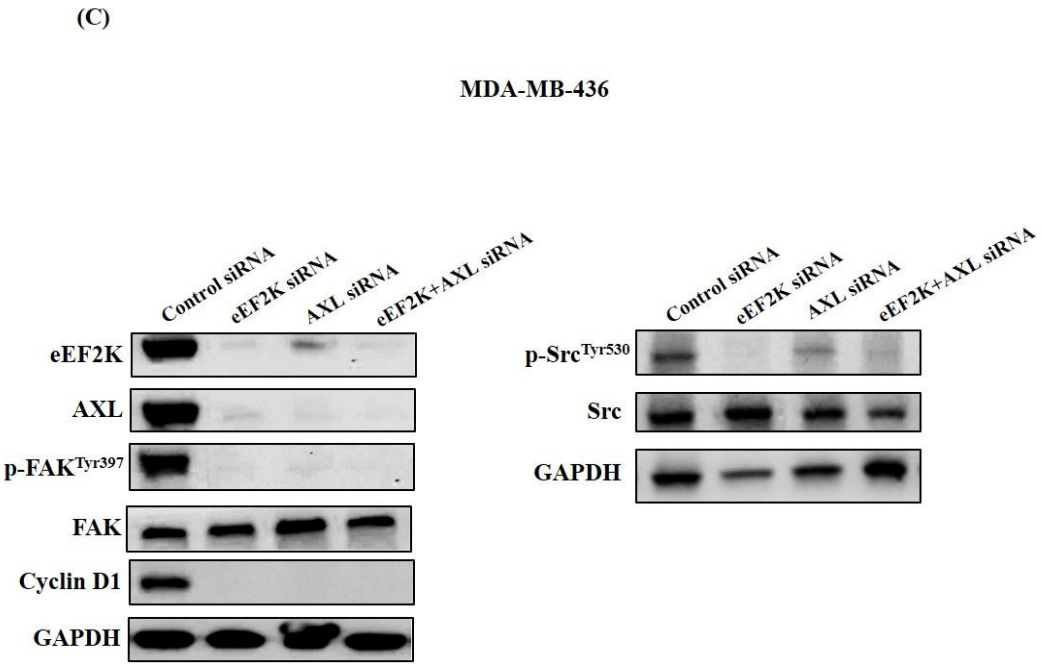

Figure 4.33. The effect of eEF2K and AXL knockdown on TNBC cells at molecular level (A) MDA-MB-231, (B) BT-20 and (C) MDA-MB-436 cell lines

4.23. Animal Studies

To elucidate the role of miR-329 as a therapeutically potential target in TNBC tumor growth, tumorigenesis and progression, MNPs based miR-329 therapy was intraperitoneally administrated into MDA-MB-231 and MDA-MB-436 orthotopic xenograft models in nude mice. About 2 weeks later of implanting the cells into the mammary fat pad of mice, MNPs-miR 329 and MNPs-miR control groups were injected weekly during four weeks of treatment. No detectable toxicity was observed in mice at the end of the treatments. The tumor volumes of each mouse were measured once a week and the results are given in Figure 4.34 and Figure 4.36 for MDA-MB-231 and MDA-MB-436 tumor model, respectively. The results demonstrate that in both model, the rate of tumor growth in the mice treated with MNPs-miR 329 is remarkably lower than that the mice treated with MNPs-miR control. The xenograft tumors were collected and analyzed by Western Blot assay for eEF2K, AXL and several downstream targets involved in cell proliferation, migration/invasion. As shown in Figure 4.35 and 4.37, in vivo delivery of miR-329 via MNPs drastically inhibited the protein levels of eEF2K or p-EF2, AXL, p-

Src, p-FAK and Cyclin D1 in MDA-MB-231 and MDA-MB-436 xenograft models in nude mice.

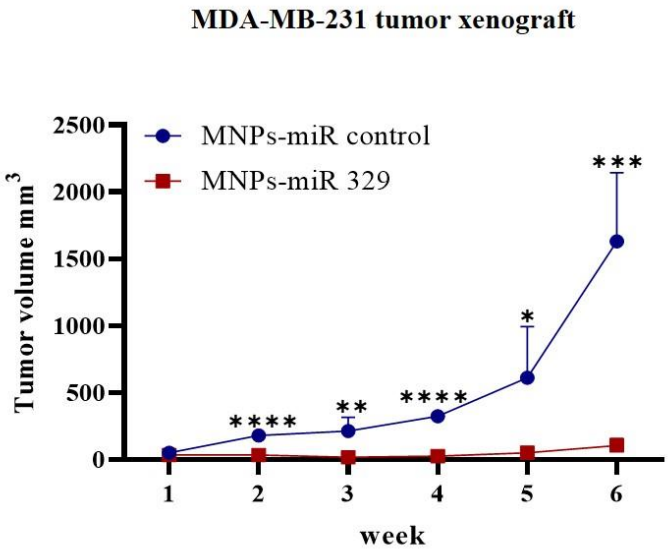

Figure 4.34. The tumor volumes of MDA-MB-231 orthotopic xenograft model in mice after MNPs-miR 329 treatment

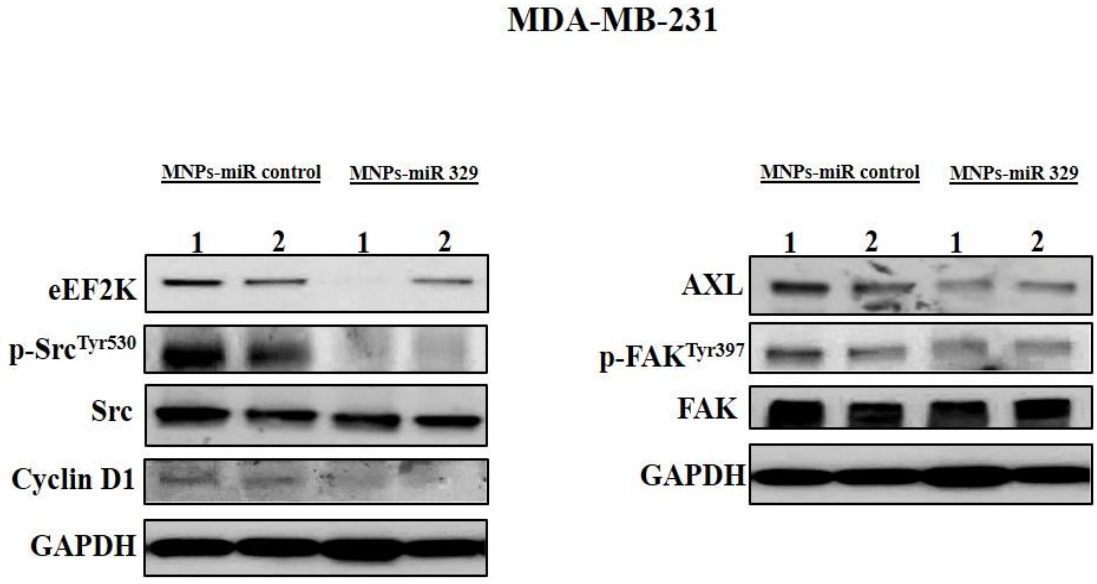

Figure 4.35. The molecular effect of MNPs-miR 329 treatment in MDA-MB-231 orthotopic xenograft model in mice

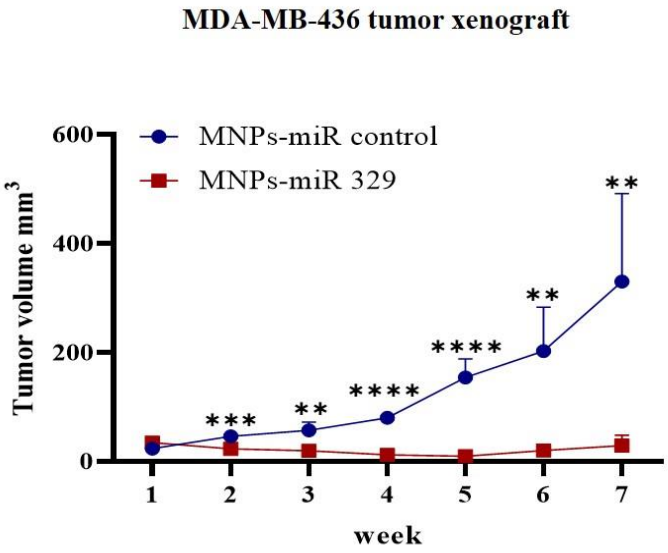

Figure 4.36. The tumor volumes of MDA-MB-436 orthotopic xenograft model in mice after MNPs-miR 329 treatment

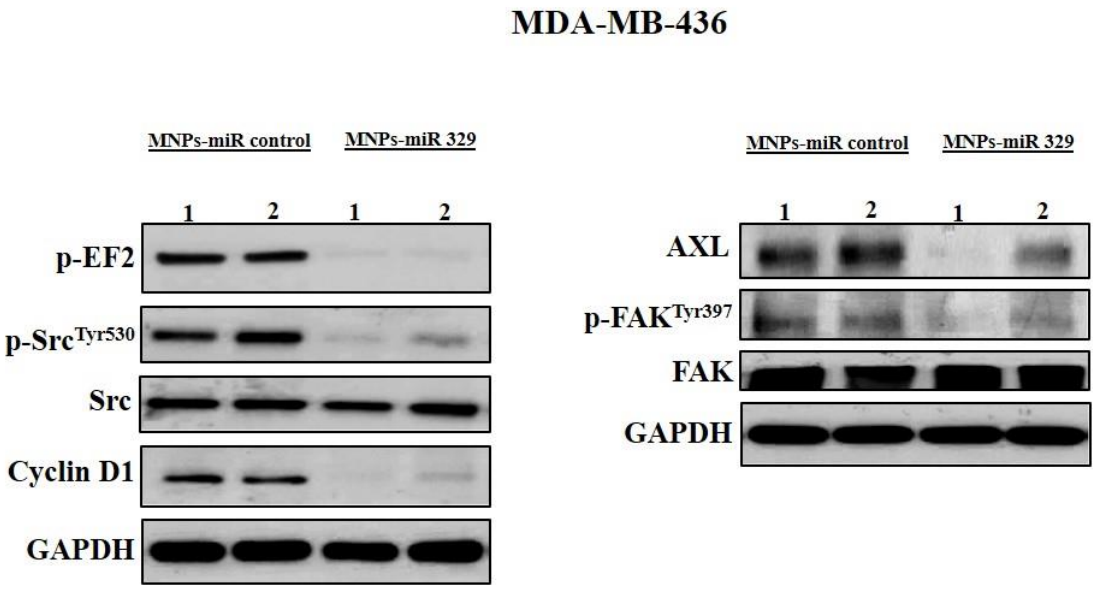

Figure 4.37. The molecular effect of MNPs-miR 329 treatment in MDA-MB-436 orthotopic xenograft model in mice.

This study reported for the first time that miR-329 mimic has a tumor suppressor role in TNBC by directly inhibiting the expression levels of eEF2K and AXL, and resulting in a drastic reduction in cell proliferation, invasion/migration and tumorigenesis. Moreover, it was also demonstrated for the first time that using novel PLL/Ser-SPIONs (in the study it was abbreviated as 'MNPs') as a transfection agent can enable successful delivery of miR-329 and hence specific downregulation of eEF2K and AXL in vitro and in vivo orthotopic tumor models, providing a highly potential and safe carrier system to be used for novel miRNA therapeutics.

Recent studies have revealed that eEF2K is a significant molecule in several cancer types such as brain, pancreatic and breast cancer [200, 201, 205, 206, 234, 235]. It is a calcium/calmodulin activated member of α-kinase family and promotes protein synthesis, induction of autophagy, apoptosis and cell cycle progression in cancer cells [236, 237]. Phosphorylation and inactivation of eEF2 (at threonine 56) regulate the activity of eEF2K and thereby protein chain elongation rate [238-240]. eEF2K is also included in cell survival during nutrient deprivation, DNA damage, metabolic stress and hypoxia via regulating the translation rate [241, 242]. It was previously reported that eEF2K is involved in several cellular processes such as cell proliferation, invasion/migration, progression and tumorigenesis of TNBC as a result of regulation in cyclin D1, c-myc, PI3K/Akt, Src, FAK signaling pathways [205, 206, 234].

AXL, the ligand of GAS6 and a member of the RTK family, plays an important role in a number of biological processes that regulate proliferation, migration, survival, invasion, autophagy, drug resistance and angiogenesis [208, 209]. The numerous studies indicating the high expression levels of AXL in ovarian, prostate, lung, pancreas and breast cancer and the remarkable correlation between the AXL expression and the tumor stage made AXL a potential oncogenic target in patients [216].

Since recent reports suggest that eEF2K and AXL are critical prognostic factors and potential molecular targets in BC, targeting strategies against those molecules may be a promising approach for the development of novel treatment options for TNBC. In a work by Bayraktar et al. [204] eEF2K was reported as highly overexpressed in TNBC cells. In addition to this, in the current study it was also demonstrated that TNBC cells have high expression levels of AXL. Furthermore, as a result of an extensive analysis of miR database, it was found that miR-329 expression is related with significantly longer survival

in TNBC patients. More important, it was demonstrated that miR-329 expression is lost or dramatically reduced in the majority of TNBC cell lines comparing to non-cancerous breast cells.

In various cancer types such as glioma, lung, melanoma, pancreatic and ER/PR(+) breast cancer, the expression of miR-329 was determined to be deregulated and inversely correlated with pathological characteristics [22-26]. However, the potential role and molecular mechanism of miR-329 as a miRNA therapeutic was not identified in TNBC.

In the present study, it was showed that in vitro and in vivo overexpression of miR-329 recapitulates the effect of eEF2K and AXL knockdown in TNBC that results in inhibition of cancer cell proliferation, migration/invasion and tumor growth/progression. Not surprisingly, in vivo delivery of miR-329 in mice elicited Src/FAK and Cyclin D1 inhibition revealing that regulation of these pathways by miR-329 is associated with eEF2K and AXL suppression. Given that results of inducing miR-329 expression or silencing eEF2K and AXL by siRNA-based strategies inhibit tumor growth in mice, it can be suggested that the targeting therapeutic strategies for miR-329/eEF2K and miR-329/AXL may provide extensive antitumor effects in consequence of inhibition of multiple oncogenic pathways.

miRNA replacement therapy has emerged as a promising therapeutic option by regulating specific genes which possess important roles in many pathological processes [243]. The potential use of therapeutic miRNAs against cancer is being investigated in clinical trials in the US [244]. The significant antitumor efficacy of ncRNA such as siRNAs and miRNAs has been proved by several recent studies if RNA molecules are delivered properly into tumors [244, 245]. Therefore, a safe and clinically feasible delivery tools are required for efficient cancer treatment.

In the current study, a nano-carrier system was developed to be used as a delivery tool for miR-329 for the in vitro and in vivo TNBC therapy. miR-329 loaded MNPs were produced, and the target proteins inhibiting and subsequently resulting cellular effects of those nano-therapy systems were investigated. MNPs have been used for many years as a drug/gene delivery tool and MRI agent with their unique properties. Small dimensions that MNPs have enable them to localize in the narrowest blood vessel and penetrate the cell membrane. In addition, they can be directed by an external magnetic field in

the targeted area to deliver their therapeutic drug or gene payload with their ferromagnetic and superparamagnetic properties [176]. In this work, using MNPs as a transfection reagent provided a safe and efficient delivery of miR-329 in vitro and in vivo resulting in a significant inhibition of eEF2K and AXL. With the enhanced permeability and retention (EPR) effect, MNPs may successfully escape the reticuloendothelial system (RES) and accumulate into the tumor. Taken together, this MNPs-miR 329 is found to be a promising and useful tool for TNBC cancer therapy. Due to the multifunctional roles of MNPs in cancer biology such as monitoring, diagnosis, targeting and therapy [172], it is also suggested that these produced MNPs may also be useful for imaging applications for cancer detection in further studies.

5. CONCLUSION

- SPIONs, APTES-SPIONs, Ser-SPIONs and PLL/Ser-SPIONs were successfully synthesized and characterized. The size range of the all produced nanoparticles was measured as between 10 and 30 nm after TEM analysis. The zeta potential of the nanoparticles was found to be as 20.50 mV, 33.03 mV, -9.20 mV and 13.10 mV for SPIONs, APTES-SPIONs, Ser-SPIONs and PLL/Ser-SPIONs, respectively, by DLS measurements. After loading PLL/Ser-SPIONs with miR-control at concentrations of 25 nM, 50 nM and 100 nM, zeta potential values of the obtained nanoparticles were measured as -11.34 mV, -12.75 mV and -14.80 mV.

- FTIR analysis results proved that all samples (Sericin, SPIONs, APTES-SPIONs, Ser-SPIONs and PLL/Ser-SPIONs) were synthesized successfully.

- SPIONs and PLL/Ser-SPIONs synthesized in the studies were found to exhibit magnetic properties by ESR analysis.

- To evaluate the in vitro degradation behaviours of PLL/Ser-SPIONs at pH 7.4 and 5.5, the nanoparticles were incubated at 37^{o}C in PBS containing lysozyme. The mass remainings (%) of the nanoparticles in 15 days were 85% and 83% incubated in pH 5.5 and 7.4, respectively. According to the obtained results, PLL/Ser-SPIONs exhibited a controllable degradation profile and fulfilled all the requirements for a proper drug delivery system.

- For the storage stability of Ser-SPIONs and PLL/Ser-SPIONs, after four weeks incubation of nanoparticles at 4^{o}C in PBS, the percentage of intact nanoparticle content was found as 92% and 98% for Ser-SPIONs and PLL/Ser-SPIONs, respectively.

- PLL/Ser-SPIONs were interacted with miR-controls having concentrations of 25 nM, 50 nM and 100 nM and the binding efficiencies (%) of each MNPs-miR control were determined using a fluorometric method. 99.3%, 98.5% and 97.7% binding efficiencies were achieved when using 25 nM, 50 nM and 100 nM of miR-control, respectively.

- The in vitro release of miR-329 from PLL/Ser-SPIONs was evaluated using various miRNA concentrations (25 nM-50 nM-100 nM). All miRNA loaded nanoparticles showed a slow and sustained release profile that contributes to prolonging miRNA effectiveness.

- The intracellular localization of produced MNPs-miR-control in MDA-MB-231 cells was evaluated via TEM analysis. According to the results, incubating the cells with the MNPs-miR control systems for 24 h led to a successful localization in cell cytoplasm.

- High uptake of control siRNA-Alexa Flour 555 loaded MNPs by MDA-MB-231 cells was observed by confocal microscopy analysis.

- Non-significant cytotoxicity and reduction in colony formation ability of bare nanoparticles against non-cancerous (L929) and TNBC cells were observed. Only very high amount of nanoparticles showed a significant toxic effect and inhibition in colony formation.

- Several miR databases were broadly investigated and showed that miR-329 expression is associated with significantly longer survival in patients with TNBC.

- RT-qPCR analysis revealed that in the majority of TNBC cell lines, miR-329 expression level is lost or markedly reduced.

- In vitro expression of miR-329 mimic using either MNPs or a commercially available transfection reagent successfully suppressed cell proliferation, colony formation, invasion and migration inhibiting the levels of eEF2K and AXL in TNBC. Downregulation of eEF2K and AXL by using specific siRNAs recapitulated the effects of ectopic expression of miR-329 and significantly reduced TNBC cell proliferation, colony formation, invasion and migration.

- In vivo delivery of miR-329 by using MNPs into TNBC orthotopic xenograft mouse models led to a drastic inhibition of tumor growth and knockdown of

eEF2K and AXL expression. In vivo inhibition of eEF2K and AXL decreased the expression levels of Src/FAK and cyclin D1 that have key roles in invasion/migration and cell cycle pathways, respectively. Remarkably, PLL/Ser-SPIONs based miR-329 therapy in mice did not cause any side effects suggesting that miR-329 mimic nano-therapy is a safe and clinically feasible approach.

In conclusion, the presented study demonstrated for the first time that miR-329 acts as a tumor suppressor molecule in TNBC and its expression is associated with cell proliferation, migration/invasion and tumorigenesis. miR-329 expression in TNBC is found to have the ability of directly targeting and inhibiting eEF2K and AXL and subsequently suppress several hallmarks of cancer. Therefore, miR-329 mimic replacement therapy may be a novel and potential therapeutic approach for TNBC. This study also revealed that PLL/Ser-SPIONs based miRNA delivery system can effectively inhibit in vivo tumor tissue growth and the target genes. This novel nano-carrier has a potential for a useful and safe approach for the delivery of miRNA-based therapeutics for cancer treatment.

6. REFERENCES

[1] P. Boyle, The globalisation of cancer, Lancet (London, England), 368 (**2006**) 629.

[2] A. Jemal, F. Bray, M.M. Center, J. Ferlay, E. Ward, D. Forman, Global cancer statistics, CA: a cancer journal for clinicians, 61 (**2011**) 69.

[3] C.M. Perou, T. Sorlie, M.B. Eisen, M. van de Rijn, S.S. Jeffrey, C.A. Rees, et al., Molecular portraits of human breast tumours, Nature, 406 (**2000**) 747.

[4] W.D. Foulkes, I.E. Smith, J.S. Reis-Filho, Triple-negative breast cancer, The New England journal of medicine, 363 (**2010**) 1938.

[5] C. Wang, S. Kar, X. Lai, W. Cai, F. Arfuso, G. Sethi, et al., Triple negative breast cancer in Asia: An insider's view, Cancer treatment reviews, 62 (**2018**) 29.

[6] R. Dent, M. Trudeau, K.I. Pritchard, W.M. Hanna, H.K. Kahn, C.A. Sawka, et al., Triple-negative breast cancer: clinical features and patterns of recurrence, Clinical cancer research : an official journal of the American Association for Cancer Research, 13 (**2007**) 4429.

[7] S. Dawood, K. Broglio, A.U. Buzdar, G.N. Hortobagyi, S.H. Giordano, Prognosis of women with metastatic breast cancer by HER2 status and trastuzumab treatment: an institutional-based review, Journal of clinical oncology : official journal of the American Society of Clinical Oncology, 28 (**2010**) 92.

[8] V. Ossovskaya, Y. Wang, A. Budoff, Q. Xu, A. Lituev, O. Potapova, et al., Exploring molecular pathways of triple-negative breast cancer, Genes & cancer, 2 (**2011**) 870.

[9] V.S. Jamdade, N. Sethi, N.A. Mundhe, P. Kumar, M. Lahkar, N. Sinha, Therapeutic targets of triple-negative breast cancer: a review, British journal of pharmacology, 172 (**2015**) 4228.

[10] C.A. Minami, D.U. Chung, H.R. Chang, Management options in triple-negative breast cancer, Breast cancer : basic and clinical research, 5 (**2011**) 175.

[11] D. Zardavas, J. Baselga, M. Piccart, Emerging targeted agents in metastatic breast cancer, Nature reviews. Clinical oncology, 10 (**2013**) 191.

[12] Y. Peng, C.M. Croce, The role of MicroRNAs in human cancer, Signal transduction and targeted therapy, 1 (**2016**) 15004.

[13] L. Zhang, Y. Ge, E. Fuchs, miR-125b can enhance skin tumor initiation and promote malignant progression by repressing differentiation and prolonging cell survival, Genes & development, 28 (**2014**) 2532.

[14] Q. Wang, J. Qin, A. Chen, J. Zhou, J. Liu, J. Cheng, et al., Downregulation of microRNA-145 is associated with aggressive progression and poor prognosis in human cervical cancer, Tumour biology : the journal of the International Society for Oncodevelopmental Biology and Medicine, 36 (**2015**) 3703.

[15] D.P. Bartel, MicroRNAs: genomics, biogenesis, mechanism, and function, Cell, 116 (**2004**) 281.

[16] K. Kleivi Sahlberg, G. Bottai, B. Naume, B. Burwinkel, G.A. Calin, A.L. Borresen-Dale, et al., A serum microRNA signature predicts tumor relapse and survival in triple-negative breast cancer patients, Clinical cancer research : an official journal of the American Association for Cancer Research, 21 (**2015**) 1207.

[17] E. D'Ippolito, M.V. Iorio, MicroRNAs and triple negative breast cancer, International journal of molecular sciences, 14 (**2013**) 22202.

[18] A. Esquela-Kerscher, F.J. Slack, Oncomirs - microRNAs with a role in cancer, Nature reviews. Cancer, 6 (**2006**) 259.

[19] M.S. Hwang, N. Yu, S.Y. Stinson, P. Yue, R.J. Newman, B.B. Allan, et al., miR-221/222 targets adiponectin receptor 1 to promote the epithelial-to-mesenchymal transition in breast cancer, PloS one, 8 (**2013**) e66502.

[20] N. Petrovic, miR-21 Might be Involved in Breast Cancer Promotion and Invasion Rather than in Initial Events of Breast Cancer Development, Molecular diagnosis & therapy, 20 (**2016**) 97.

[21] M. Tanic, K. Yanowsky, C. Rodriguez-Antona, R. Andres, I. Marquez-Rodas, A. Osorio, et al., Deregulated miRNAs in hereditary breast cancer revealed a role for miR-30c in regulating KRAS oncogene, PloS one, 7 (**2012**) e38847.

[22] Y. Mo, R.H. Fang, J. Wu, Y. Si, S.Q. Jia, Q. Li, et al., MicroRNA-329 upregulation impairs the HMGB2/beta-catenin pathway and regulates cell biological behaviors in melanoma, Journal of cellular physiology, 234 (**2019**) 23518.

[23] B. Xiao, L. Tan, B. He, Z. Liu, R. Xu, MiRNA-329 targeting E2F1 inhibits cell proliferation in glioma cells, Journal of translational medicine, 11 (**2013**) 172.

[24] C.-C. Sun, S.-J. Li, F. Zhang, J.-Y. Pan, L. Wang, C.-L. Yang, et al., Hsa-miR-329 exerts tumor suppressor function through down-regulation of MET in non-small cell lung cancer, Oncotarget, 7 (**2016**) 21510.

[25] X. Wang, X. Lu, T. Zhang, C. Wen, M. Shi, X. Tang, et al., mir-329 restricts tumor growth by targeting grb2 in pancreatic cancer, Oncotarget, 7 (**2016**) 21441.

[26] H. Kang, C. Kim, H. Lee, J.G. Rho, J.W. Seo, J.W. Nam, et al., Downregulation of microRNA-362-3p and microRNA-329 promotes tumor progression in human breast cancer, Cell death and differentiation, 23 (**2016**) 484.

[27] T.C. Roberts, M.J. Wood, Therapeutic targeting of non-coding RNAs, Essays in biochemistry, 54 (**2013**) 127.

[28] N. Hosseinahli, M. Aghapour, P.H.G. Duijf, B. Baradaran, Treating cancer with microRNA replacement therapy: A literature review, Journal of cellular physiology, 233 (**2018**) 5574.

[29] L. Aagaard, J.J. Rossi, RNAi therapeutics: principles, prospects and challenges, Advanced drug delivery reviews, 59 (**2007**) 75.

[30] X. Wang, B. Yu, W. Ren, X. Mo, C. Zhou, H. He, et al., Enhanced hepatic delivery of siRNA and microRNA using oleic acid based lipid nanoparticle formulations, Journal of controlled release : official journal of the Controlled Release Society, 172 (**2013**) 690.

[31] H.W. Yang, C.Y. Huang, C.W. Lin, H.L. Liu, C.W. Huang, S.S. Liao, et al., Gadolinium-functionalized nanographene oxide for combined drug and microRNA delivery and magnetic resonance imaging, Biomaterials, 35 (**2014**) 6534.

[32] B. Bakhshandeh, M. Soleimani, M. Hafizi, N. Ghaemi, A comparative study on nonviral genetic modifications in cord blood and bone marrow mesenchymal stem cells, Cytotechnology, 64 (**2012**) 523.

[33] H. Yin, R.L. Kanasty, A.A. Eltoukhy, A.J. Vegas, J.R. Dorkin, D.G. Anderson, Non-viral vectors for gene-based therapy, Nature reviews. Genetics, 15 (**2014**) 541.

[34] M. Abdelrahman, L. Douziech Eyrolles, S.Y. Alkarib, K. Herve-Aubert, S. Ben Djemaa, H. Marchais, et al., siRNA delivery system based on magnetic nanovectors: Characterization and stability evaluation, European journal of pharmaceutical sciences : official journal of the European Federation for Pharmaceutical Sciences, 106 (**2017**) 287.

[35] S.K. Yen, P. Padmanabhan, S.T. Selvan, Multifunctional iron oxide nanoparticles for diagnostics, therapy and macromolecule delivery, Theranostics, 3 (**2013**) 986.

[36] J.P. Williams, P. Southern, A. Lissina, H.C. Christian, A.K. Sewell, R. Phillips, et al., Application of magnetic field hyperthermia and superparamagnetic iron oxide nanoparticles to HIV-1-specific T-cell cytotoxicity, International journal of nanomedicine, 8 (**2013**) 2543.

[37] A. Mahapatro, D.K. Singh, Biodegradable nanoparticles are excellent vehicle for site directed in-vivo delivery of drugs and vaccines, Journal of nanobiotechnology, 9 (**2011**) 55.

[38] S. Sharifi, H. Seyednejad, S. Laurent, F. Atyabi, A.A. Saei, M. Mahmoudi, Superparamagnetic iron oxide nanoparticles for in vivo molecular and cellular imaging, Contrast media & molecular imaging, 10 (**2015**) 329.

[39] H.A. Wahba, H.A. El-Hadaad, Current approaches in treatment of triple-negative breast cancer, Cancer biology & medicine, 12 (**2015**) 106.

[40] J. Collignon, L. Lousberg, H. Schroeder, G. Jerusalem, Triple-negative breast cancer: treatment challenges and solutions, Breast cancer (Dove Medical Press), 8 (**2016**) 93.

[41] C. Fitzmaurice, D. Abate, N. Abbasi, H. Abbastabar, F. Abd-Allah, O. Abdel-Rahman, et al., Global, Regional, and National Cancer Incidence, Mortality, Years of Life Lost, Years Lived With Disability, and Disability-Adjusted Life-Years for 29 Cancer Groups, 1990 to 2017: A Systematic Analysis for the Global Burden of Disease Study, JAMA oncology, DOI 10.1001/jamaoncol.2019.2996(**2019**).

[42] V. Ozmen, Breast Cancer in Turkey: Clinical and Histopathological Characteristics (Analysis of 13.240 Patients), The journal of breast health, 10 (**2014**) 98.

[43] V. Ozmen, T. Ozmen, V. Dogru, Breast Cancer in Turkey; An Analysis of 20.000 Patients with Breast Cancer, European journal of breast health, 15 (**2019**) 141.

[44] J.-R. Jhan, E.R. Andrechek, Triple-negative breast cancer and the potential for targeted therapy, Pharmacogenomics, 18 (**2017**) 1595.

[45] S. Libson, M. Lippman, A review of clinical aspects of breast cancer, International review of psychiatry (Abingdon, England), 26 (**2014**) 4.

[46] M. Adhami, A.A. Haghdoost, B. Sadeghi, R. Malekpour Afshar, Candidate miRNAs in human breast cancer biomarkers: a systematic review, Breast cancer (Tokyo, Japan), 25 (**2018**) 198.

[47] N. Eliyatkin, E. Yalcin, B. Zengel, S. Aktas, E. Vardar, Molecular Classification of Breast Carcinoma: From Traditional, Old-Fashioned Way to A New Age, and A New Way, The journal of breast health, 11 (**2015**) 59.

[48] T. Ahmadzada, G. Reid, D.R. McKenzie, Fundamentals of siRNA and miRNA therapeutics and a review of targeted nanoparticle delivery systems in breast cancer, Biophysical reviews, 10 (**2018**) 69.

[49] S.K. Yeo, J.L. Guan, Breast Cancer: Multiple Subtypes within a Tumor?, Trends in cancer, 3 (**2017**) 753.

[50] P. Kumar, R. Aggarwal, An overview of triple-negative breast cancer, Archives of gynecology and obstetrics, 293 (**2016**) 247.

[51] T. Sorlie, C.M. Perou, R. Tibshirani, T. Aas, S. Geisler, H. Johnsen, et al., Gene expression patterns of breast carcinomas distinguish tumor subclasses with clinical implications, Proceedings of the National Academy of Sciences of the United States of America, 98 (**2001**) 10869.

[52] X. Dai, L. Xiang, T. Li, Z. Bai, Cancer Hallmarks, Biomarkers and Breast Cancer Molecular Subtypes, Journal of Cancer, 7 (**2016**) 1281.

[53] M. Kalimutho, K. Parsons, D. Mittal, J.A. Lopez, S. Srihari, K.K. Khanna, Targeted Therapies for Triple-Negative Breast Cancer: Combating a Stubborn Disease, Trends in pharmacological sciences, 36 (**2015**) 822.

[54] F. Penault-Llorca, N. Radosevic-Robin, Ki67 assessment in breast cancer: an update, Pathology, 49 (**2017**) 166.

[55] S.Y. Bae, S. Kim, J.H. Lee, H.C. Lee, S.K. Lee, W.H. Kil, et al., Poor prognosis of single hormone receptor- positive breast cancer: similar outcome as triple-negative breast cancer, BMC cancer, 15 (**2015**) 138.

[56] R. Haque, S.A. Ahmed, G. Inzhakova, J. Shi, C. Avila, J. Polikoff, et al., Impact of breast cancer subtypes and treatment on survival: an analysis spanning two decades, Cancer epidemiology, biomarkers & prevention : a publication of the American Association for Cancer Research, cosponsored by the American Society of Preventive Oncology, 21 (**2012**) 1848.

[57] P. Eroles, A. Bosch, J.A. Perez-Fidalgo, A. Lluch, Molecular biology in breast cancer: intrinsic subtypes and signaling pathways, Cancer treatment reviews, 38 (**2012**) 698.

[58] G. Cancello, P. Maisonneuve, N. Rotmensz, G. Viale, M.G. Mastropasqua, G. Pruneri, et al., Progesterone receptor loss identifies Luminal B breast cancer subgroups at higher risk of relapse, Annals of oncology : official journal of the European Society for Medical Oncology, 24 (**2013**) 661.

[59] F. Ades, D. Zardavas, I. Bozovic-Spasojevic, L. Pugliano, D. Fumagalli, E. de Azambuja, et al., Luminal B breast cancer: molecular characterization, clinical management, and future perspectives, Journal of clinical oncology : official journal of the American Society of Clinical Oncology, 32 (**2014**) 2794.

[60] M. Kittaneh, A.J. Montero, S. Gluck, Molecular profiling for breast cancer: a comprehensive review, Biomarkers in cancer, 5 (**2013**) 61.

[61] S.J. Schnitt, Classification and prognosis of invasive breast cancer: from morphology to molecular taxonomy, Modern pathology : an official journal of the United States and Canadian Academy of Pathology, Inc, 23 Suppl 2 (**2010**) S60.

[62] J.S. Ross, E.A. Slodkowska, W.F. Symmans, L. Pusztai, P.M. Ravdin, G.N. Hortobagyi, The HER-2 receptor and breast cancer: ten years of targeted anti-HER-2 therapy and personalized medicine, The oncologist, 14 (**2009**) 320.

[63] M. Sana, H.J. Malik, Current and emerging breast cancer biomarkers, Journal of cancer research and therapeutics, 11 (**2015**) 508.

[64] C. Peng, W. Ma, W. Xia, W. Zheng, Integrated analysis of differentially expressed genes and pathways in triplenegative breast cancer, Molecular medicine reports, 15 (**2017**) 1087.

[65] E.A. Rakha, D.S. Tan, W.D. Foulkes, I.O. Ellis, A. Tutt, T.O. Nielsen, et al., Are triple-negative tumours and basal-like breast cancer synonymous?, Breast cancer research : BCR, 9 (**2007**) 404; author reply 405.

[66] E.A. Rakha, M.E. El-Sayed, A.R. Green, A.H. Lee, J.F. Robertson, I.O. Ellis, Prognostic markers in triple-negative breast cancer, Cancer, 109 (**2007**) 25.

[67] C.K. Anders, L.A. Carey, Biology, metastatic patterns, and treatment of patients with triple-negative breast cancer, Clinical breast cancer, 9 Suppl 2 (**2009**) S73.

[68] L. Carey, E. Winer, G. Viale, D. Cameron, L. Gianni, Triple-negative breast cancer: disease entity or title of convenience?, Nature reviews. Clinical oncology, 7 (**2010**) 683.

[69] F.M. Blows, K.E. Driver, M.K. Schmidt, A. Broeks, F.E. van Leeuwen, J. Wesseling, et al., Subtyping of breast cancer by immunohistochemistry to investigate a relationship between subtype and short and long term survival: a collaborative analysis of data for 10,159 cases from 12 studies, PLoS medicine, 7 (**2010**) e1000279.

[70] A.M. Gonzalez-Angulo, K.M. Timms, S. Liu, H. Chen, J.K. Litton, J. Potter, et al., Incidence and outcome of BRCA mutations in unselected patients with triple receptor-negative breast cancer, Clinical cancer research : an official journal of the American Association for Cancer Research, 17 (**2011**) 1082.

[71] J.M. Lebert, R. Lester, E. Powell, M. Seal, J. McCarthy, Advances in the systemic treatment of triple-negative breast cancer, Current oncology (Toronto, Ont.), 25 (**2018**) S142.

[72] B.G. Haffty, Q. Yang, M. Reiss, T. Kearney, S.A. Higgins, J. Weidhaas, et al., Locoregional relapse and distant metastasis in conservatively managed triple negative early-stage breast cancer, Journal of clinical oncology : official journal of the American Society of Clinical Oncology, 24 (**2006**) 5652.

[73] L.G. Fulford, J.S. Reis-Filho, K. Ryder, C. Jones, C.E. Gillett, A. Hanby, et al., Basal-like grade III invasive ductal carcinoma of the breast: patterns of metastasis and long-term survival, Breast cancer research : BCR, 9 (**2007**) R4.

[74] R. Dent, W.M. Hanna, M. Trudeau, E. Rawlinson, P. Sun, S.A. Narod, Pattern of metastatic spread in triple-negative breast cancer, Breast cancer research and treatment, 115 (**2009**) 423.

[75] P.L. Nguyen, A.G. Taghian, M.S. Katz, A. Niemierko, R.F. Abi Raad, W.L. Boon, et al., Breast cancer subtype approximated by estrogen receptor, progesterone receptor, and HER-2 is associated with local and distant recurrence after breast-conserving therapy, Journal of clinical oncology : official journal of the American Society of Clinical Oncology, 26 (**2008**) 2373.

[76] K.D. Voduc, M.C. Cheang, S. Tyldesley, K. Gelmon, T.O. Nielsen, H. Kennecke, Breast cancer subtypes and the risk of local and regional relapse, Journal of clinical oncology : official journal of the American Society of Clinical Oncology, 28 (**2010**) 1684.

[77] S. Dawood, Triple-negative breast cancer: epidemiology and management options, Drugs, 70 (**2010**) 2247.

[78] J.E. Panoff, J. Hurley, C. Takita, I.M. Reis, W. Zhao, V. Sujoy, et al., Risk of locoregional recurrence by receptor status in breast cancer patients receiving modern systemic therapy and post-mastectomy radiation, Breast cancer research and treatment, 128 (**2011**) 899.

[79] B.S. Abdulkarim, J. Cuartero, J. Hanson, J. Deschenes, D. Lesniak, S. Sabri, Increased risk of locoregional recurrence for women with T1-2N0 triple-negative breast cancer treated with modified radical mastectomy without adjuvant radiation therapy compared with breast-conserving therapy, Journal of clinical oncology : official journal of the American Society of Clinical Oncology, 29 (**2011**) 2852.

[80] J. Wang, M. Shi, R. Ling, Y. Xia, S. Luo, X. Fu, et al., Adjuvant chemotherapy and radiotherapy in triple-negative breast carcinoma: a prospective randomized controlled multi-center trial, Radiotherapy and oncology : journal of the European Society for Therapeutic Radiology and Oncology, 100 (**2011**) 200.

[81] R. Ismail-Khan, M.M. Bui, A review of triple-negative breast cancer, Cancer control : journal of the Moffitt Cancer Center, 17 (**2010**) 173.

[82] N. Berrada, S. Delaloge, F. Andre, Treatment of triple-negative metastatic breast cancer: toward individualized targeted treatments or chemosensitization?, Annals of oncology : official journal of the European Society for Medical Oncology, 21 Suppl 7 (**2010**) vii30.

[83] K.D. Amos, B. Adamo, C.K. Anders, Triple-negative breast cancer: an update on neoadjuvant clinical trials, International journal of breast cancer, 2012 (**2012**) 385978.

[84] S. Cleator, W. Heller, R.C. Coombes, Triple-negative breast cancer: therapeutic options, The Lancet. Oncology, 8 (**2007**) 235.

[85] F. Kassam, K. Enright, R. Dent, G. Dranitsaris, J. Myers, C. Flynn, et al., Survival outcomes for patients with metastatic triple-negative breast cancer: implications for clinical practice and trial design, Clinical breast cancer, 9 (**2009**) 29.

[86] S. Verma, L. Provencher, R. Dent, Emerging trends in the treatment of triple-negative breast cancer in Canada: a survey, Current oncology (Toronto, Ont.), 18 (**2011**) 180.

[87] S. Badve, D.J. Dabbs, S.J. Schnitt, F.L. Baehner, T. Decker, V. Eusebi, et al., Basal-like and triple-negative breast cancers: a critical review with an emphasis on the implications for pathologists and oncologists, Modern pathology : an official journal of the United States and Canadian Academy of Pathology, Inc, 24 (**2011**) 157.

[88] S.P. Shah, A. Roth, R. Goya, A. Oloumi, G. Ha, Y. Zhao, et al., The clonal and mutational evolution spectrum of primary triple-negative breast cancers, Nature, 486 (**2012**) 395.

[89] M.D. Burstein, A. Tsimelzon, G.M. Poage, K.R. Covington, A. Contreras, S.A. Fuqua, et al., Comprehensive genomic analysis identifies novel subtypes and targets of triple-negative breast cancer, Clinical cancer research : an official journal of the American Association for Cancer Research, 21 (**2015**) 1688.

[90] V.G. Abramson, B.D. Lehmann, T.J. Ballinger, J.A. Pietenpol, Subtyping of triple-negative breast cancer: implications for therapy, Cancer, 121 (**2015**) 8.

[91] B.D. Lehmann, J.A. Bauer, X. Chen, M.E. Sanders, A.B. Chakravarthy, Y. Shyr, et al., Identification of human triple-negative breast cancer subtypes and preclinical models for selection of targeted therapies, The Journal of clinical investigation, 121 (**2011**) 2750.

[92] H. Masuda, K.A. Baggerly, Y. Wang, Y. Zhang, A.M. Gonzalez-Angulo, F. Meric-Bernstam, et al., Differential response to neoadjuvant chemotherapy among 7 triple-negative breast cancer molecular subtypes, Clinical cancer research : an official journal of the American Association for Cancer Research, 19 (**2013**) 5533.

[93] B.D. Lehmann, J.A. Bauer, J.M. Schafer, C.S. Pendleton, L. Tang, K.C. Johnson, et al., PIK3CA mutations in androgen receptor-positive triple negative breast cancer confer sensitivity to the combination of PI3K and androgen receptor inhibitors, Breast cancer research : BCR, 16 (**2014**) 406.

[94] G. Elgar, T. Vavouri, Tuning in to the signals: noncoding sequence conservation in vertebrate genomes, Trends in genetics : TIG, 24 (**2008**) 344.

[95] G. Romano, D. Veneziano, M. Acunzo, C.M. Croce, Small non-coding RNA and cancer, Carcinogenesis, 38 (**2017**) 485.

[96] E. Pennisi, Genomics. ENCODE project writes eulogy for junk DNA, Science (New York, N.Y.), 337 (**2012**) 1159.

[97] A.F. Palazzo, E.S. Lee, Non-coding RNA: what is functional and what is junk?, Frontiers in genetics, 6 (**2015**) 2.

[98] O. Slaby, R. Laga, O. Sedlacek, Therapeutic targeting of non-coding RNAs in cancer, The Biochemical journal, 474 (**2017**) 4219.

[99] M.G. Dozmorov, C.B. Giles, K.A. Koelsch, J.D. Wren, Systematic classification of non-coding RNAs by epigenomic similarity, BMC bioinformatics, 14 Suppl 14 (**2013**) S2.

[100] M. Acunzo, G. Romano, D. Wernicke, C.M. Croce, MicroRNA and cancer--a brief overview, Advances in biological regulation, 57 (**2015**) 1.

[101] M. Esteller, Non-coding RNAs in human disease, Nature reviews. Genetics, 12 (**2011**) 861.

[102] R.C. Lee, R.L. Feinbaum, V. Ambros, The C. elegans heterochronic gene lin-4 encodes small RNAs with antisense complementarity to lin-14, Cell, 75 (**1993**) 843.

[103] T. Nogimori, K. Furutachi, K. Ogami, N. Hosoda, S.I. Hoshino, A novel method for stabilizing microRNA mimics, Biochemical and biophysical research communications, 511 (**2019**) 422.

[104] R. Garzon, G.A. Calin, C.M. Croce, MicroRNAs in Cancer, Annual review of medicine, 60 (**2009**) 167.

[105] A. Kozomara, S. Griffiths-Jones, miRBase: integrating microRNA annotation and deep-sequencing data, Nucleic acids research, 39 (**2011**) D152.

[106] R. Garzon, G. Marcucci, C.M. Croce, Targeting microRNAs in cancer: rationale, strategies and challenges, Nature reviews. Drug discovery, 9 (**2010**) 775.

[107] D.P. Bartel, MicroRNAs: target recognition and regulatory functions, Cell, 136 (**2009**) 215.

[108] R.C. Friedman, K.K. Farh, C.B. Burge, D.P. Bartel, Most mammalian mRNAs are conserved targets of microRNAs, Genome research, 19 (**2009**) 92.

[109] E. Berezikov, V. Guryev, J. van de Belt, E. Wienholds, R.H. Plasterk, E. Cuppen, Phylogenetic shadowing and computational identification of human microRNA genes, Cell, 120 (**2005**) 21.

[110] P. Jakob, U. Landmesser, Role of microRNAs in stem/progenitor cells and cardiovascular repair, Cardiovascular research, 93 (**2012**) 614.

[111] N.H. Tolia, L. Joshua-Tor, Slicer and the argonautes, Nature chemical biology, 3 (**2007**) 36.

[112] I. Lee, S.S. Ajay, J.I. Yook, H.S. Kim, S.H. Hong, N.H. Kim, et al., New class of microRNA targets containing simultaneous 5'-UTR and 3'-UTR interaction sites, Genome research, 19 (**2009**) 1175.

[113] G.A. Calin, C. Sevignani, C.D. Dumitru, T. Hyslop, E. Noch, S. Yendamuri, et al., Human microRNA genes are frequently located at fragile sites and genomic regions involved in cancers, Proceedings of the National Academy of Sciences of the United States of America, 101 (**2004**) 2999.

[114] A. Lujambio, S. Ropero, E. Ballestar, M.F. Fraga, C. Cerrato, F. Setien, et al., Genetic unmasking of an epigenetically silenced microRNA in human cancer cells, Cancer research, 67 (**2007**) 1424.

[115] R. Munker, G.A. Calin, MicroRNA profiling in cancer, Clinical science (London, England : 1979), 121 (**2011**) 141.

[116] S. Volinia, G.A. Calin, C.G. Liu, S. Ambs, A. Cimmino, F. Petrocca, et al., A microRNA expression signature of human solid tumors defines cancer gene targets, Proceedings of the National Academy of Sciences of the United States of America, 103 (**2006**) 2257.

[117] W. Ji, B. Sun, C. Su, Targeting MicroRNAs in Cancer Gene Therapy, Genes, 8 (**2017**).

[118] M. Kobayashi, K. Sawada, T. Kimura, Is microRNA replacement therapy promising treatment for cancer?, Non-coding RNA Investigation, 2 (**2018**).

[119] Y. Pekarsky, C.M. Croce, Is miR-29 an oncogene or tumor suppressor in CLL?, Oncotarget, 1 (**2010**) 224.

[120] G.A. Calin, C.D. Dumitru, M. Shimizu, R. Bichi, S. Zupo, E. Noch, et al., Frequent deletions and down-regulation of micro- RNA genes miR15 and miR16 at 13q14 in chronic lymphocytic leukemia, Proceedings of the National Academy of Sciences of the United States of America, 99 (**2002**) 15524.

[121] K. Lin, M. Farahani, Y. Yang, G.G. Johnson, M. Oates, M. Atherton, et al., Loss of MIR15A and MIR16-1 at 13q14 is associated with increased TP53 mRNA, de-repression of BCL2 and adverse outcome in chronic lymphocytic leukaemia, British journal of haematology, 167 (**2014**) 346.

[122] S. Roush, F.J. Slack, The let-7 family of microRNAs, Trends in cell biology, 18 (**2008**) 505.

[123] H. Jiang, G. Zhang, J.H. Wu, C.P. Jiang, Diverse roles of miR-29 in cancer (review), Oncology reports, 31 (**2014**) 1509.

[124] S.P. Nana-Sinkam, C.M. Croce, MicroRNA regulation of tumorigenesis, cancer progression and interpatient heterogeneity: towards clinical use, Genome biology, 15 (**2014**) 445.

[125] R. Rupaimoole, F.J. Slack, MicroRNA therapeutics: towards a new era for the management of cancer and other diseases, Nature reviews. Drug discovery, 16 (**2017**) 203.

[126] E. van Rooij, S. Kauppinen, Development of microRNA therapeutics is coming of age, EMBO molecular medicine, 6 (**2014**) 851.

[127] H. Ling, M. Fabbri, G.A. Calin, MicroRNAs and other non-coding RNAs as targets for anticancer drug development, Nature reviews. Drug discovery, 12 (**2013**) 847.

[128] A.G. Bader, D. Brown, M. Winkler, The promise of microRNA replacement therapy, Cancer research, 70 (**2010**) 7027.

[129] A.G. Bader, D. Brown, J. Stoudemire, P. Lammers, Developing therapeutic microRNAs for cancer, Gene therapy, 18 (**2011**) 1121.

[130] J.C. Henry, A.C. Azevedo-Pouly, T.D. Schmittgen, MicroRNA replacement therapy for cancer, Pharmaceutical research, 28 (**2011**) 3030.

[131] X. Zhao, F. Pan, C.M. Holt, A.L. Lewis, J.R. Lu, Controlled delivery of antisense oligonucleotides: a brief review of current strategies, Expert opinion on drug delivery, 6 (**2009**) 673.

[132] S. Essex, G. Navarro, P. Sabhachandani, A. Chordia, M. Trivedi, S. Movassaghian, et al., Phospholipid-modified PEI-based nanocarriers for in vivo siRNA therapeutics against multidrug-resistant tumors, Gene therapy, 22 (**2015**) 257.

[133] J.G. Parvani, M.W. Jackson, Silencing the roadblocks to effective triple-negative breast cancer treatments by siRNA nanoparticles, Endocrine-related cancer, 24 (**2017**) R81.

[134] Y. Chen, D.Y. Gao, L. Huang, In vivo delivery of miRNAs for cancer therapy: challenges and strategies, Advanced drug delivery reviews, 81 (**2015**) 128.

[135] A.E. Arnold, P. Czupiel, M. Shoichet, Engineered polymeric nanoparticles to guide the cellular internalization and trafficking of small interfering ribonucleic acids, Journal of controlled release : official journal of the Controlled Release Society, 259 (**2017**) 3.

[136] M. Gujrati, A. Vaidya, Z.R. Lu, Multifunctional pH-Sensitive Amino Lipids for siRNA Delivery, Bioconjugate chemistry, 27 (**2016**) 19.

[137] S.W. Young, M. Stenzel, J.L. Yang, Nanoparticle-siRNA: A potential cancer therapy?, Critical reviews in oncology/hematology, 98 (**2016**) 159.

[138] S. Kasar, E. Salerno, Y. Yuan, C. Underbayev, D. Vollenweider, M.F. Laurindo, et al., Systemic in vivo lentiviral delivery of miR-15a/16 reduces malignancy in the NZB de novo mouse model of chronic lymphocytic leukemia, Genes and immunity, 13 (**2012**) 109.

[139] M.S. Kumar, S.J. Erkeland, R.E. Pester, C.Y. Chen, M.S. Ebert, P.A. Sharp, et al., Suppression of non-small cell lung tumor development by the let-7 microRNA family, Proceedings of the National Academy of Sciences of the United States of America, 105 (**2008**) 3903.

[140] Y.P. Liu, M.A. Vink, J.T. Westerink, E. Ramirez de Arellano, P. Konstantinova, O. Ter Brake, et al., Titers of lentiviral vectors encoding shRNAs and miRNAs are reduced by different mechanisms that require distinct repair strategies, RNA (New York, N.Y.), 16 (**2010**) 1328.

[141] M.R. Brandt, A.G. Kirste, T. Pozzuto, S. Schubert, R. Kandolf, H. Fechner, et al., Adenovirus vector-mediated RNA interference for the inhibition of human parvovirus B19 replication, Virus research, 176 (**2013**) 155.

[142] W. Lou, Q. Chen, L. Ma, J. Liu, Z. Yang, J. Shen, et al., Oncolytic adenovirus co-expressing miRNA-34a and IL-24 induces superior antitumor activity in experimental tumor model, Journal of molecular medicine (Berlin, Germany), 91 (**2013**) 715.

[143] F. Borel, M.A. Kay, C. Mueller, Recombinant AAV as a platform for translating the therapeutic potential of RNA interference, Molecular therapy : the journal of the American Society of Gene Therapy, 22 (**2014**) 692.

[144] J. Kota, R.R. Chivukula, K.A. O'Donnell, E.A. Wentzel, C.L. Montgomery, H.W. Hwang, et al., Therapeutic microRNA delivery suppresses tumorigenesis in a murine liver cancer model, Cell, 137 (**2009**) 1005.

[145] L.M. Stanek, S.P. Sardi, B. Mastis, A.R. Richards, C.M. Treleaven, T. Taksir, et al., Silencing mutant huntingtin by adeno-associated virus-mediated RNA interference ameliorates disease manifestations in the YAC128 mouse model of Huntington's disease, Human gene therapy, 25 (**2014**) 461.

[146] L.B. Couto, K.A. High, Viral vector-mediated RNA interference, Current opinion in pharmacology, 10 (**2010**) 534.

[147] K. Pauwels, R. Gijsbers, J. Toelen, A. Schambach, K. Willard-Gallo, C. Verheust, et al., State-of-the-art lentiviral vectors for research use: risk assessment and biosafety recommendations, Current gene therapy, 9 (**2009**) 459.

[148] R. Hendrickx, N. Stichling, J. Koelen, L. Kuryk, A. Lipiec, U.F. Greber, Innate immunity to adenovirus, Human gene therapy, 25 (**2014**) 265.

[149] Y. Seow, M.J. Wood, Biological gene delivery vehicles: beyond viral vectors, Molecular therapy : the journal of the American Society of Gene Therapy, 17 (**2009**) 767.

[150] H. Lv, S. Zhang, B. Wang, S. Cui, J. Yan, Toxicity of cationic lipids and cationic polymers in gene delivery, Journal of controlled release : official journal of the Controlled Release Society, 114 (**2006**) 100.

[151] D.K. Mishra, N. Balekar, P.K. Mishra, Nanoengineered strategies for siRNA delivery: from target assessment to cancer therapeutic efficacy, Drug delivery and translational research, 7 (**2017**) 346.

[152] I. Fernandez-Pineiro, I. Badiola, A. Sanchez, Nanocarriers for microRNA delivery in cancer medicine, Biotechnology advances, 35 (**2017**) 350.

[153] K. Tatiparti, S. Sau, S.K. Kashaw, A.K. Iyer, siRNA Delivery Strategies: A Comprehensive Review of Recent Developments, Nanomaterials (Basel, Switzerland), 7 (**2017**).

[154] K. Wang, F.M. Kievit, M. Zhang, Nanoparticles for cancer gene therapy: Recent advances, challenges, and strategies, Pharmacological research, 114 (**2016**) 56.

[155] D. Bedi, J.W. Gillespie, V.A. Petrenko, Jr., A. Ebner, M. Leitner, P. Hinterdorfer, et al., Targeted delivery of siRNA into breast cancer cells via phage fusion proteins, Molecular pharmaceutics, 10 (**2013**) 551.

[156] K. Hirota, H. Terada, Endocytosis of particle formulations by macrophages and its application to clinical treatment, Molecular regulation of endocytosis, 1 (**2012**).

[157] S.S. Davis, Biomedical applications of nanotechnology--implications for drug targeting and gene therapy, Trends in biotechnology, 15 (**1997**) 217.

[158] S. Govindarajan, J. Sivakumar, P. Garimidi, N. Rangaraj, J.M. Kumar, N.M. Rao, et al., Targeting human epidermal growth factor receptor 2 by a cell-penetrating peptide-affibody bioconjugate, Biomaterials, 33 (**2012**) 2570.

[159] M.S. Draz, B.A. Fang, P. Zhang, Z. Hu, S. Gu, K.C. Weng, et al., Nanoparticle-mediated systemic delivery of siRNA for treatment of cancers and viral infections, Theranostics, 4 (**2014**) 872.

[160] D. Dong, W. Gao, Y. Liu, X.R. Qi, Therapeutic potential of targeted multifunctional nanocomplex co-delivery of siRNA and low-dose doxorubicin in breast cancer, Cancer letters, 359 (**2015**) 178.

[161] S. Honary, F. Zahir, Effect of zeta potential on the properties of nano-drug delivery systems-a review (Part 2), Tropical Journal of Pharmaceutical Research, 12 (**2013**) 265.

[162] P. Zou, Y. Yu, Y.A. Wang, Y. Zhong, A. Welton, C. Galban, et al., Superparamagnetic iron oxide nanotheranostics for targeted cancer cell imaging and pH-dependent intracellular drug release, Molecular pharmaceutics, 7 (**2010**) 1974.

[163] L.S. Wang, M.C. Chuang, J.A. Ho, Nanotheranostics--a review of recent publications, International journal of nanomedicine, 7 (**2012**) 4679.

[164] A.S. Wadajkar, J.U. Menon, K.T. Nguyen, Polymer-Coated Magnetic Nanoparticles for Cancer Diagnosis and Therapy, Reviews in Nanoscience and Nanotechnology, 1 (**2012**) 284.

[165] F. Dilnawaz, A. Singh, C. Mohanty, S.K. Sahoo, Dual drug loaded superparamagnetic iron oxide nanoparticles for targeted cancer therapy, Biomaterials, 31 (**2010**) 3694.

[166] H.J. Lee, Y.T. Nguyen, M. Muthiah, H. Vu-Quang, R. Namgung, W.J. Kim, et al., MR traceable delivery of p53 tumor suppressor gene by PEI-functionalized superparamagnetic iron oxide nanoparticles, Journal of biomedical nanotechnology, 8 (**2012**) 361.

[167] S. Balivada, R.S. Rachakatla, H. Wang, T.N. Samarakoon, R.K. Dani, M. Pyle, et al., A/C magnetic hyperthermia of melanoma mediated by iron(0)/iron oxide core/shell magnetic nanoparticles: a mouse study, BMC cancer, 10 (**2010**) 119.

[168] S. Prijic, L. Prosen, M. Cemazar, J. Scancar, R. Romih, J. Lavrencak, et al., Surface modified magnetic nanoparticles for immuno-gene therapy of murine mammary adenocarcinoma, Biomaterials, 33 (**2012**) 4379.

[169] H. Xu, Z.P. Aguilar, L. Yang, M. Kuang, H. Duan, Y. Xiong, et al., Antibody conjugated magnetic iron oxide nanoparticles for cancer cell separation in fresh whole blood, Biomaterials, 32 (**2011**) 9758.

[170] T. Indira, P. Lakshmi, Magnetic nanoparticles–a review, Int. J. Pharm. Sci. Nanotechnol, 3 (**2010**) 1035.

[171] C. Fang, F.M. Kievit, O. Veiseh, Z.R. Stephen, T. Wang, D. Lee, et al., Fabrication of magnetic nanoparticles with controllable drug loading and release through a simple assembly approach, Journal of controlled release : official journal of the Controlled Release Society, 162 (**2012**) 233.

[172] P.B. Santhosh, N.P. Ulrih, Multifunctional superparamagnetic iron oxide nanoparticles: promising tools in cancer theranostics, Cancer letters, 336 (**2013**) 8.

[173] C.C. Berry, S. Wells, S. Charles, G. Aitchison, A.S. Curtis, Cell response to dextran-derivatised iron oxide nanoparticles post internalisation, Biomaterials, 25 (**2004**) 5405.

[174] A.K. Gupta, M. Gupta, Synthesis and surface engineering of iron oxide nanoparticles for biomedical applications, Biomaterials, 26 (**2005**) 3995.

[175] M.M. Lin, D.K. Kim, A.J. El Haj, J. Dobson, Development of superparamagnetic iron oxide nanoparticles (SPIONS) for translation to clinical applications, IEEE transactions on nanobioscience, 7 (**2008**) 298.

[176] S.C. McBain, H.H. Yiu, J. Dobson, Magnetic nanoparticles for gene and drug delivery, International journal of nanomedicine, 3 (**2008**) 169.

[177] T. Sasayama, M. Nishihara, T. Kondoh, K. Hosoda, E. Kohmura, MicroRNA-10b is overexpressed in malignant glioma and associated with tumor invasive factors, uPAR and RhoC, International Journal of Cancer, 125 (**2009**) 1407.

[178] Y.H. Chang, F. Yin, G.F. Fan, M. Zhao, Down-regulation of miR-329-3p is associated with worse prognosis in patients with cervical cancer, Eur Rev Med Pharmacol Sci, 21 (**2017**) 4045.

[179] W. Li, J. Liang, Z. Zhang, H. Lou, L. Zhao, Y. Xu, et al., MicroRNA-329-3p targets MAPK1 to suppress cell proliferation, migration and invasion in cervical cancer, Oncology reports, 37 (**2017**) 2743.

[180] J. Xu, J. Zhang, LncRNA TP73-AS1 is a novel regulator in cervical cancer via miR-329-3p/ARF1 axis, Journal of cellular biochemistry, 121 (**2020**) 344.

[181] H. Yang, Q. Li, W. Zhao, D. Yuan, H. Zhao, Y. Zhou, miR-329 suppresses the growth and motility of neuroblastoma by targeting KDM1A, FEBS Letters, 588 (**2014**) 192.

[182] W. Jiang, J. Liu, T. Xu, X. Yu, MiR-329 suppresses osteosarcoma development by downregulating Rab10, FEBS Letters, 590 (**2016**) 2973.

[183] D. Li, Z. Tao, Downregulation of serum miR-329 is an unfavorable prognostic biomarker in head and neck squamous cell carcinoma, INTERNATIONAL JOURNAL OF CLINICAL AND EXPERIMENTAL PATHOLOGY, 10 (**2017**) 3157.

[184] Z. Li, X. Yu, Y. Wang, J. Shen, W.K. Wu, J. Liang, et al., By downregulating TIAM1 expression, microRNA-329 suppresses gastric cancer invasion and growth, Oncotarget, 6 (**2015**) 17559.

[185] L. Cai, Q. Chen, S. Fang, M. Lian, M. Cai, MicroRNA-329 inhibits cell proliferation and tumor growth while facilitates apoptosis via negative regulation of KDM1A in gastric cancer, Journal of cellular biochemistry, 119 (**2018**) 3338.

[186] B. Li, M. Huang, M. Liu, S. Wen, F. Sun, MicroRNA329 serves a tumor suppressive role in colorectal cancer by directly targeting transforming growth factor beta1, Molecular medicine reports, 16 (**2017**) 3825.

[187] J. Yin, X. Shen, M. Li, F. Ni, L. Xu, H. Lu, miR-329 regulates the sensitivity of 5-FU in chemotherapy of colorectal cancer by targeting E2F1, Oncology letters, 16 (**2018**) 3587.

[188] J. Ye, J. Lei, Q. Fang, Y. Shen, W. Xia, X. Hu, et al., miR-4666-3p and miR-329 Synergistically Suppress the Stemness of Colorectal Cancer Cells via Targeting TGF-β/Smad Pathway, Frontiers in Oncology, 9 (**2019**).

[189] L. Wu, F. Pei, X. Men, K. Wang, D. Ma, miR-329 inhibits papillary thyroid cancer progression via direct targeting WNT1, Oncology letters, 16 (**2018**) 3561.

[190] C.H. Liao, Y. Liu, Y.F. Wu, S.W. Zhu, R.Y. Cai, L. Zhou, et al., microRNA-329 suppresses epithelial-to-mesenchymal transition and lymph node metastasis in bile duct cancer by inhibiting laminin subunit beta 3, Journal of cellular physiology, 234 (**2019**) 17786.

[191] Z.G. Hu, C.W. Zheng, H.Z. Su, Y.L. Zeng, C.J. Lin, Z.Y. Guo, et al., MicroRNA-329-mediated PTTG1 downregulation inactivates the MAPK signaling pathway to suppress cell proliferation and tumor growth in cholangiocarcinoma, Journal of cellular biochemistry, 120 (**2019**) 9964.

[192] J. Zhou, W. Li, J. Guo, G. Li, F. Chen, J. Zhou, Downregulation of miR-329 promotes cell invasion by regulating BRD4 and predicts poor prognosis in hepatocellular carcinoma, Tumour biology : the journal of the International Society for Oncodevelopmental Biology and Medicine, 37 (**2016**) 3561.

[193] C.C. Sun, S.J. Li, F. Zhang, J.Y. Pan, L. Wang, C.L. Yang, et al., Hsa-miR-329 exerts tumor suppressor function through down-regulation of MET in non-small cell lung cancer, Oncotarget, 7 (**2016**) 21510.

[194] P. Li, J. Dong, X. Zhou, W. Sun, H. Huang, T. Chen, et al., Expression patterns of microRNA-329 and its clinical performance in diagnosis and prognosis of breast cancer, OncoTargets and therapy, 10 (**2017**) 5711.

[195] P. Wang, Y. Luo, H. Duan, S. Xing, J. Zhang, D. Lu, et al., MicroRNA 329 suppresses angiogenesis by targeting CD146, Molecular and cellular biology, 33 (**2013**) 3689.

[196] R. Liu, C.G. Proud, Eukaryotic elongation factor 2 kinase as a drug target in cancer, and in cardiovascular and neurodegenerative diseases, Acta pharmacologica Sinica, 37 (**2016**) 285.

[197] J.W. Kenney, C.E. Moore, X. Wang, C.G. Proud, Eukaryotic elongation factor 2 kinase, an unusual enzyme with multiple roles, Advances in biological regulation, 55 (**2014**) 15.

[198] X.Y. Liu, L. Zhang, Y. Zhang, J.M. Yang, Roles of eEF-2 kinase in cancer, Chinese medical journal, 125 (**2012**) 2908.

[199] X. Wang, J. Xie, C.G. Proud, Eukaryotic Elongation Factor 2 Kinase (eEF2K) in Cancer, Cancers, 9 (**2017**) 162.

[200] A.A. Ashour, A.A. Abdel-Aziz, A.M. Mansour, S.N. Alpay, L. Huo, B. Ozpolat, Targeting elongation factor-2 kinase (eEF-2K) induces apoptosis in human pancreatic cancer cells, Apoptosis : an international journal on programmed cell death, 19 (**2014**) 241.

[201] A.A. Ashour, N. Gurbuz, S.N. Alpay, A.A. Abdel-Aziz, A.M. Mansour, L. Huo, et al., Elongation factor-2 kinase regulates TG2/beta1 integrin/Src/uPAR pathway and epithelial-mesenchymal transition mediating pancreatic cancer cells invasion, Journal of cellular and molecular medicine, 18 (**2014**) 2235.

[202] C.M. Xie, X.Y. Liu, K.W. Sham, J.M. Lai, C.H. Cheng, Silencing of EEF2K (eukaryotic elongation factor-2 kinase) reveals AMPK-ULK1-dependent autophagy in colon cancer cells, Autophagy, 10 (**2014**) 1495.

[203] Y. Zhang, Y. Cheng, L. Zhang, X. Ren, K.J. Huber-Keener, S. Lee, et al., Inhibition of eEF-2 kinase sensitizes human glioma cells to TRAIL and down-regulates Bcl-xL expression, Biochemical and biophysical research communications, 414 (**2011**) 129.

[204] R. Bayraktar, M. Pichler, P. Kanlikilicer, C. Ivan, E. Bayraktar, N. Kahraman, et al., MicroRNA 603 acts as a tumor suppressor and inhibits triple-negative breast cancer tumorigenesis by targeting elongation factor 2 kinase, Oncotarget, 8 (**2017**) 11641.

[205] I. Tekedereli, S.N. Alpay, C.D. Tavares, Z.E. Cobanoglu, T.S. Kaoud, I. Sahin, et al., Targeted silencing of elongation factor 2 kinase suppresses growth and sensitizes tumors to doxorubicin in an orthotopic model of breast cancer, PloS one, 7 (**2012**) e41171.

[206] Z. Hamurcu, A. Ashour, N. Kahraman, B. Ozpolat, FOXM1 regulates expression of eukaryotic elongation factor 2 kinase and promotes proliferation, invasion and tumorgenesis of human triple negative breast cancer cells, Oncotarget, 7 (**2016**) 16619.

[207] J.P. O'Bryan, R.A. Frye, P.C. Cogswell, A. Neubauer, B. Kitch, C. Prokop, et al., axl, a transforming gene isolated from primary human myeloid leukemia cells, encodes a novel receptor tyrosine kinase, Molecular and cellular biology, 11 (**1991**) 5016.

[208] R.M. Linger, A.K. Keating, H.S. Earp, D.K. Graham, TAM receptor tyrosine kinases: biologic functions, signaling, and potential therapeutic targeting in human cancer, Advances in cancer research, 100 (**2008**) 35.

[209] S.J. Holland, A. Pan, C. Franci, Y. Hu, B. Chang, W. Li, et al., R428, a selective small molecule inhibitor of Axl kinase, blocks tumor spread and prolongs survival in models of metastatic breast cancer, Cancer research, 70 (**2010**) 1544.

[210] J.B. Koorstra, C.A. Karikari, G. Feldmann, S. Bisht, P.L. Rojas, G.J. Offerhaus, et al., The Axl receptor tyrosine kinase confers an adverse prognostic influence in pancreatic cancer and represents a new therapeutic target, Cancer biology & therapy, 8 (**2009**) 618.

[211] T. Sawabu, H. Seno, T. Kawashima, A. Fukuda, Y. Uenoyama, M. Kawada, et al., Growth arrest-specific gene 6 and Axl signaling enhances gastric cancer cell survival via Akt pathway, Molecular carcinogenesis, 46 (**2007**) 155.

[212] Y.X. Zhang, P.G. Knyazev, Y.V. Cheburkin, K. Sharma, Y.P. Knyazev, L. Orfi, et al., AXL is a potential target for therapeutic intervention in breast cancer progression, Cancer research, 68 (**2008**) 1905.

[213] W. Sun, J. Fujimoto, T. Tamaya, Coexpression of Gas6/Axl in human ovarian cancers, Oncology, 66 (**2004**) 450.

[214] P.P. Sainaghi, L. Castello, L. Bergamasco, M. Galletti, P. Bellosta, G.C. Avanzi, Gas6 induces proliferation in prostate carcinoma cell lines expressing the Axl receptor, Journal of cellular physiology, 204 (**2005**) 36.

[215] Y.S. Shieh, C.Y. Lai, Y.R. Kao, S.G. Shiah, Y.W. Chu, H.S. Lee, et al., Expression of axl in lung adenocarcinoma and correlation with tumor progression, Neoplasia (New York, N.Y.), 7 (**2005**) 1058.

[216] G. Berclaz, H.J. Altermatt, V. Rohrbach, I. Kieffer, E. Dreher, A.C. Andres, Estrogen dependent expression of the receptor tyrosine kinase axl in normal and malignant human breast, Annals of oncology : official journal of the European Society for Medical Oncology, 12 (**2001**) 819.

[217] M. Mackiewicz, K. Huppi, J.J. Pitt, T.H. Dorsey, S. Ambs, N.J. Caplen, Identification of the receptor tyrosine kinase AXL in breast cancer as a target for

the human miR-34a microRNA, Breast cancer research and treatment, 130 (**2011**) 663.

[218] S.K. Das, T. Dey, S.C. Kundu, Fabrication of sericin nanoparticles for controlled gene delivery, RSC Advances, 4 (**2014**) 2137.

[219] M.K. Yoo, I.Y. Park, I.Y. Kim, I.K. Park, J.S. Kwon, H.J. Jeong, et al., Superparamagnetic iron oxide nanoparticles coated with mannan for macrophage targeting, Journal of nanoscience and nanotechnology, 8 (**2008**) 5196.

[220] A. Bandhu, S. Mukherjee, S. Acharya, S. Modak, S.K. Brahma, D. Das, et al., Dynamic magnetic behaviour and Mössbauer effect measurements of magnetite nanoparticles prepared by a new technique in the co-precipitation method, Solid State Communications, 149 (**2009**) 1790.

[221] A.K. Hauser, M.I. Mitov, E.F. Daley, R.C. McGarry, K.W. Anderson, J.Z. Hilt, Targeted iron oxide nanoparticles for the enhancement of radiation therapy, Biomaterials, 105 (**2016**) 127.

[222] I. Koh, X. Wang, B. Varughese, L. Isaacs, S.H. Ehrman, D.S. English, Magnetic Iron Oxide Nanoparticles for Biorecognition: Evaluation of Surface Coverage and Activity, The Journal of Physical Chemistry B, 110 (**2006**) 1553.

[223] A. Aires, S.M. Ocampo, D. Cabrera, L.d.l. Cueva, G. Salas, F.J. Teran, et al., BSA-coated magnetic nanoparticles for improved therapeutic properties, Journal of Materials Chemistry B, 3 (**2015**) 6239.

[224] Z. Karahaliloğlu, E. Kilicay, P. Alpaslan, B. Hazer, E. Baki Denkbas, Enhanced antitumor activity of epigallocatechin gallate–conjugated dual-drug-loaded polystyrene–polysoyaoil–diethanol amine nanoparticles for breast cancer therapy, Journal of Bioactive and Compatible Polymers, 33 (**2018**) 38.

[225] D.C. Castrillón Martínez, C.L. Zuluaga, A. Restrepo-Osorio, C. Álvarez-López, Characterization of sericin obtained from cocoons and silk yarns, Procedia Engineering, 200 (**2017**) 377.

[226] E. Yalcin, G. Kara, E. Celik, F.A. Pinarli, G. Saylam, C. Sucularli, et al., Preparation and characterization of novel albumin-sericin nanoparticles as siRNA delivery vehicle for laryngeal cancer treatment, Preparative biochemistry & biotechnology, 49 (**2019**) 659.

[227] J. Saha, M. Mondal, M. Sheikh, M. Habib, Extraction, Structural and Functional Properties of Silk Sericin Biopolymer from Bombyx mori Silk Cocoon Waste, Journal of Textile Science & Engineering, 09 (**2019**).

[228] A.K. Bordbar, A.A. Rastegari, R. Amiri, E. Ranjbakhsh, M. Abbasi, A.R. Khosropour, Characterization of modified magnetite nanoparticles for albumin immobilization, Biotechnology research international, 2014 (**2014**) 705068.

[229] S. Villa, P. Riani, F. Locardi, F. Canepa, Functionalization of Fe_3O_4 NPs by Silanization: Use of Amine (APTES) and Thiol (MPTMS) Silanes and Their Physical Characterization, Materials (Basel), 9 (**2016**) 826.

[230] M. Seifan, A. Ebrahiminezhad, Y. Ghasemi, A.K. Samani, A. Berenjian, Amine-modified magnetic iron oxide nanoparticle as a promising carrier for application in bio self-healing concrete, Applied microbiology and biotechnology, 102 (**2018**) 175.

[231] K. Langer, M.G. Anhorn, I. Steinhauser, S. Dreis, D. Celebi, N. Schrickel, et al., Human serum albumin (HSA) nanoparticles: reproducibility of preparation process and kinetics of enzymatic degradation, International journal of pharmaceutics, 347 (**2008**) 109.

[232] A. Woods, E. Bicer, C. Apfelthaler, K. Bruce, L. Dailey, B. Forbes, Albumin Nanoparticles for Drug Delivery to the Lungs-In Vitro Investigation of Biodegradation as a Mechanism of Clearance, Drug Delivery to the Lungs, 24 (**2013**).

[233] L. Shang, Q.-y. Wang, K.-l. Chen, J. Qu, Q.-h. Zhou, J.-b. Luo, et al., SPIONs/DOX loaded polymer nanoparticles for MRI detection and efficient cell targeting drug delivery, Rsc Advances, 7 (**2017**) 47715.

[234] J.C. Liu, V. Voisin, S. Wang, D.Y. Wang, R.A. Jones, A. Datti, et al., Combined deletion of Pten and p53 in mammary epithelium accelerates triple-negative breast cancer with dependency on eEF2K, EMBO molecular medicine, 6 (**2014**) 1542.

[235] X.Y. Liu, L. Zhang, J. Wu, L. Zhou, Y.-J. Ren, W.-Q. Yang, et al., Inhibition of elongation factor-2 kinase augments the antitumor activity of Temozolomide against glioma, PloS one, 8 (**2013**) e81345.

[236] X. Wang, W. Li, M. Williams, N. Terada, D.R. Alessi, C.G. Proud, Regulation of elongation factor 2 kinase by p90(RSK1) and p70 S6 kinase, The EMBO journal, 20 (**2001**) 4370.

[237] C.E. Moore, S. Regufe da Mota, H. Mikolajek, C.G. Proud, A conserved loop in the catalytic domain of eukaryotic elongation factor 2 kinase plays a key role in its substrate specificity, Molecular and cellular biology, 34 (**2014**) 2294.

[238] C.D. Tavares, J.P. O'Brien, O. Abramczyk, A.K. Devkota, K.S. Shores, S.B. Ferguson, et al., Calcium/calmodulin stimulates the autophosphorylation of elongation factor 2 kinase on Thr-348 and Ser-500 to regulate its activity and calcium dependence, Biochemistry, 51 (**2012**) 2232.

[239] C.G. Proud, Regulation and roles of elongation factor 2 kinase, Portland Press Ltd., 2015.

[240] C.D.J. Tavares, S.B. Ferguson, D.H. Giles, Q. Wang, R.M. Wellmann, J.P. O'Brien, et al., The molecular mechanism of eukaryotic elongation factor 2 kinase activation, J Biol Chem, 289 (**2014**) 23901.

[241] E. Connolly, S. Braunstein, S. Formenti, R.J. Schneider, Hypoxia inhibits protein synthesis through a 4E-BP1 and elongation factor 2 kinase pathway controlled by mTOR and uncoupled in breast cancer cells, Molecular and cellular biology, 26 (**2006**) 3955.

[242] G.J. Browne, C.G. Proud, Regulation of peptide-chain elongation in mammalian cells, European journal of biochemistry, 269 (**2002**) 5360.

[243] J.K. Lam, M.Y. Chow, Y. Zhang, S.W. Leung, siRNA Versus miRNA as Therapeutics for Gene Silencing, Molecular therapy. Nucleic acids, 4 (**2015**) e252.

[244] G. Misso, M.T. Di Martino, G. De Rosa, A.A. Farooqi, A. Lombardi, V. Campani, et al., Mir-34: a new weapon against cancer?, Molecular therapy. Nucleic acids, 3 (**2014**) e194.

[245] B. Ozpolat, A.K. Sood, G. Lopez-Berestein, Liposomal siRNA nanocarriers for cancer therapy, Advanced drug delivery reviews, 66 (**2014**) 110.

EKLER

EK 1: Ethics Committee Approval

All animal studies were conducted according to an experimental protocol by Assoc. Prof. Dr. Bülent ÖZPOLAT and approved by the MD Anderson Institutional Animal Care and Use Committee. (Protocol Number: 00000838-RN02).

EK 2: Presentations Related to the Thesis

Kara G., Malekghasemi S., Denkbas E.B., “Preparation and Characterization of Magnetic Sericin Nanoparticles”, NanoTech Poland International Conference and Exhibition, 1-3 June 2017, Poznan, Poland